

# **Recharge and discharge of near-surface groundwater in Forsmark**

## **Comparison of classification methods**

Kent Werner, Golder Associates AB

Per-Olof Johansson, Artesia Grundvattenkonsult AB

Lars Brydsten, Umeå University

Emma Bosson, Sten Berglund  
Svensk Kärnbränslehantering AB

Mats Tröjbom, Mopelikan

Helena Nyman, SWECO Position AB

March 2007

**Svensk Kärnbränslehantering AB**

Swedish Nuclear Fuel  
and Waste Management Co  
Box 5864  
SE-102 40 Stockholm Sweden  
Tel 08-459 84 00  
+46 8 459 84 00  
Fax 08-661 57 19  
+46 8 661 57 19



# **Recharge and discharge of near-surface groundwater in Forsmark**

## **Comparison of classification methods**

Kent Werner, Golder Associates AB

Per-Olof Johansson, Artesia Grundvattenkonsult AB

Lars Brydsten, Umeå University

Emma Bosson, Sten Berglund  
Svensk Kärnbränslehantering AB

Mats Tröjbom, Mopelikan

Helena Nyman, SWECO Position AB

March 2007

# Abstract

This report presents and compares data and models for identification of near-surface groundwater recharge and discharge (RD) areas in Forsmark. The general principles of groundwater recharge and discharge are demonstrated and applied to interpret hydrological and hydrogeological observations made in the Forsmark area. “Continuous” RD classification methods considered in the study include topographical modelling, map overlays, and hydrological-hydrogeological flow modelling. “Discrete” (point) methods include field-based and hydrochemistry-based RD classifications of groundwater monitoring well locations. The topographical RD modelling uses the digital elevation model as the only input. The map overlays use background maps of Quaternary deposits, soils, and ground- and field layers of the vegetation/land use map. Further, the hydrological-hydrogeological modelling is performed using the MIKE SHE-MIKE 11 software packages, taking into account e.g. topography, meteorology, hydrogeology, and geometry of watercourses and lakes.

The best between-model agreement is found for the topography-based model and the MIKE SHE-MIKE 11 model. The agreement between the topographical model and the map overlays is less good. The agreement between the map overlays on the one hand, and the MIKE SHE and field-based RD classifications on the other, is thought to be less good, as inferred from the comparison made with the topography-based model. However, much improvement of the map overlays can likely be obtained, e.g. by using “weights” and calibration (such exercises were outside the scope of the present study). For field-classified “recharge wells”, there is a good agreement to the hydrochemistry-based (Piper plot) well classification, but less good for the field-classified “discharge wells”. In addition, the concentration of the age-dating parameter tritium shows low variability among recharge wells, but a large spread among discharge wells. The usefulness of hydrochemistry-based RD classification of the Forsmark area is thought to be limited, for instance due to calcite-rich soils and local/shallow groundwater flow systems.

Updated RD classifications of the Forsmark area should be made when further data and updated models are available. Based on the findings in this study, it is recommended that the MIKE SHE-MIKE 11 model primarily is used for this purpose. MIKE SHE-MIKE 11 (in combination with groundwater flow models of the deep rock) has the largest potential to identify the most important subset of the near-surface groundwater discharge areas, i.e. discharge areas receiving groundwater that passes the intended repository volume along its flow path. The remaining methods presented in the study should primarily be used as support for the MIKE SHE-MIKE 11 modelling. The supporting data set should include a field-based RD classification of the entire set of monitoring wells in Forsmark (and possibly also other objects of interest), as well as an updated hydrochemistry-based RD classification. However, the present results indicate that Piper plots and single “age parameters” (such as tritium, used as example here) provide too inconsistent information to be of practical use for RD classification. In order to evaluate the applicability of hydrochemistry-based methods to assess groundwater flow patterns in Forsmark, hydrochemical data need to be analyzed further and compared to updated MIKE SHE-MIKE 11 modelling results.

# Sammanfattning

Denna rapport presenterar och jämför data och modeller för identifiering av ytnära in- och utströmningsområden (RD; eng. recharge-discharge) för grundvatten i Forsmark. De allmänna principerna för grundvattnets in- och utströmning presenteras och tillämpas för tolkning av hydrologiska och hydrogeologiska observationer i Forsmark. ”Kontinuerliga” RD-klassificeringsmetoder som beaktas i studien inkluderar topografisk modellering, kartpålägg och hydrologisk-hydrogeologisk flödesmodellering. ”Diskreta” (punkt)metoder inkluderar fältbaserad och hydrokemibaserad RD-klassificering av grundvattenrör i jord. Den topografiska RD-modelleringen använder endast den digitala höjdmodellen som indata. Kartpåläggen utgår från bakgrundskartor över kvartära avlagringar, jordmån samt botten- och fältlager i kartan över vegetation och markanvändning. Den hydrologiska-hydrogeologiska modelleringen utförs med programpaketet MIKE SHE-MIKE 11, som använder data bland annat på topografi, meteorologi, hydrogeologi samt geometri på vattendrag och sjöar.

Den bästa modellöverensstämmelsen erhålls mellan den topografibaserade modellen och MIKE SHE-MIKE 11-modellen. Det är sämre överensstämmelse mellan den topografiska modellen och kartpåläggen. Överensstämmelsen mellan kartpåläggen å ena sidan, och MIKE SHE-MIKE 11 och den fältbaserade RD-klassificeringen å den andra, bedöms vara mindre god, baserat på jämförelsen med den topografibaserade modellen. Förbättringar av klassningen utgående från kartpålägg bör dock vara möjliga, till exempel genom att tillämpa ”viktningar” och kalibrering (vilket låg utanför ramen för denna studie). För fältklassade ”inströmningsrör” är det god överensstämmelse med den hydrokemibaserade (Piperdiagram) rörklassificeringen, men sämre för fältklassade ”utströmningsrör”. Dessutom uppvisar koncentrationen av åldersparametern tritium låg variation mellan inströmningsrör, men stor spridning mellan utströmningsrör. Nyttan med hydrokemiskt baserad RD-klassificering av Forsmarksområdet bedöms vara begränsad, bland annat på grund av jordens höga kalcitinhåll samt lokal/ytnära grundvattenströmning.

Uppdaterade RD-klassificeringar av Forsmarksområdet bör utföras när ytterligare data och uppdaterade modeller är tillgängliga. Baserat på slutsatserna från denna studie, rekommenderas att MIKE SHE-MIKE 11-modellen främst används för detta syfte. MIKE SHE-MIKE 11 (i kombination med grundvattenflödesmodeller av det djupa berget) har den största potentialen att kunna identifiera den viktigaste delmängden av de ytnära utströmningsområdena, det vill säga utströmningsområden för grundvatten som passerar den tänkta förvarsvolymen längs flödesvägen. De övriga metoder som presenteras i studien bör främst användas som stöd för MIKE SHE-MIKE 11-modelleringen. Stödande data bör inkludera fältbaserad RD-klassificering av samtliga grundvattenrör i Forsmark (möjligen också av andra intressanta objekt), samt en uppdaterad hydrokemibaserad RD-klassificering. Resultaten från denna studie indikerar att Piperdiagram och enstaka åldersparametrar (till exempel tritium, som här används som exempel) ger alltför inkonsekvent information för att vara praktiskt användbar för RD-klassificering. För att kunna utvärdera användbarheten av hydrokemibaserade metoder för bedömning av grundvattnets flödesmönster i Forsmark, bör hydrokemiska data analyseras vidare och även jämföras med resultat från MIKE SHE-MIKE 11-modelleringen.

# Contents

<b>1</b>	<b>Introduction</b>	7
1.1	Background	7
1.2	Objectives and scope	7
1.3	Overview of methods and data	8
<b>2</b>	<b>Groundwater recharge and discharge areas</b>	9
2.1	Background	9
2.1.1	Influence of topography	9
2.1.2	Combined influences of topography and geological variability	11
2.1.3	Transient effects	13
2.1.4	The influence of the upper boundary condition	15
2.2	The Forsmark area	15
2.2.1	Topography and hydrogeology	15
2.2.2	Groundwater recharge	18
2.2.3	Groundwater levels	20
2.2.4	Implications of site characteristics for recharge-discharge area patterns	25
<b>3</b>	<b>Presentation of RD classification methods</b>	29
3.1	Topographical RD model	29
3.2	Map overlays	32
3.3	Hydrological-hydrogeological modelling using MIKE SHE	35
3.4	Field classification of groundwater monitoring well locations	38
3.4.1	Methodology	38
3.4.2	Results	40
3.5	Hydrochemical classification of groundwater monitoring well locations	46
3.5.1	Some observations concerning RD-hydrochemistry relations in the Forsmark area	46
3.5.2	Major chemical elements	47
3.5.3	Redox and groundwater age	48
<b>4</b>	<b>Comparison between RD classification methods</b>	53
4.1	Topographical model and map overlays	53
4.2	Topographical model and MIKE SHE	55
4.3	Methods for classification of groundwater monitoring well locations	57
4.3.1	Topographical classifications	58
4.3.2	RD classifications	58
<b>5</b>	<b>Summary and conclusions</b>	65
	<b>References</b>	69

# 1 Introduction

## 1.1 Background

Proper identification and characterization of groundwater recharge and discharge areas are important issues for many applications, related to a geological repository for spent nuclear fuel. In case of radionuclide leakage from such a repository, which in the Swedish concept is located in the rock at a depth of 400–700 m, radionuclides would be transported by groundwater flow in rock and Quaternary deposits towards groundwater discharge areas. Such areas may be located either at the ground surface or at the bottom of surface waters. An important issue for safety assessment is hence the identification of discharge areas receiving groundwater that passes the intended repository volume along its flow path.

The Forsmark area, located near the coast in mid-eastern Sweden, is one of two candidate sites for a geological repository for spent nuclear fuel (the other site is the Simpevarp area in south-eastern Sweden). In accordance with the description above, identification and characterization of groundwater discharge areas are important components of the site investigations at these sites, and also for the associated site descriptive modelling.

Previous studies of groundwater recharge and discharge in the Forsmark area have been focused on conceptual models based on geological, hydrogeological and hydrochemical data, and numerical modelling of ground- and surface water flow /Follin et al. 2005, Johansson et al. 2005, SKB 2005, Tröjbom and Söderbäck 2006, Juston et al. 2007/. The present report attempts to integrate different types of data and models (of which some have not been used before for Forsmark) for characterization of the water flow systems in the Forsmark area. In particular, the report summarizes and compares some methods that potentially could be utilized for classification of the Forsmark area in terms of groundwater recharge and discharge areas.

## 1.2 Objectives and scope

A set of field and modelling studies are presented, performed in support of the Forsmark site description. Specifically, these studies have been performed with the general objective of investigating the spatial and temporal patterns of groundwater recharge and discharge at the site. The report aims to investigate methods and parameters that may be useful for describing recharge-discharge patterns. In particular, the report analyses the differences between recharge-discharge classifications, which are the outcomes of the classification methods considered herein.

The specific objectives of the present work are to:

- Present and compare different methods for spatially continuous delineations of groundwater recharge and discharge areas.
- Present and compare (i) a physical-hydrological field classification and (ii) a hydrochemical classification of the locations of groundwater monitoring wells installed in Quaternary deposits in Forsmark, in terms of recharge and discharge areas.

The considered studies are limited to and use data from the surface and near-surface water flow systems only. In practise, this limitation implies that all input data used in the present work are obtained from the ground surface (such as the topographical description) and the Quaternary deposits above the rock (such as data from groundwater monitoring wells).

Note that the report frequently uses the abbreviations “R” for groundwater recharge, and “D” for groundwater discharge. For instance, “recharge-discharge classification” is in the report for brevity written as “RD classification”.

### 1.3 Overview of methods and data

As indicated in the previous section, groundwater RD characteristics can be analysed using two main types of data:

- Data available “continuously” over the whole study area, e.g. topographical maps, maps of Quaternary deposits and vegetation/land use, and results from numerical water flow modelling. Obviously, such information is available in the form of grid cells and therefore discrete. Although commonly presented as uniformly available over the whole area, it should be noted that the information could be associated with different degrees of uncertainty in different areas. This study includes the following continuous data for the Forsmark area: (i) A topographical RD map /Brydsten 2006/, (ii) the vegetation/land use map /Boresjö Bronge and Wester 2002, 2003/, (iii) the soil map /Lundin et al. 2004/, (iv) the map of Quaternary deposits /Sohlenius et al. 2004/, and (v) an RD map obtained by hydrological-hydrogeological modelling /Johansson et al. 2005/.
- Data available at discrete locations, here in the form of data from groundwater monitoring wells; this study includes a physical-hydrological field classification and a hydrochemical classification in terms of RD of such wells in the Forsmark area.

## 2 Groundwater recharge and discharge areas

### 2.1 Background

#### 2.1.1 Influence of topography

Groundwater recharge areas and groundwater discharge areas are usually defined as areas where groundwater flow has a downward and upward flow component, respectively. A groundwater flow system (or groundwater basin) is defined as a three-dimensional closed system, containing the entire flow paths followed by all the water recharging the system (see, e.g. /Freeze and Witherspoon 1967, Freeze and Cherry 1979/).

The influence of the topography on groundwater flow systems on different scales was demonstrated in the pioneering work by Tóth /Tóth 1962, 1963/. In Sweden, similar and independent studies were performed by Gustafsson (see, e.g. /Gustafsson 1968/). /Tóth 1963/ used analytical solutions to the equation for steady-state groundwater flow, assuming homogeneous and isotropic groundwater basins. He considered the case of an undulating groundwater table along a constant gentle regional slope, approximating the groundwater table by a sine function. Hence, Tóth used a fixed hydraulic head as the upper boundary, in the form of a subdued replica of the topography of the ground surface. Depending on the ratio between the depth and the lateral extent of the investigated basins, and the amplitude of the undulating groundwater table, Tóth demonstrated that groundwater flow systems may occur on three characteristic scales: local, intermediate, and regional systems.

According to Tóth's definitions, a local groundwater flow system has its recharge area at a topographic high and its discharge area at an adjacent topographic low. For intermediate systems, one or more topographic highs and lows may be located between the recharge and discharge areas, although these areas are not associated to the highest and lowest locations within the groundwater basin. Finally, the recharge area of a regional system occupies the upstream water divide of the basin, and its discharge area is located at the main (regional) valley bottom, i.e. at the lowest location of the basin.

This topographical influence on the groundwater flow pattern, and the locations of groundwater recharge and discharge, is schematically illustrated in the vertical cross sections in Figures 2-1 to 2-3. These figures show the configuration of stationary groundwater flow (visualized by flow paths) along a regional slope, for different amplitudes of the local topographic relief: 0.5, 5, and 10 m. The figures have been generated by use of the analytical element code TWODAN /Fitts 2004/, considering a hypothetical groundwater basin of length 1.2 km. The depth of the basin is 600 m at the downstream (left) edge of all sections. A closed flow system is assumed, with no groundwater flow across the left and right boundaries, or across the bottom boundary of the basin.

Following /Tóth 1963/, the configuration of the undulating groundwater table in Figures 2-1 to 2-3 is approximated by a sine function (a wavelength of 480 m is used here). Further, a regional slope of 1/50 is assumed. The sine curve is shifted by +0.75 wavelengths along the positive horizontal axis and by the amplitude along the positive vertical axis. These shifts are made to produce a main valley with hydraulic head = 0 at the downstream edge, a regional high at the upstream edge, and two local valleys and highs along the regional slope.

As illustrated in Figure 2-1, a constant gentle regional slope and small amplitude of the local relief (0.5 m) result in flow along the slope being essentially horizontal. Groundwater recharge is evenly distributed along the upstream (right) part of the basin, whereas groundwater discharge takes place along its downstream part; the hinge line (the line separating recharge and discharge) is located midway along the slope.



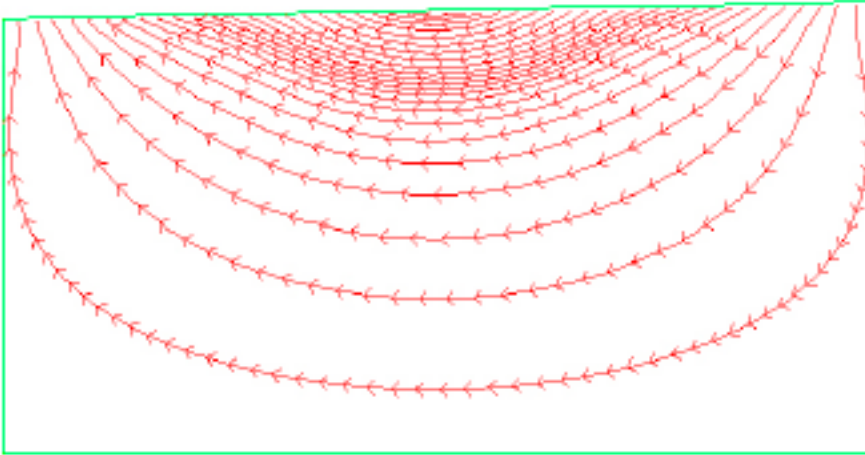


**Figure 2-1.** Visualization of stationary flow paths along a regional slope (topographic gradient 1/50). The length and depth of the basin is 1.2 km and 600 m, respectively. The amplitude of the undulating groundwater table is 0.5 m.

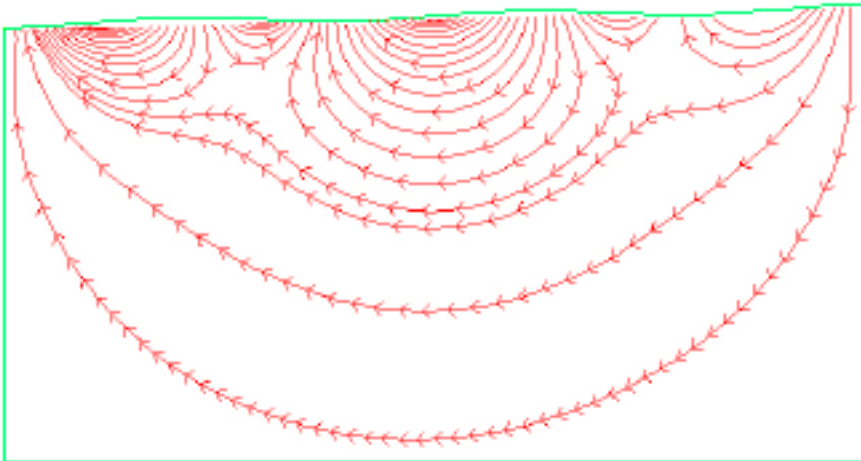


**Figure 2-2.** Visualization of stationary flow paths along a regional slope (topographic gradient 1/50). The length and depth of the basin is 1.2 km and 600 m, respectively. The amplitude of the undulating groundwater table is 5 m.

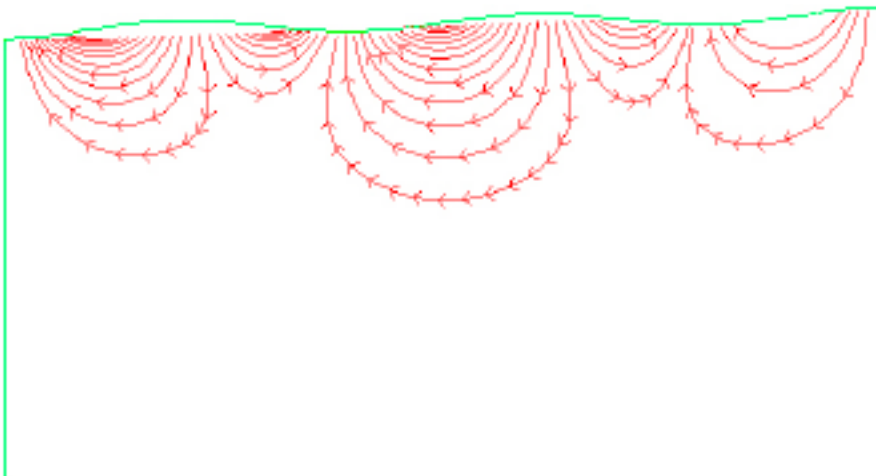


**Figure 2-3.** Visualization of stationary flow paths along a regional slope (topographic gradient 1/50). The length and depth of the basin is 1.2 km and 600 m, respectively. The amplitude of the undulating groundwater table is 10 m.

Higher amplitude of the local relief (Figure 2-2) results in flow systems on all the scales defined by Tóth: Local, intermediate and regional. The flow paths that visualize the regional system span the whole basin, from the regional high to the main valley. Flow paths associated with the intermediate system extend from a recharge area at a local high (located downstream from the regional high), to the discharge area at the main valley. Moreover, there are several local systems, having their recharge areas at topographic highs and their discharge areas at adjacent topographic lows.

Compared to the simple flow system in Figure 2-1, the occurrence of flow systems on different scales as illustrated in Figure 2-2 have important implications for the concept of groundwater recharge and discharge areas. Considering a topographic high, Figure 2-2 shows that even a relatively small difference in the location of recharge may make the difference between water entering a local, an intermediate or a regional flow system. Further, Figure 2-2 shows that there are more discharge areas associated with local flow systems, compared to those associated with larger-scale systems; the regional flow system has only one discharge area.

The figure also shows that “near-surface” groundwater in a certain discharge area may consist of a mix of water, associated with flow systems on different scales. In the main valley in Figure 2-2, a near-surface groundwater sample could contain water associated with flow systems on all scales.

A consequence of the above observations is that the terms recharge and discharge for undulating terrain, typical for many areas in Sweden, must be associated with a spatial scale. A parcel of water entering the groundwater table at a certain recharge location may follow flow paths down to small or large depths. Further, water entering the ground surface or the bottom of a surface water body in a discharge area may be associated with a local, an intermediate or a regional flow system, or a mix of them.

Referring to Chapter 1, this report considers near-surface recharge and discharge, i.e. recharge and discharge areas as they can be identified and characterized from data obtained at or near the ground surface. In fact, focusing on near-surface data implies a broadening of the study, compared with a study focusing on the conditions deeper below the ground surface. Most likely, only a small subset of the recharge and discharge areas identified in the present study coincide with intermediate or regional recharge-discharge areas.

Doubling the terrain amplitude to 10 m (Figure 2-3) implies that there are only local flow systems; no flow path traverses the entire basin, and no flow path has one or more topographic highs and lows between the recharge and discharge areas. As shown by /Tóth 1963/, the amplitude at which this occurs depends on the ratio between the depth and the lateral extent of the basin. If this ratio is small, a system consisting of local flow systems occurs for smaller amplitudes.

### **2.1.2 Combined influences of topography and geological variability**

Using numerical solutions to the steady-state groundwater flow equation /Freeze and Witherspoon 1967/ were the first to investigate both the influence of topography and (simple cases of) spatially variable hydraulic conductivity on groundwater flow. They showed that such variability may have strong influence on flow paths between recharge and discharge areas.

The cross sections in Figures 2-4 to 2-6 schematically illustrate the large influence of even simple cases of spatial heterogeneity on groundwater flow paths. The principal cases considered here were also investigated in /Freeze and Witherspoon 1967/. Figure 2-4 shows another hypothetical groundwater basin, having a length of 3.7 km and a depth of 750 m, along a regional slope (slope 1/300). As in Figures 2-1 to 2-3, the undulating groundwater table along the regional slope is approximated by a sine function, in this case with a wavelength of c. 1,050 m and relatively small amplitude (1.5 m). Figure 2-4 shows a homogeneous case, for which even this small local relief produces several local flow systems, one intermediate system and a regional system.

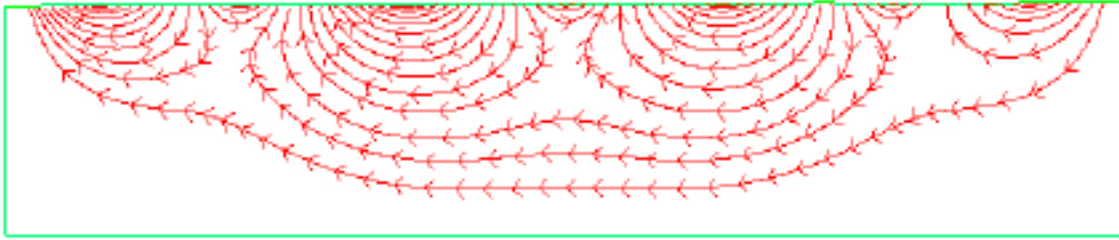


**Figure 2-4.** Visualization of stationary flow paths along a regional slope (topographic gradient 1/300) along a homogeneous groundwater basin. The length and depth of the basin is 3.7 km and 750 m, respectively, and the amplitude of the undulating groundwater table is 1.5 m.

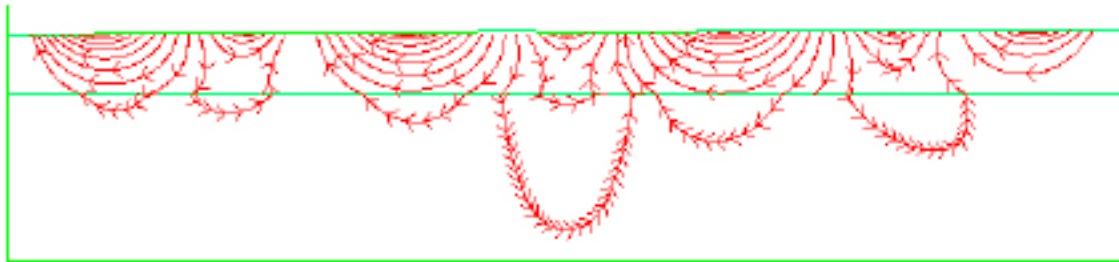


**Figure 2-5.** Visualization of stationary flow paths along a regional slope (topographic gradient 1/300) along a layered groundwater basin. The length and depth of the basin is 3.7 km and 750 m, respectively, and the amplitude of the undulating groundwater table is 1.5 m. The hydraulic conductivity contrast between the lower and the upper layer is 1/100.

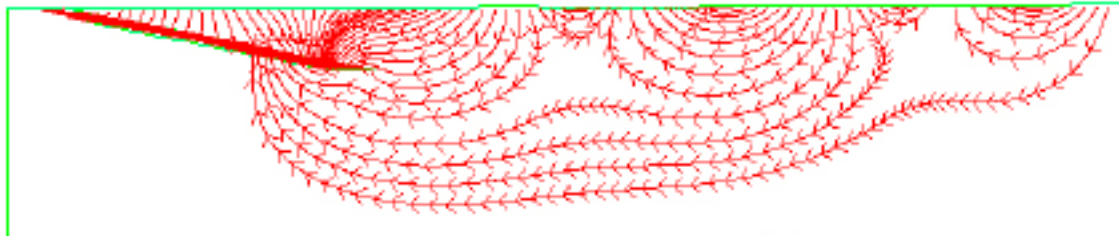


**Figure 2-6.** Visualization of stationary flow paths along a regional slope along a groundwater basin with a sub-horizontal layer. The length and depth of the basin is 3.7 km and 750 m, respectively, and the amplitude of the undulating groundwater table is 1.5 m. The hydraulic conductivity contrast between the layer and the rest of the basin is 100/1.

A low-permeable layer has been added in the lower 550 m of the cross section in Figure 2-5, with a hydraulic conductivity of 1/100 of the conductivity of the upper 200 m. This case could, for instance, represent a zone of high-permeable rock overlying low-permeable rock. A higher hydraulic conductivity in the upper part of the cross section removes the intermediate and regional flow systems, hence resulting in local flow systems only.

In Figure 2-6, a sub-horizontal layer, with a width of 150 m, has been added to the homogeneous case in Figure 2-4. This layer, extending from a depth of 200 m and outcropping in the vicinity of the main valley, has 100 times higher hydraulic conductivity than the rest of the cross section. For example, this case could represent a deformation zone within rock. /Freeze and Witherspoon 1967/ found that such “stratigraphic pinch outs” may imply that recharge and discharge take place at locations that can not be anticipated solely based on the topography of the ground surface or the groundwater table. As shown in Figure 2-6, the high-permeable layer

effectively acts as a “collector drain”, causing a convergence of flow paths associated with local, intermediate and regional systems; all flow paths within the sub-horizontal layer are directed towards the ground surface.

In the present context, it is also of interest to mention a recent investigation by /Ericsson et al. 2006/. Using eastern Småland (a province in south-eastern Sweden) as case study, /Ericsson et al. 2006/ presented an extensive groundwater modelling study, investigating the relative impact of a number of factors on the pattern of “suprascale” (large-regional scale) groundwater flow, including topography and geological variability. In the context of that study, “suprascale” flow paths are referred to as flow paths with lengths greater than 10 km, starting at a depth of 500 m in the rock. Examples of investigated factors include local topographic undulation, and spatially variable hydrogeological properties, including anisotropy (direction-dependent properties) and vertical/horizontal deformation zones in the rock.

The main conclusions from the study are listed below:

- The topographical undulation has larger impact on regional groundwater flow than spatially variable hydraulic conductivity, including lithological units and regional deformation zones. In Sweden, the groundwater table usually follows the topography, due to the large potential groundwater recharge and the low-permeable rock.
- The second most important factor is depth-dependent and anisotropic hydraulic conductivity. Compared to homogeneous conditions, a depth-decreasing hydraulic conductivity, and/or a higher vertical than horizontal hydraulic conductivity, reduce the number of regional flow paths, and increase the number of local flow paths. Conversely, a higher horizontal than vertical hydraulic conductivity implies more regional-scale flow paths, and fewer local flow paths.
- Deformation zones and dolerite dikes in the rock are of tertiary importance, demonstrating relatively larger impact on local-scale flow, compared to regional-scale groundwater flow.
- The study shows that an increasing model complexity (i.e. taking into account more factors) increases the number of local flow paths, and reduce the number of regional flow paths. Assuming hydrogeological conditions typical for Sweden, there are much more local groundwater flow paths, compared to regional flow paths.

An illustrative example from /Ericsson et al. 2006/ is shown in Figure 2-7, visualizing model-calculated groundwater discharge areas at the ground surface, for a complex simulation case. This case takes into account lithological units, vertical deformation zones and vertical dolerite dikes with depth-decreasing hydraulic conductivity, and Quaternary deposits above the rock. The discharge areas are visualized by particle tracking, where particles are released uniformly across all onshore parts of the model area (size 80 by 130 km), at a depth of 500 m in the rock.

Figure 2-7 shows that groundwater flow paths, starting at a large depth (500 m), end in discharge areas across the whole model area. In the onshore parts, the discharge areas are mainly located along major valleys, pits, watercourses, and lakes. There are no discharge areas in local topographic highs, but rather in valleys and pits surrounding such highs.

### **2.1.3 Transient effects**

Transient meteorological conditions imply that the extents of recharge and discharge areas may vary in time. For typical conditions in Sweden, with relatively small basins and undulating terrain, the extents of discharge areas increase during wet periods /Grip and Rodhe 1985/. This phenomenon is exemplified in Figure 2-8, by pre-site investigation numerical modelling results for the Forsmark area /Holmén and Forsman 2005/. In this particular simulation example, the areal fraction of discharge areas varies between c. 25% and 75% during a normal year. Note that the figure is shown only for illustrative purposes; it was produced as part of a general modelling study, performed prior to the site investigations in Forsmark.

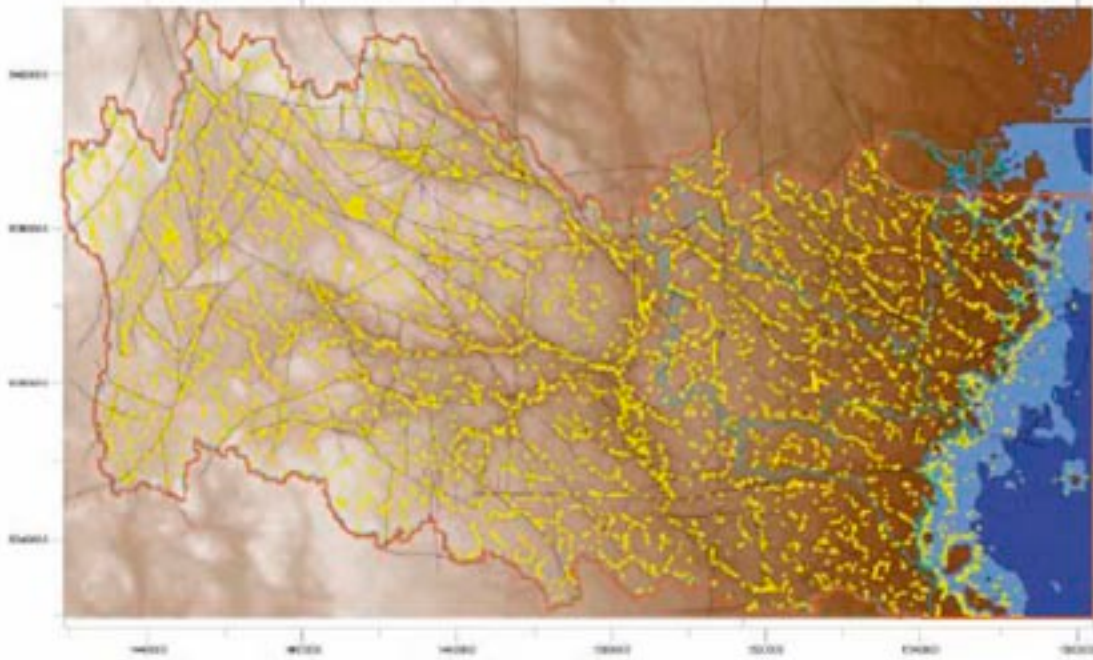


Figure 2-7. Particle-tracking visualization of groundwater discharge areas (yellow dots) at the ground surface across the eastern Småland case study area /Ericsson et al. 2006/. Particles are released uniformly onshore, at a depth of 500 m.

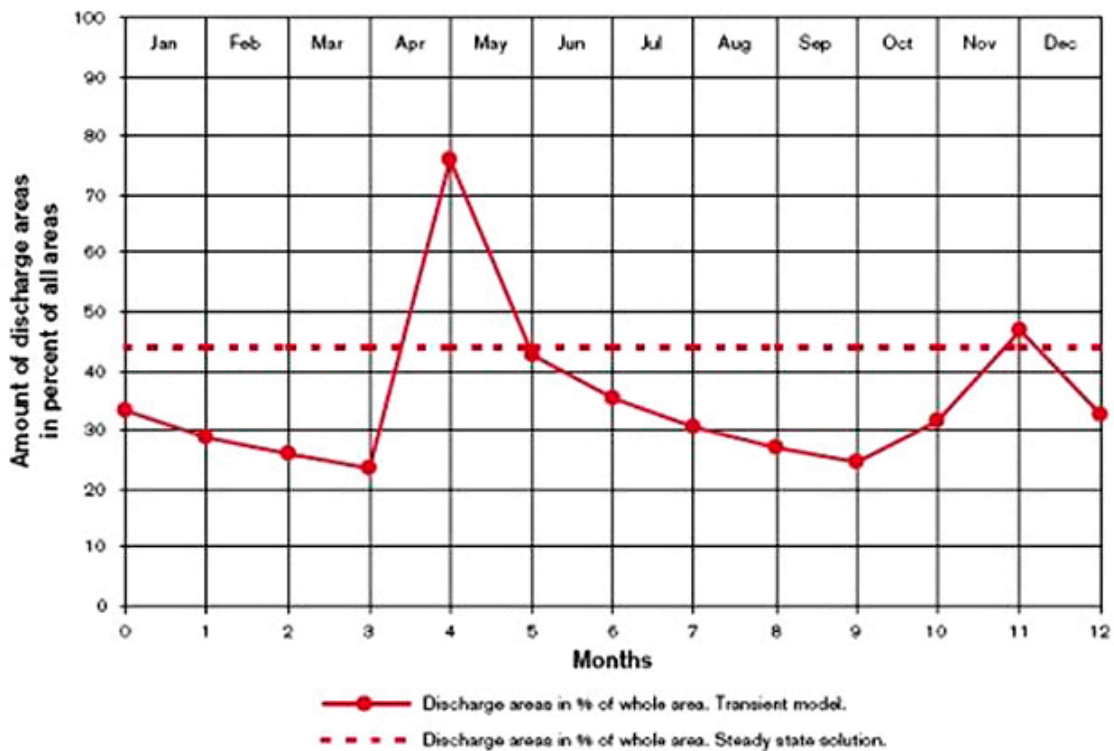


Figure 2-8. Pre-site investigation modelling results, showing the relative amount (%) of groundwater discharge areas in Forsmark during a normal year /Holmén and Forsman 2005/. The solid line represents results obtained using time-varying precipitation (monthly averages), whereas the annual average precipitation is used as input to produce the dotted line.

#### **2.1.4 The influence of the upper boundary condition**

A potentially important issue in numerical groundwater flow modelling is the influence of the upper boundary condition on the extent of model-calculated recharge and discharge areas. In principle, the upper boundary condition may be in the form of specified head or specified flux. The influence of the upper boundary on the overall modelling results has been tested in previous groundwater flow modelling of the Forsmark site /SKB 2005/.

As base case, the head on the top surface was set to the topographic height. Offshore, the head was set equal to the depth of the sea multiplied by the relative density of the Baltic Sea to freshwater. A variant was to use a flux-type boundary condition, with a potential infiltration of  $200 \text{ mm}\cdot\text{year}^{-1}$ . One further variant was to fix the head at the ground surface only in the discharge areas, and lower the head in the recharge areas by an amount in accordance with the observed variability in the elevation of the groundwater table. The objective of the latter variant was to study the implications of a topographically specified head for groundwater flow at repository depth, by reducing the impact of local topographic gradients relative to the regional topographic gradient.

It was found that similar results were obtained by using a topographically specified head or a specified flux. However, it was concluded that more variants of the hydraulic properties of the Quaternary deposits need to be considered in forthcoming modelling, probably using a specified flux as upper boundary and a high resolution of the computational grid.

## **2.2 The Forsmark area**

Unless stated otherwise, the present description of the Forsmark site is based on data available in the Forsmark version 2.2 data set. The regional model area and the candidate area of the Forsmark site investigation are shown in Figure 2-9. It can be seen that forest land dominates the candidate area and its surroundings and that wetlands are frequent.

### **2.2.1 Topography and hydrogeology**

The preliminary conceptual and descriptive model of the surface hydrology and near-surface hydrogeology in /Johansson et al. 2005/ considered the area north-east of the main water divide of the catchment area of Forsmarksån, between the nuclear power plant in the north and Kallrigafjärden in the south, see Figure 2-10. As shown in this figure, the area is situated almost entirely below 20 m above sea level and is characterized by small-scale topography.

In the conceptual and descriptive modelling, it was assumed that surface water and near-surface groundwater divides coincide. The boundary towards Forsmarksån was assumed to be a surface water and groundwater divide (i.e. a no-flow boundary). Also the north-western boundary was modelled as a surface water and groundwater divide. The boundaries towards the cooling water canal and the Baltic Sea were set as prescribed head boundaries, which mean that they normally act as outflow boundaries. However, the flat topography allows sea water inflow to some of the lakes during periods of very high sea water levels.

No major watercourses flow through the area northeast of the main water divide to the watercourse Forsmarksån. The brooks downstream Lake Gunnarsboträsket, Lake Eckarfjärden and Lake Gällsboträsket carry water most of the year, but can still be dry for long time periods during dry years. Fens and marshes are frequent in the more low-lying parts of the area. The gytta in these wetlands can rest directly on till, or be underlain by clayey gytta and/or sand and clay above the till. This means that the hydraulic contact with the surrounding groundwater system varies among the wetlands in the area. Till is the dominating type of Quaternary deposit, covering approximately 75% of the area considered in the detailed mapping, see Figure 2-11.



Figure 2-9. The regional model area and the candidate area of the Forsmark site investigation.

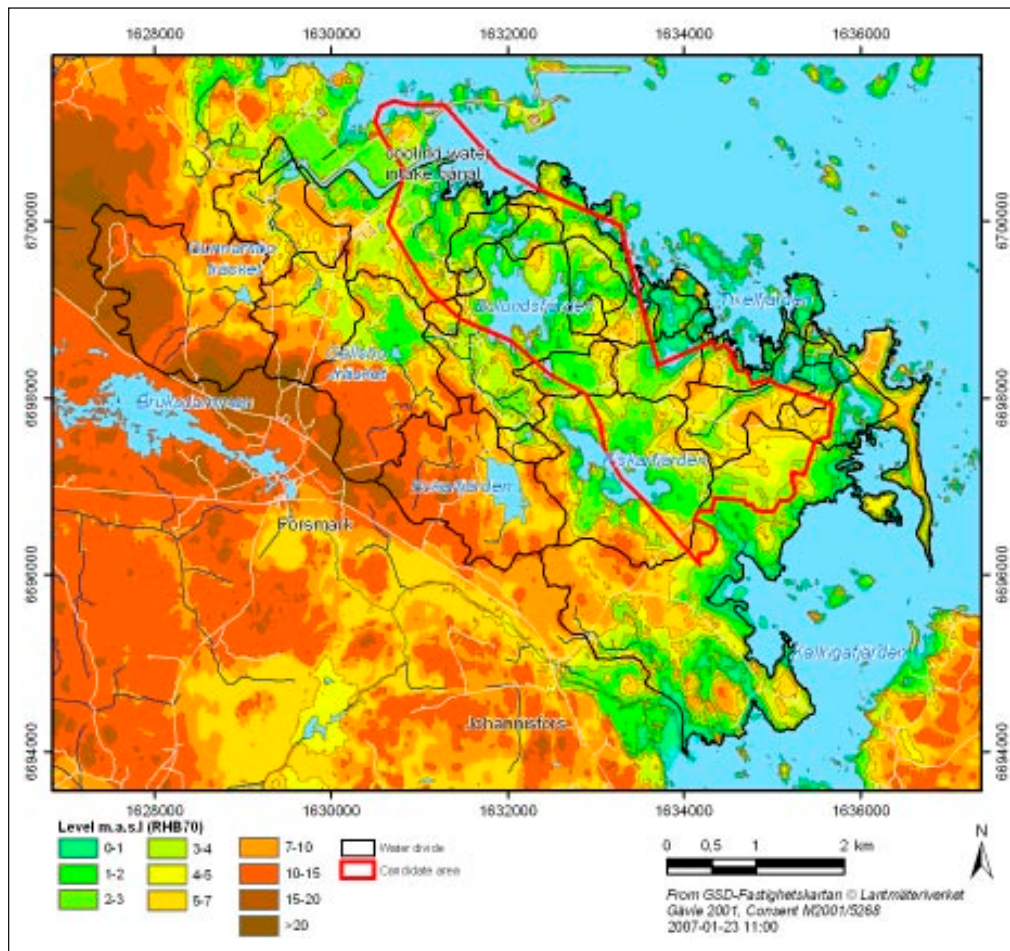


Figure 2-10. Topographical map of the candidate area and its surroundings, and surface water divides.

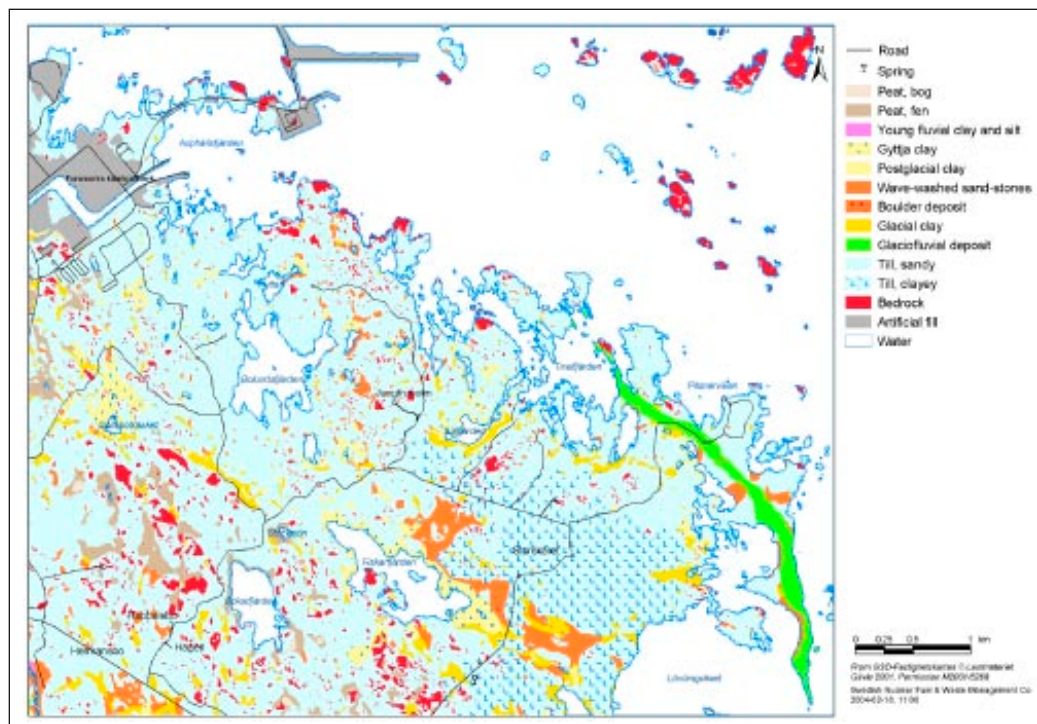


Figure 2-11. Detailed map of Quaternary deposits /Sohlenius et al. 2004/.



Rock outcrops are frequent, but constitute only approximately 5% of the area. Wave-washed sand and gravel, clay, gyttja clay and peat cover 3–4% each. The only glaciofluvial deposit, the Börstilåsen esker, runs in a north-south direction along the coast (cf. the “green belt” in Figure 2-11). The Quaternary deposits are shallow, with an average depth of c. 5 m for the whole Forsmark area /Nyman et al. 2007/. The greatest depth to rock, recorded in a drilling south-east of Lake Fiskarfjärden, is 16 m.

From generic and site-specific data it is known that in the uppermost part of the till, the hydraulic conductivity and the specific yield are much higher than further down in the profile /Lind and Lundin 1990, Lundin et al. 2004/. This is mainly due to soil forming processes, probably with ground frost as the single most important process, resulting in higher porosity and formation of macropores. However, wave washing also implies that the till at exposed locations is coarser at the soil surface, and at some locations coarse out-washed material has been deposited. Based on the site-specific data, the saturated hydraulic conductivity in the uppermost part of the till can be estimated to  $10^{-5}$ – $10^{-4}$  m/s and the specific yield to between 10% and 20%, with the higher values close to the surface. The total porosity can typically be estimated to 30–40%, mainly depending on depth. Below the depth interval strongly influenced by the soil forming processes, the hydraulic conductivity and the porosity of the till are considerably lower. The results from the slug tests indicate a higher hydraulic conductivity in the Quaternary deposit/rock contact zone than in the till itself, with geometric mean values of  $1.3 \cdot 10^{-5}$  m/s and  $1.2 \cdot 10^{-6}$  m/s, respectively (not including wells installed below open water) /Johansson et al. 2005/. The total porosity and the specific yield of the till below the upper one metre can typically be estimated to 20–30% and 2–5%, respectively.

The stratigraphy of bottom sediments in lakes has been investigated, and typical profiles have been identified for some of the lakes /Hedenström 2003, 2004, Vikström 2005/. Typically, the sediment stratigraphy from down and up is glacial and/or postglacial clay, sand and gravel, and nested layers of gyttja in different fractions. The clay layer is missing in major parts of the area below Lake Bolundsfjärden.

The rock hydrogeological conditions in Forsmark reveal a significant hydraulic anisotropy within a tectonic lens, which covers the body of the candidate area. The upper c. 150 m of rock contains high-transmissive horizontal fractures/sheet joints. These fractures/sheet joints occur at different elevations in the percussion-drilled boreholes /Gentzschein et al. 2006/, but are found to interconnect hydraulically across large distances (1–2 km) /Gokall-Norman et al. 2005, Gokall-Norman and Ludvigson 2006/. The horizontal fractures/sheet joints have transmissivities in the range c.  $1 \cdot 10^{-6}$ – $1 \cdot 10^{-3}$  m<sup>2</sup>/s (hydraulic conductivity c.  $1 \cdot 10^{-6}$ – $1 \cdot 10^{-3}$  m/s) /Gentzschein et al. 2006/.

The rock in between the horizontal fractures/sheet joints, however, is considerably less conductive (hydraulic conductivity c.  $1 \cdot 10^{-11}$ – $1 \cdot 10^{-8}$  m/s), except where it is intersected by transmissive steeply-dipping or gently-dipping deformation zones. Below the uppermost c. 150 m of rock, the high-transmissive horizontal fractures/sheet joints vanish totally, the conductive fracture frequency becomes very low, and the few fractures present are fairly low-transmissive (fracture transmissivity c.  $1 \cdot 10^{-10}$ – $1 \cdot 10^{-7}$  m<sup>2</sup>/s) /SKB 2006/. In some of the 1,000 m deep cored boreholes, there are almost no flowing fractures observed below c. 200 m depth, which is exceptional in a national perspective.

### 2.2.2 Groundwater recharge

Direct recharge from rainfall/snowmelt is the dominant source of groundwater recharge. The 30-year average annual precipitation at the site (corrected for measurement losses, mainly wind losses) has been calculated to 559 mm, based on data from surrounding SMHI stations /SMHI 2005/. The mean annual precipitation for the period Oct. 2004–Sep. 2006 was 519 mm (552 and 487 mm for each of the two years, respectively). The potential evapotranspiration,

calculated for the same period by the Penman equation according to /Eriksson 1981/, is 517 mm (507 and 527 mm, respectively). The annual variation in rainfall/snowmelt and potential evapotranspiration for the whole period with site measurements is shown in Figure 2-12.

The annual variation in rainfall/snowmelt and evapotranspiration typically results in large flows in the brooks during late autumn and during spring following snowmelt, see Figure 2-13. The mean annual discharge, for the same period as above, is 147 mm (139 and 154 mm for each of the two years, respectively). Subtracting this value from the precipitation for the same period, leaves 373 mm for actual evapotranspiration and storage changes. A rough estimate of the changes of the surface water and subsurface storages during the period indicates a decrease in storage of c. 25 mm. This means that the mean annual evapotranspiration was c. 385 mm, i.e. c. 130 mm less than the potential evapotranspiration.

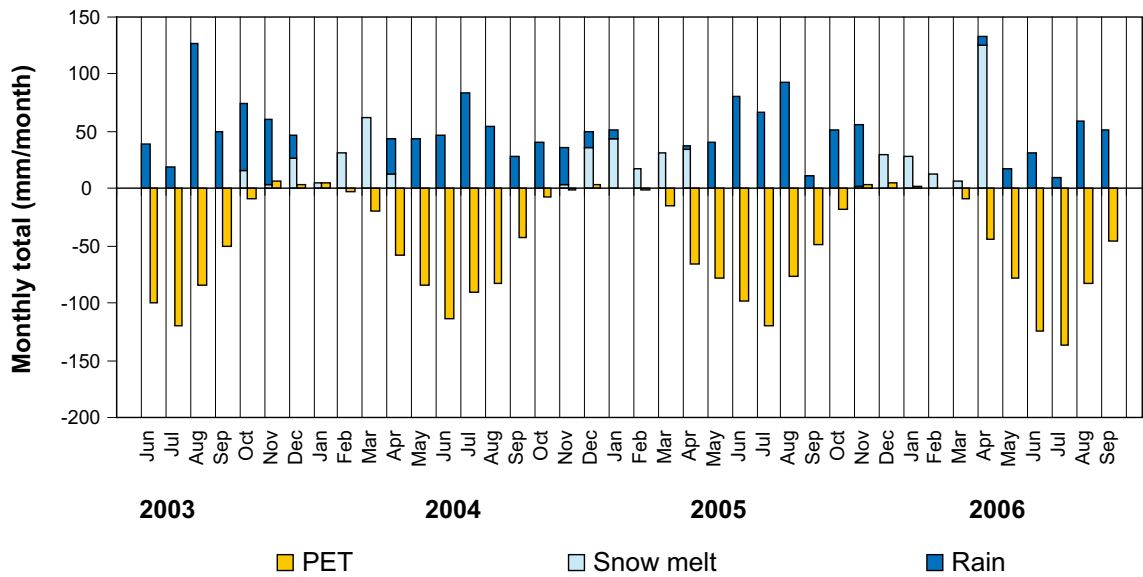


**Figure 2-12.** Annual variations in rainfall/snowmelt and potential evapotranspiration (PET).

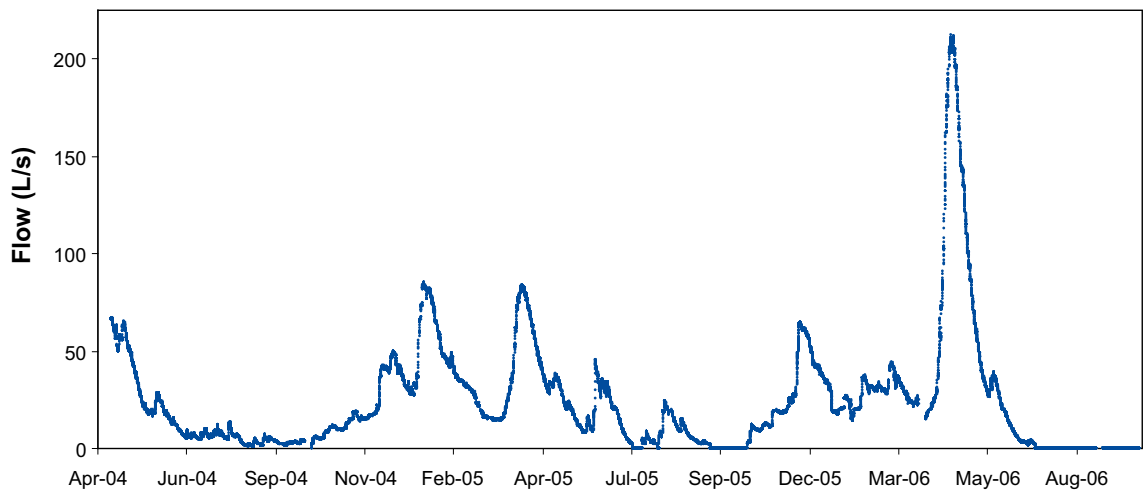


**Figure 2-13.** Surface water discharge in Bolundsbacken just upstream of the inflow to Lake Bolundsfjärden, from the start of the measurements up to data freeze 2.2 (Sep. 30, 2006). The catchment area is 5.6 km<sup>2</sup>.

### 2.2.3 Groundwater levels

There is a strong correlation between the groundwater levels and the discharge of the brooks, i.e. the same seasonal pattern can be seen in the groundwater levels as in the surface discharge, see Figure 2-14. Generally, the groundwater levels are very shallow in the area, see Figure 2-15. Also in recharge areas the groundwater levels are close to the ground surface during long periods of the year.

The decline of the groundwater levels in the Quaternary deposits during dry periods is enhanced by direct and indirect water uptake by vegetation from the groundwater zone. There have been observations of diurnal variations of the groundwater level due to variation in evapotranspiration /Johansson et al. 2005, Juston et al. 2007/. The water uptake by vegetation also causes decline of groundwater levels in the vicinity of the lakes during dry summer periods, such that groundwater levels sometimes are below lake water levels. This decline changes the lakes to potential recharge areas, see Figure 2-16.



**Figure 2-14.** Groundwater levels in two groundwater monitoring wells in typical recharge and discharge areas, SFM0019 and SFM0014, respectively.

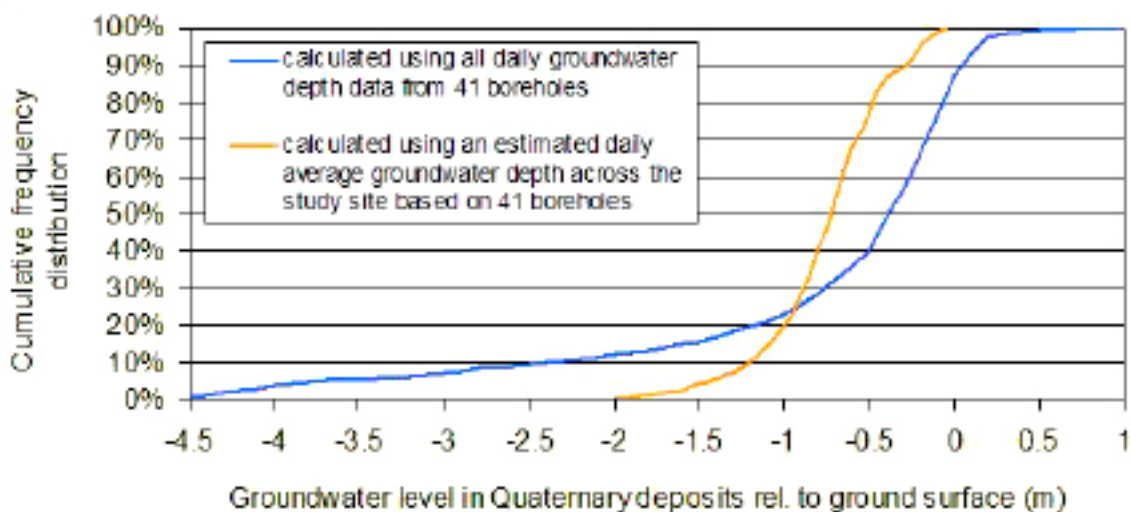


**Figure 2-15.** Groundwater levels expressed as depth below ground in 41 monitoring wells in Quaternary deposits.

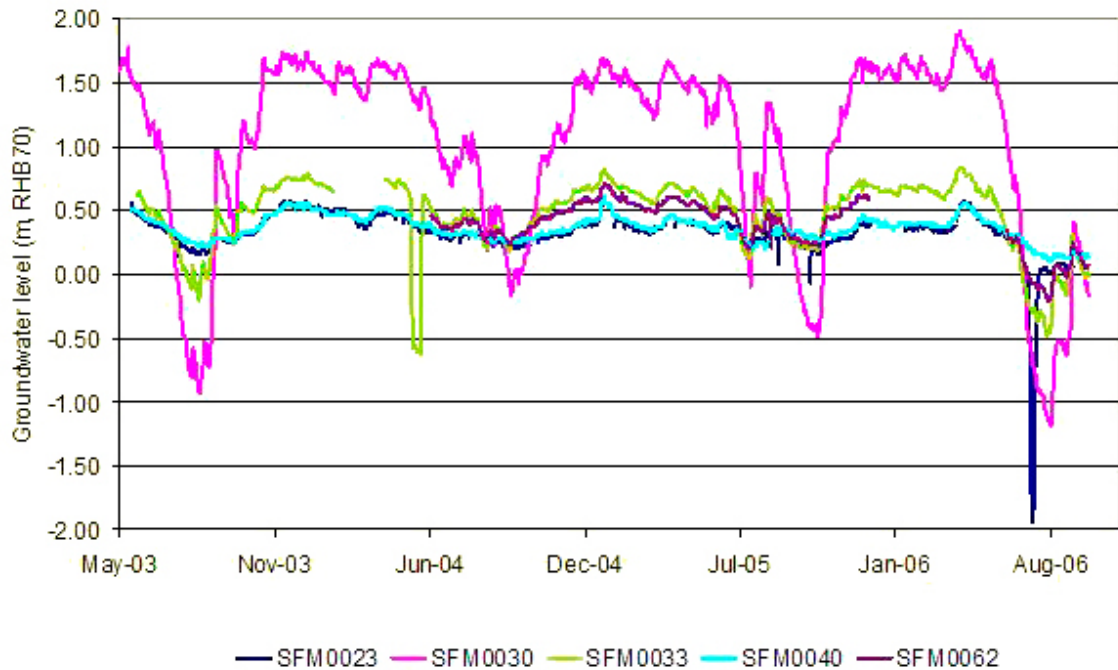


**Figure 2-16.** Water level in, below and close to Lake Bolundsfjärden. SFM0040 = lake water level, SFM0023 = groundwater level in till below the middle of the lake, SFM0062 = groundwater level in till below the lake (close to the shore), SFM0033 = groundwater level in till c. 50 m from the lake, SFM0030 = groundwater level in till c. 100 m from the lake.

An interesting observation is that within the tectonic lens, the groundwater level in the rock is low and relatively flat. The average groundwater level (point water head) is between 0 and 1.1 m (elevation system RHB70) in all percussion-drilled boreholes, except for two almost dry sections, see Figures 2-17 and 2-18.

In terms of spatial variability, groundwater levels in the Quaternary deposits are quite different to the levels in the rock. In contrast to groundwater levels in rock, the levels in the Quaternary deposits are strongly correlated to the ground surface elevation, see Figures 2-19 and 2-20.

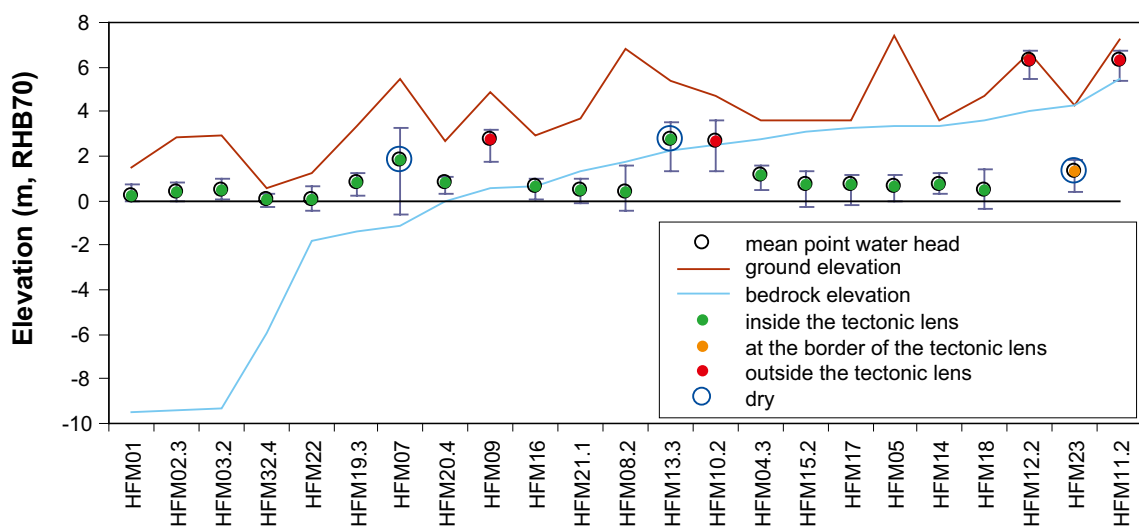


**Figure 2-17.** Mean groundwater levels (point water heads) in percussion-drilled boreholes. With exception for two “dry” sections, the ground water level within the tectonic lens varies very little, from 0.0 to 1.14 m (elevation system RHB70). Note that only wells with more than 150 days of level data are included.

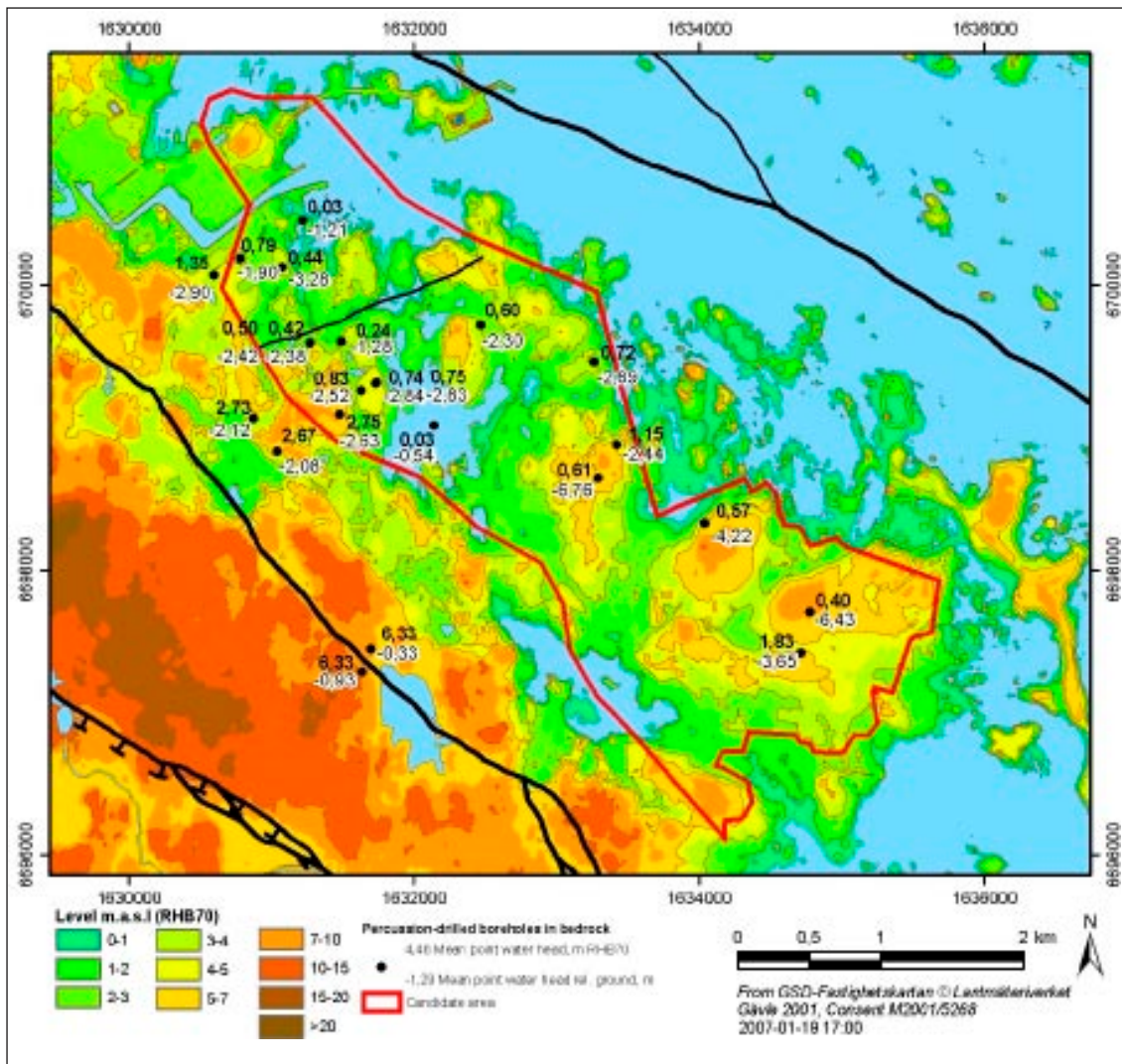


Figure 2-18. Mean groundwater levels in percussion-drilled boreholes (point water heads in the uppermost sections of the boreholes) expressed as elevation (elevation system RHB70) and relative to ground surface.

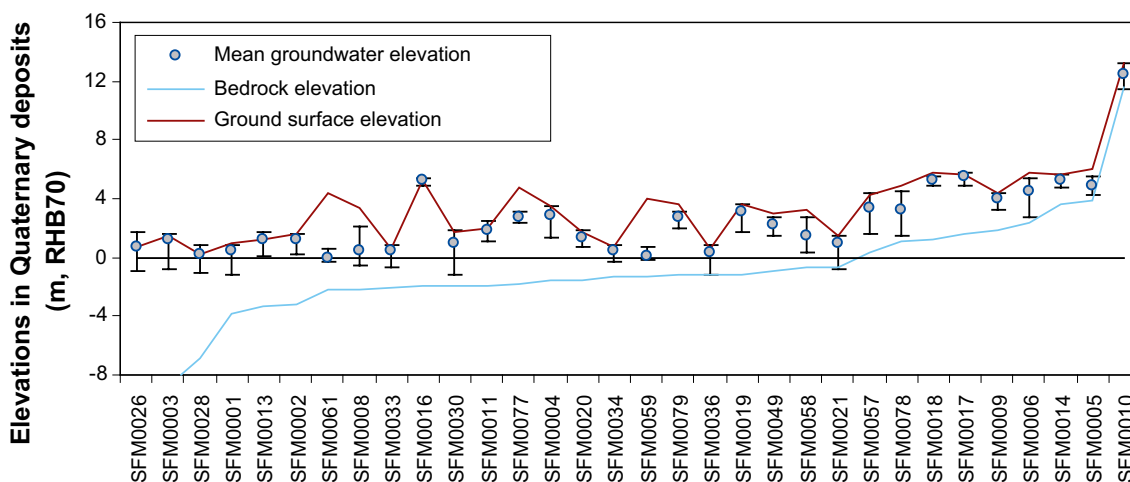
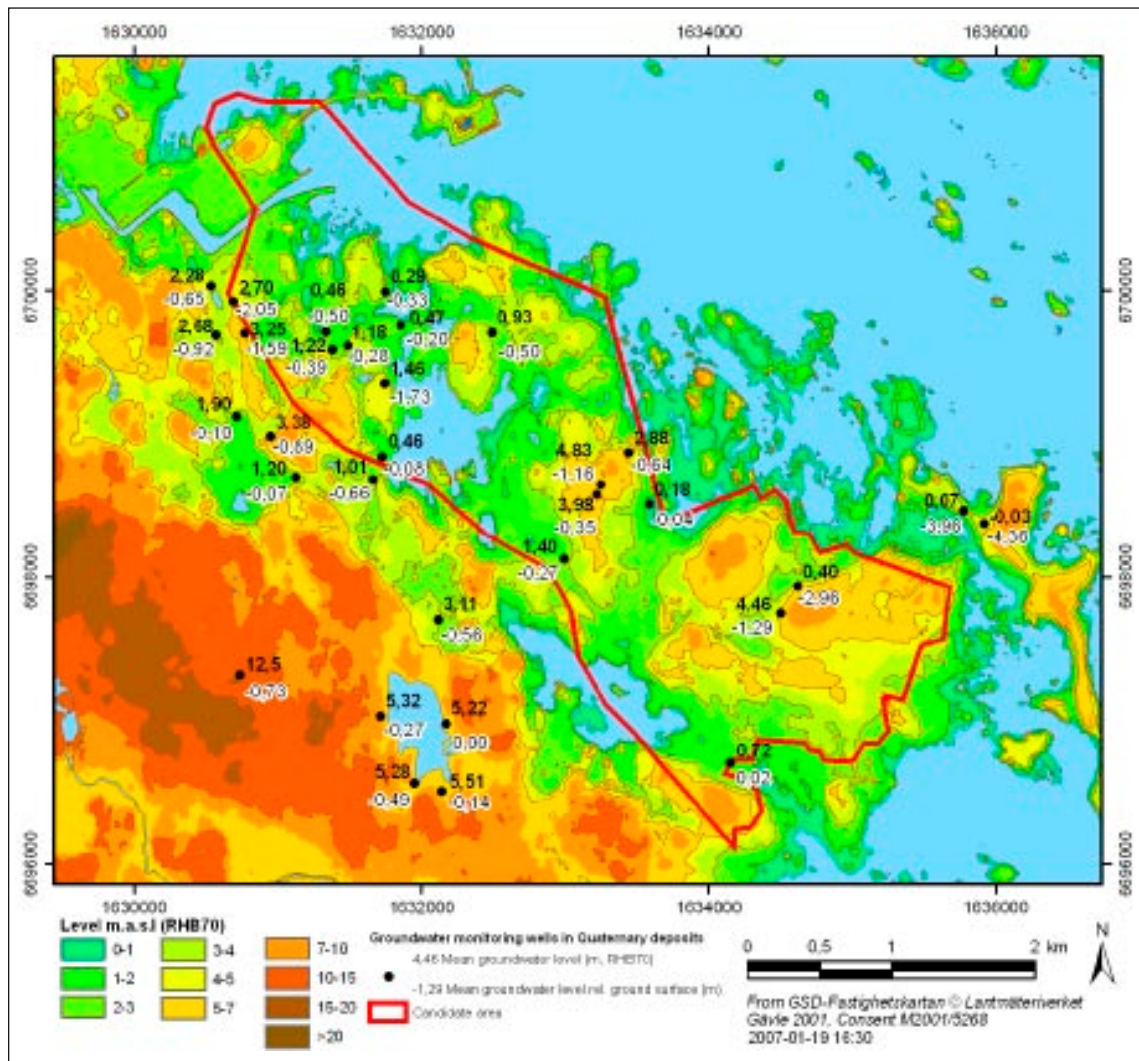


Figure 2-19. Mean groundwater levels in Quaternary deposits (only wells with more than 150 days of level data are included). The close correlation of groundwater levels and ground levels is clear. The only exceptions are SFM0059 and SFM0061, which are placed in a glaciofluvial deposit, Börstilåsen.



**Figure 2-20.** Mean groundwater levels in Quaternary deposits, expressed as elevation (m) in elevation system RHB70, and relative to ground surface.

Another interesting observation is that at locations where groundwater levels are measured both in Quaternary deposits and rock, the groundwater level in the rock is often considerably lower than in the overburden, see Figures 2-21 and 2-22. This feature is most pronounced within the tectonic lens.

In the example shown in Figure 2-22, the groundwater levels in the Quaternary deposits are at all times well above the point water heads in the rock. This seems to be typical when the wells in the Quaternary deposits are situated in typical recharge areas. When there are nearby wells in Quaternary deposits in typical discharge areas, these levels can be below the point water heads in the rock, see Figure 2-23 for an example from Core drill site 4 (located outside the tectonic lens). However, within the tectonic lens there are no examples of cases of groundwater levels in Quaternary deposits being constantly below point water heads in rock, considering nearby wells/boreholes. However, such conditions can prevail during dry summer periods; see Figure 2-24 for an example from Core drill site 6.

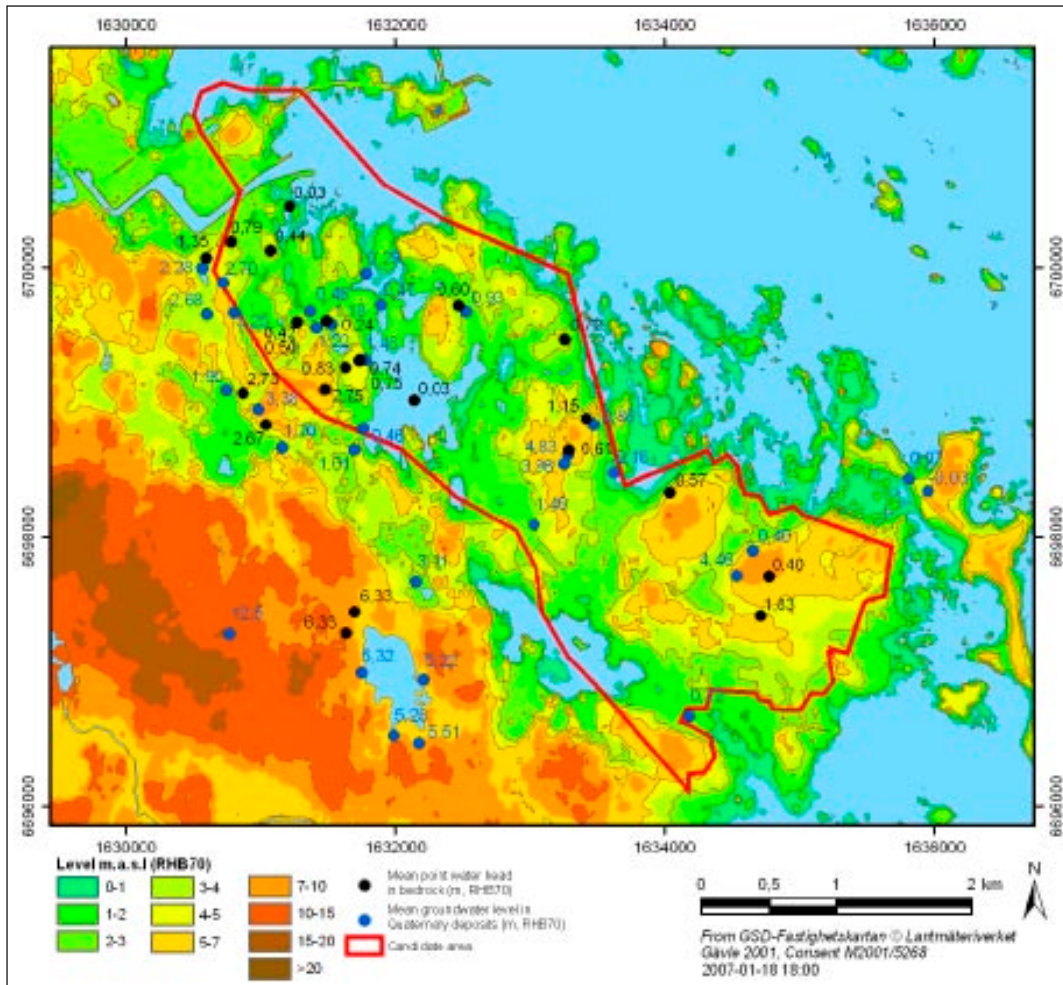


Figure 2-21. Mean groundwater levels in Quaternary deposits and point water heads (elevation system RHB70) in the uppermost sections of percussion-drilled boreholes in rock.

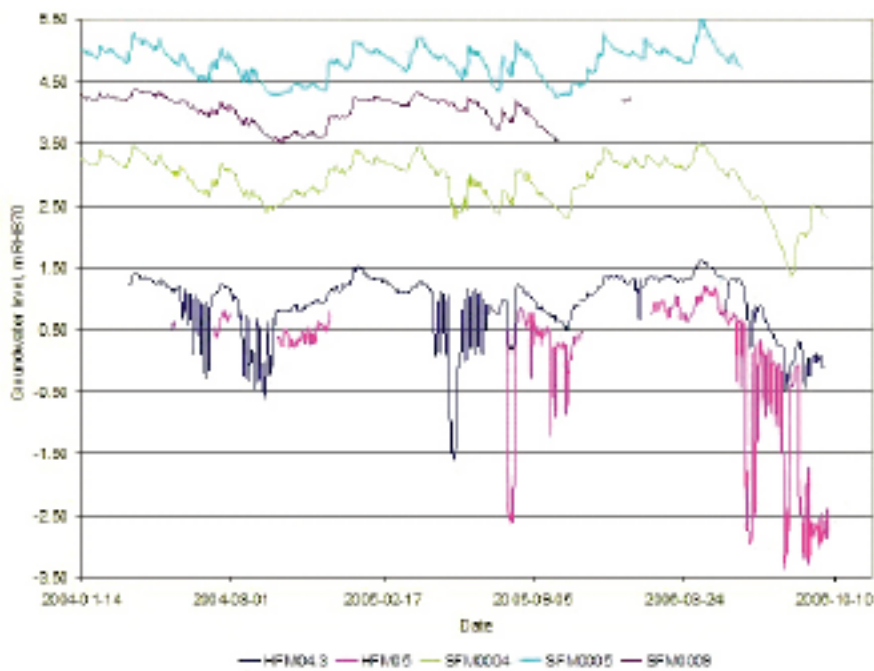
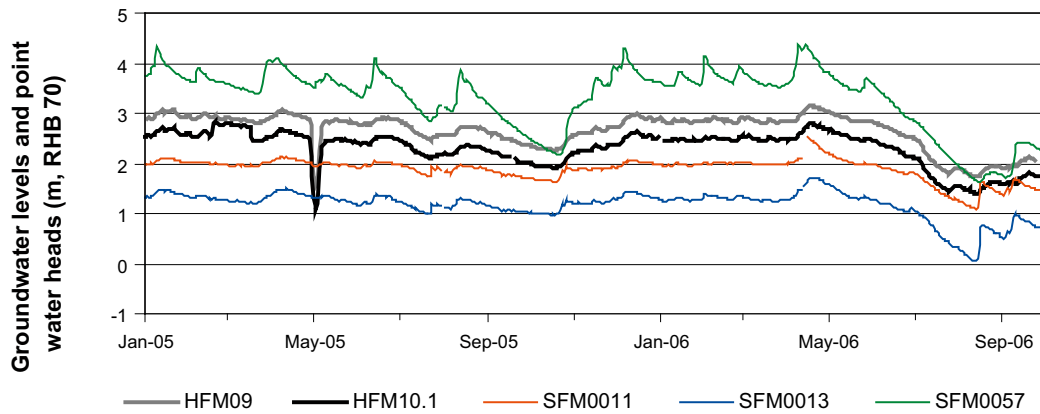
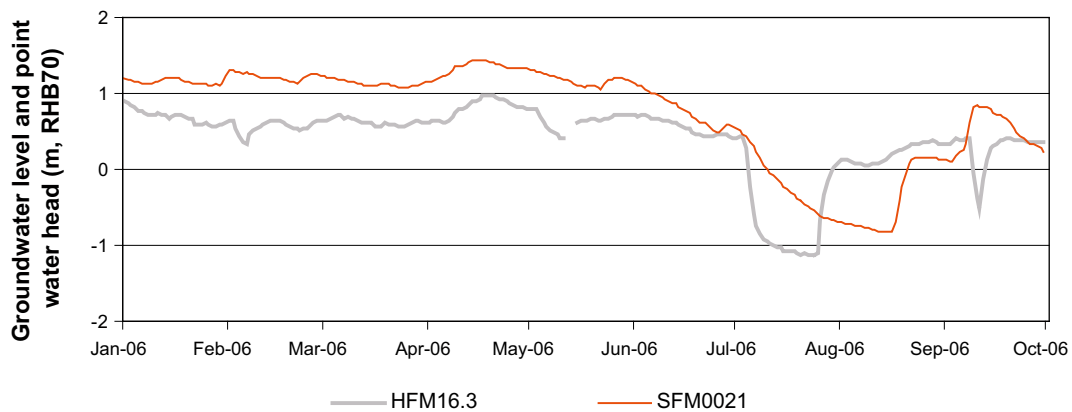


Figure 2-22. Groundwater levels in rock (HFM) and in Quaternary deposits (SFM) in wells in close proximity at Core drill site 2. Disturbances from pumping in well HFM05 can be seen also in well HFM04.



**Figure 2-23.** Groundwater levels in rock (HFM) and in Quaternary deposits (SFM) in wells/boreholes in close proximity at Core drill site 4. SFM0057 is considered to be located in a recharge area, whereas SFM0011 and SFM0013 are located in typical discharge areas.



**Figure 2-24.** Groundwater levels in rock (HFM) and in Quaternary deposits (SFM) in wells/boreholes in close proximity at Core drill site 6.

The situation with a higher groundwater level in Quaternary deposits than in the rock prevails even in the middle of Bolundsfjärden, see Figure 2-25. As shown in this figure, the lake water level and the groundwater level in the till below the lake are continuously above the point water heads in the percussion-drilled borehole. The salinity of the groundwater is almost the same in the till and in the four sections in the rock borehole, which means that the differences in levels can not be explained by differences in water density. The salinity of the groundwater is somewhat higher than the salinity of present sea water, with electrical conductivities of c. 1,200 compared to c. 900 mS/m in the sea. The salinity of the lake water may vary due to intrusion of sea water; for the presented time period, the electrical conductivity was c. 70 mS/m.

## 2.2.4 Implications of site characteristics for recharge-discharge area patterns

Ample access to water from precipitation for groundwater recharge during large parts of the year, a flat terrain and a relatively low hydraulic conductivity result in very shallow groundwater levels in Quaternary deposits in the Forsmark area (see Figures 2-14 and 2-15). This situation requires a clear definition of groundwater recharge. A common definition is “the process by which water is added to the zone of saturation” (cf. Section 2.1.1). However, for the conditions in Forsmark, there is a large difference between gross and net recharge. The diurnal groundwater level fluctuations and the conditions in the vicinity of the lakes (see Figure 2-16 for an example) clearly illustrate the influence of evapotranspiration on the groundwater zone



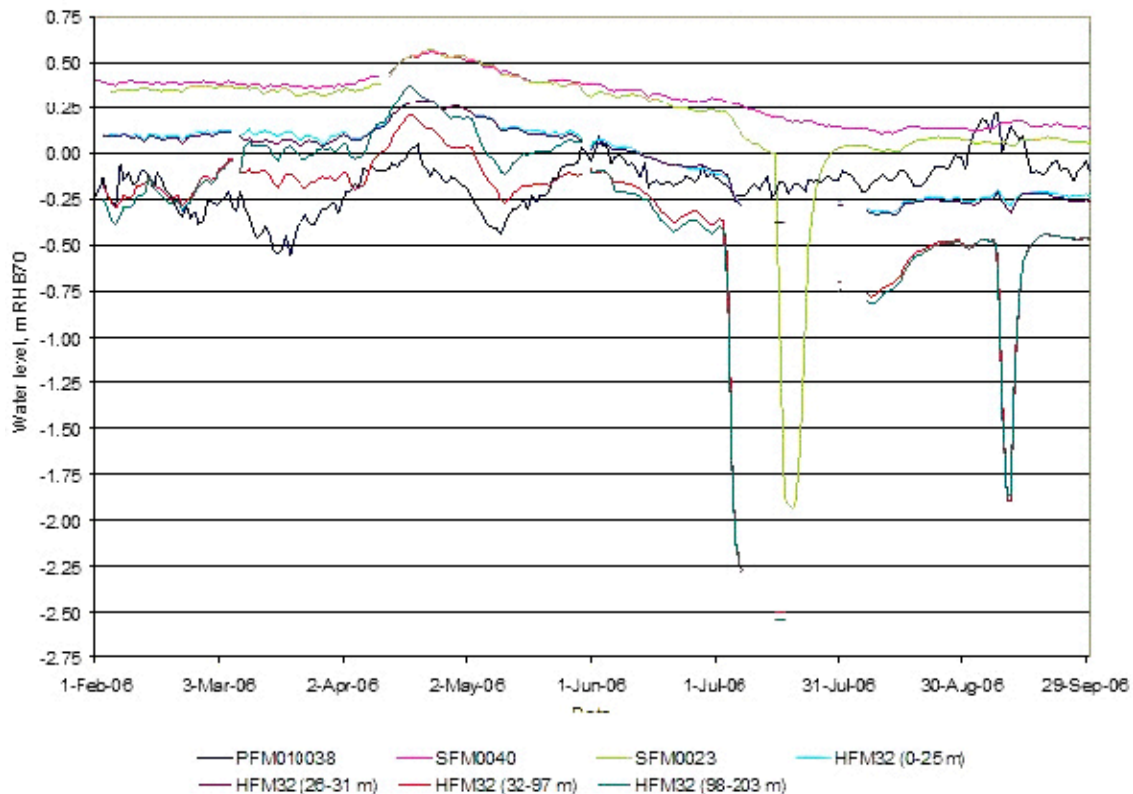


**Figure 2-25.** Comparison of the sea level (PFM010038), lake level (SFM0040), the groundwater level in the till below the lake (SFM0023) and at four different depths in the rock.

during dry periods. Furthermore, it can be useful to use the terms groundwater recharge and groundwater discharge for the groundwater flow from one hydrogeological unit (flow domain) to another.

In Forsmark, precipitation is the dominant source of groundwater recharge. However, as shown in Figure 2-16, during summer the lakes in the area may act as recharge sources to the till in the immediate vicinity of the lakes. Due to the low vertical hydraulic conductivity of the bottom sediments, the resulting water fluxes can be assumed to be small. Also the Baltic Sea can potentially act as a source for groundwater recharge, especially during periods of high sea water levels. However, there is a weak correlation between the sea water level on the one hand, and the groundwater levels in Quaternary deposits and point water heads in rock on the other /Juston et al. 2007/.

The low regional topographical gradient and the small-scale topography combined with the strongly decreasing hydraulic conductivities with depth, both in the Quaternary deposits and in the rock, promote the formation of local groundwater flow systems. Such systems are in accordance with the principles illustrated in Figures 2-4 and 2-5; the spatial scales in these exemplifying figures, including the regional slope of the groundwater level and its local-scale amplitude, are comparable with those of the Forsmark candidate area.

Generally higher groundwater levels in Quaternary deposits than point water heads in rock in large parts of the area (Figures 2-22 to 2-25) make these parts potential recharge areas. However, the decreasing hydraulic conductivity with depth in the Quaternary deposits, as well as a probable anisotropy with lower vertical hydraulic conductivities, prevent abundant downward flow. This results in a close correlation between the groundwater levels in the Quaternary deposits and the topography (Figures 2-20 and 2-21), steeper groundwater level gradients in the Quaternary deposits, and the formation of local, shallow groundwater flow systems in the Quaternary deposits.

The low and flat groundwater level (point water heads) in rock within the tectonic lens (Figures 2-17 and 2-18) is an indication of a well-connected hydraulic system of relatively high hydraulic conductivity /SKB 2006/. This conclusion is promoted by results from pumping tests showing distinct responses over large distances /Gokall-Norman et al. 2005, Gokall-Norman and Ludvigson 2006/. The hydraulic conductivity of the well-connected system of horizontal and sub-horizontal fractures in the upper c. 150 m of the rock is large enough to transmit local recharge as well as possible upward flow from greater depth at only a small gradient, which can be compared to the effect of a high-conductive fracture zone as illustrated in Figure 2-6. A considerable anisotropy with a much higher horizontal than vertical hydraulic conductivity in the upper part of the rock, confirmed by site specific data /Gentzschein et al. 2006/, promotes the formation of shallow but long flow paths in the upper part c. 150 m of the rock.

Obviously, the presence of highly transmissive structures in the uppermost part of the rock is potentially of importance for the groundwater flow pattern within the target volume. A tentative hydrogeological description of the rock within this volume is the presence of a “hydraulic cage” /SKB 2006/. According to this tentative description, the sub-horizontal fractures that occur in the uppermost part of the rock above the hydraulic cage short circuit the recharge from above and constitutes the real discharge elevation for deeper groundwater flows (cf. Figure 2-6).

A situation with local, shallow flow systems overlaying intermediate deeper systems, as illustrated in Figures 2-4 to 2-6, implies that stagnation points exist, surrounded by areas of more or less stagnant water. The situation in the middle of Lake Bolundsfjärden, with a higher water level in the lake and in the till below the lake compared to the underlying rock (Figure 2-26), indicates that no groundwater from depth can discharge into this part of the lake. Figure 2-26 also show that the point water heads in the rock is above the sea level for approximately half of the available time series. The flat groundwater level in the upper part of the rock within the tectonic lens, with average levels varying between 0 and 1 m (elevation system RHB70) indicates, beside a good hydraulic connectivity, that the absolute groundwater levels are determined by the sea level. However, the temporal variation of point water heads are mainly influenced by direct or indirect groundwater recharge from precipitation, and only very weakly correlated to variations in sea water level. This indicates that the hydraulic contact between the groundwater system observed in the percussion-drilled boreholes and the sea is not through highly transmissive fractures outcropping below the sea, but rather indirect via low-transmissive fractures or sediments. Furthermore, the available data indicate that due to the temporal variations of sea water and groundwater levels, the sea can act both as a potential recharge and discharge area, depending on the varying difference between the two levels.

The permeability and storage characteristics of the till imply that below a depth of approximately 0.5 metre, very little water needs to be added to raise the groundwater table. For instance, a groundwater recharge of 10 mm would result in a groundwater level rise of c. 20 to 50 cm. During periods of ample groundwater recharge, the groundwater level, also in most recharge areas, reaches the uppermost part of the soil profile (Figure 2-14). The shallow, highly dynamic groundwater levels in the Quaternary deposits cause a temporal variation in the extensions of recharge and discharge areas of the local, shallow flow systems, which can be compared to the modelling results presented in Figure 2-8. However, not all discharge areas are necessarily saturated up to the ground surface, due to water flow in the upper, most permeable part of the soil profile. In unsaturated discharge areas, the soil water deficit is usually very small, meaning that groundwater levels respond quickly to rainfall and snowmelt and contribute to runoff generation /Grip and Rodhe 1985/. So-called saturated overland flow appears in discharge areas where the groundwater level reaches the ground surface.

Another example of transient recharge-discharge area patterns is the situation where the lakes turns into potential recharge areas during dry summer periods; see Figure 2-16 for an example from Lake Bolundsfjärden. The actual recharge during such periods depends on the hydraulic contact between the lakes and the groundwater zone, i.e. the hydraulic conductivity of the bottom sediments. Drillings in the lake sediments show relatively thick sediments, at most locations consisting of gyttja and thin layers of clay. In Lake Bolundsfjärden, the clay

layer appears to be missing under large parts of the lake. However, pumping tests at Lake Bolundsfjärden indicate low-permeable bottom sediments /Werner and Lundholm 2004, Gokall-Norman et al. 2005, Gokall-Norman and Ludvigson 2006/. Further, site-specific data indicate that the phenomenon of reversed hydraulic gradients during dry summer conditions also appears in the vicinity of major wetlands. The wetlands can either be in direct contact with the groundwater zone, or act as separate hydrological systems, in case they are underlain by low-permeable bottom materials.

A third observation of transient behaviour is that at some locations with groundwater level data both from Quaternary deposits and rock, the mostly downward gradient is reversed during dry summer periods; see Figure 2-24 for an example. The influence of water uptake by vegetation, either indirect or direct from groundwater in the Quaternary deposits, implies a gradient that enables recharge from the rock to the Quaternary deposits.

### 3 Presentation of RD classification methods

This chapter presents some methods for identification of near-surface groundwater recharge and discharge areas, applied to the Forsmark area. Sections 3.1 and 3.3 demonstrate the use of topographical and hydrological-hydrogeological modelling, respectively, whereas Section 3.2 shows the use of maps for RD classifications. Sections 3.4 and 3.5 describe classification of groundwater monitoring well locations, using a physical-hydrological field method and a method based on hydrochemical data, respectively.

#### 3.1 Topographical RD model

/Brydsten 2006/ presents a topographical modelling study, in which the digital elevation model (DEM; spatial resolution 10 m) of the Forsmark area is used as the only input data for identification of recharge and discharge areas.

In the model evaluation step, potential recharge and discharge areas are identified within a sub area in Forsmark (see Figure 3-1). Using the Real Estate Map (in Swedish: Fastighetskartan) and a detailed orienteering map, /Brydsten 2006/ classifies lakes, watercourses (brooks) and

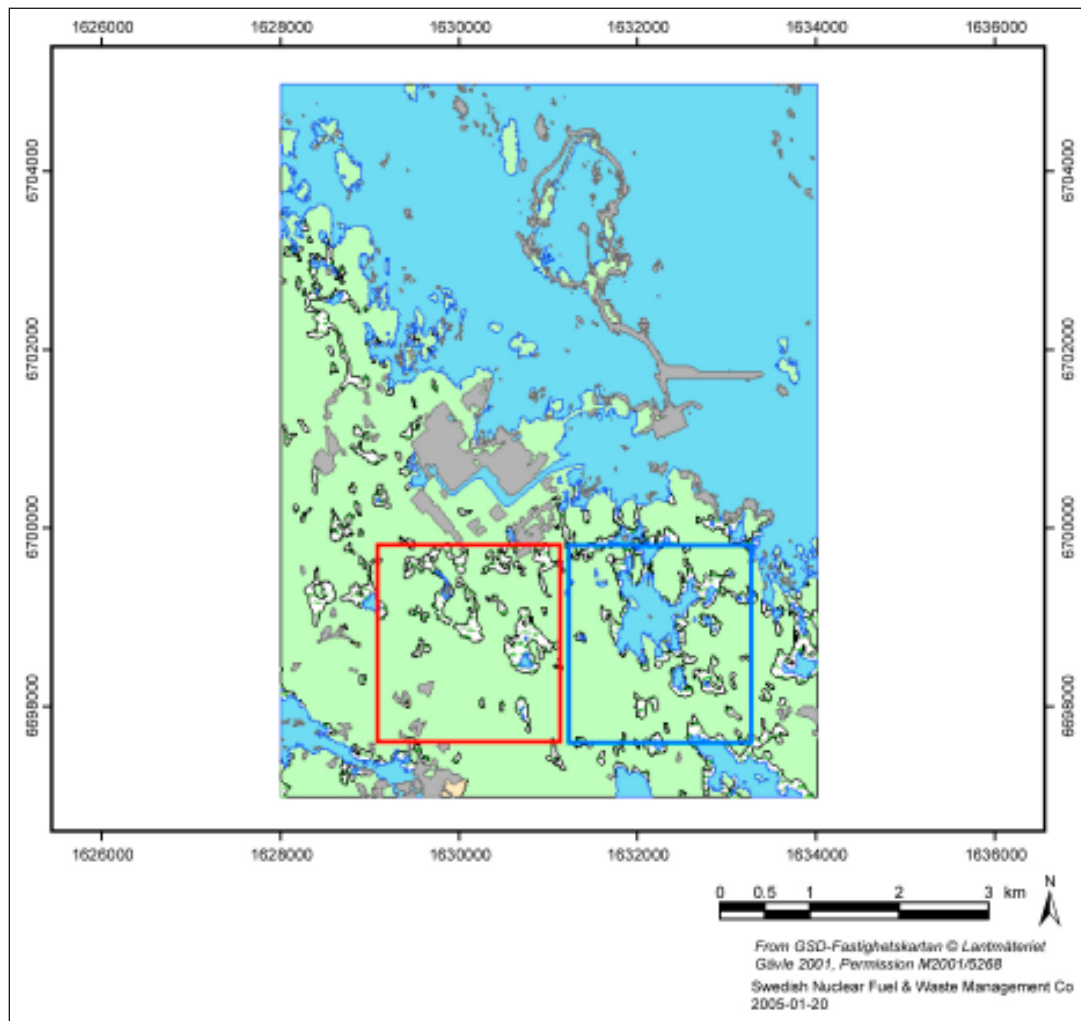


**Figure 3-1.** Extension of the model evaluation/calibration area (red frame) and the model validation area (blue frame) for the topographical model of Forsmark /Brydsten 2006/.

wetlands as potential discharge areas; the topographical RD model assumes that discharge occurs at lakes, watercourses and wetlands, but nowhere else. The remaining areas are classified as potential recharge areas. (The orienteering map of Forsmark, map number C 293:1, is in scale 1:10,000 and is produced by Forsmarks IF. The Real Estate Map has SKB GIS database references XXX\_XX\_XXX\_3150, \_3322, \_3381, \_3382, \_3421, \_3423, \_3442, \_3443, and \_3460-3485; XXX\_XX\_XXX = LMV\_FM\_FJA).

In the model calibration step, recharge and discharge areas are identified in five classes (see below) within the same sub area as in the model evaluation step:

- “Most likely recharge areas” (MLR) are identified by means of geomorphological classification using the Landserf software /Wood 1996/. The geomorphometrical classification is based on the first and second order differentials of the DEM, by use of which a number of curvature parameters are calculated. These parameters are subsequently used to classify six geomorphological features: peak, ridge, pass, plane, channel, and pit. Peaks and ridges are assumed to represent MLR. The curvature parameters are calculated for each DEM cell in the calibration area, where the parameter values depend on the size of the rectangular N by N window (N denotes the number of DEM grid cells), centred at each DEM grid cell, and the slope tolerance value. Multiple runs were made using different sets of window sizes and slope tolerance values, aiming to find the parameter combination for which the smallest number of DEM cells that are classified as MLR coincide with potential discharge areas (actual lakes, watercourses and wetlands). It was found that for N = 11 (i.e. window size 110 m by 110 m) and for a slope tolerance of 4 degrees, 3.3% of the ridges and peaks interfere with potential discharge areas. Due to the flat topography, the curvature values are extremely low in the Forsmark area, implying that even small errors in the DEM can lead to erroneous curvature values, and hence erroneous geomorphological classification /Johansson et al. 2005, Brydsten 2006/.
- “Most likely discharge areas” (MLD) are identified using the functions “Basin fill” (simulating lakes) and “Flow accumulation” in ArcGIS. The Flow accumulation function calculates the number of up-slope DEM grid cells and the accumulated flow, based on a flow direction grid. A high flow accumulation value indicates a high probability for a groundwater discharge area. Watercourses were identified as DEM grid cells with flow accumulation values > 200. One observation is that the Basin fill function produces somewhat larger and deeper lakes than the actual lakes in the area. The reason for this is that the DEM seldom contains the correct geographical location of the actual lake threshold, due to the regularly spaced DEM grid cells. The distance between the true location of the lake threshold and the nearest “DEM point” can be up to 5 metres in a 10-metre DEM.
- Having identified the MLR and MLD, approximately 50% of the calibration area remains unclassified. These remaining areas are classified using the topographical wetness index (TWI). This index characterizes the likelihood for soil saturation /Beven and Kirkby 1979/. High TWI values characterize geographical locations with high flow accumulation values and flat slopes; a high TWI-value indicates a probable discharge area. In the TWI distribution for the unclassified areas, /Brydsten 2006/ uses TWI values lower than the 3<sup>rd</sup> quartile (TWI < 4.9) of the TWI distribution to identify “Probable recharge areas” (PR). Moreover, TWI values higher than the 1<sup>st</sup> quartile (TWI > 7.2) identifies the “Probable discharge areas” (PD). Finally, TWI values in the intermediate range (4.9 < TWI < 7.2) remain unclassified, corresponding to 22% of the total model area.

The performance of the topographical RD classification model is tested in the model validation step, using a validation area located east of the calibration area. However, only the Real Estate Map is available for the validation area. 500 DEM cells were randomly chosen in potential discharge areas within the validation area, i.e. lakes, watercourses and wetlands. All other areas are considered as potential recharge areas. An independent validation was also tested considering recharge areas, using rock outcrops on the detailed map of Quaternary deposits /Sohlenius et al. 2004/ to identify potential recharge areas. For each of the two validation steps

(considering recharge areas and discharge areas, respectively), the model validation shows that the topographical model produces a deviating classification of only c. 1% of these areas.

The topographical classification methodology is summarized in Table 3-1 below.

**Table 3-1. Summary of classification methodology applied in the topographical model /Brydsten 2006/.**

Class	Method of classification	Indicator
Most likely recharge areas (MLR)	Geomorphological classification (Landserf 2.1 /Wood 1996/)	Peaks and ridges
Probable recharge areas (PR)	Topographical wetness index	TWI < 4.9
Undefined (U)	Topographical wetness index	$4.9 \leq TWI \leq 7.2$
Probable discharge areas (PD)	Topographical wetness index	$TWI > 7.2$
Most likely discharge areas (MLD)	ArcGIS (Basin fill function) Flow accumulation function (Hydrological modelling extension)	Lakes Brooks

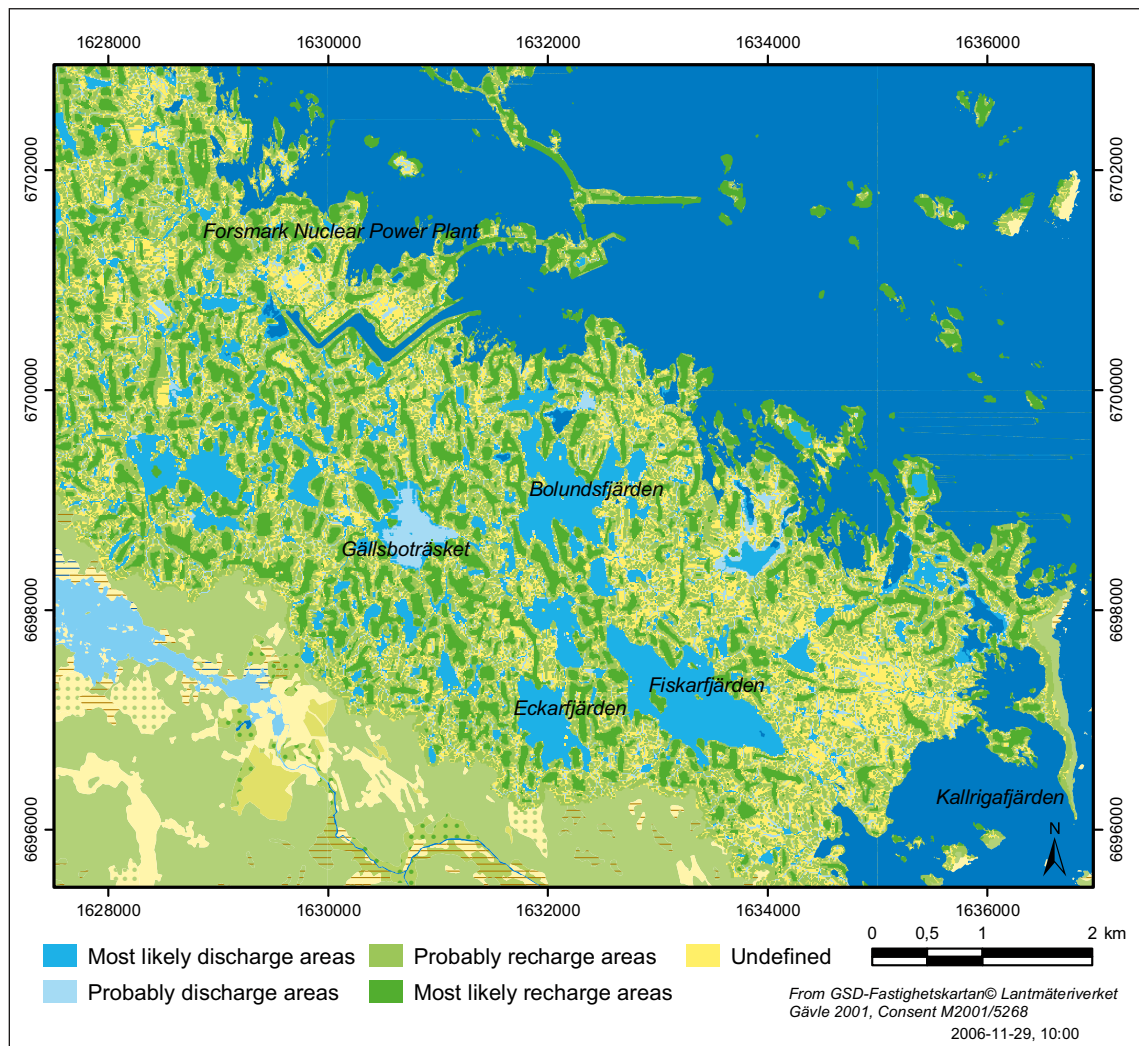


**Figure 3-2.** Topographical model of recharge and discharge areas in Forsmark. The area is divided into five classes: Most likely discharge areas, Probably discharge areas, Undefined, Probably recharge areas, and Most likely recharge areas.

## 3.2 Map overlays

Indicators such as vegetations types, soil types and types of Quaternary deposits (abbreviated QD) may potentially be used for characterization of the near-surface hydrological-hydrogeological conditions, including groundwater recharge-discharge patterns. As part of this study, a number of pre-existing digital maps (stored in SKB's GIS database) of the Forsmark area were used for RD classification. The following maps were used:

- Vegetation/land use map /Boresjö Bronge and Wester 2002, 2003/: The ground layer and the field layer were utilized in this study. SKB GIS database reference: SDEADM.SWP\_OST\_BIO\_1256.
- Map of QD /Sohlenius et al. 2004/. SKB GIS database reference: SDEADM.SGU\_FM\_GEO\_1935.
- Soil map /Lundin et al. 2004/. SKB GIS database reference: SDEADM.SLU\_FM\_GEO\_1901.

One reason for choosing these maps/layers as illustrative examples, is that they represent information that is relatively easily obtained from “normally” existing maps and/or in the field. As shown in Tables 3-2 and 3-3, each RD class in each map contains both recharge and discharge areas. Hence, RD maps produced by the types of background maps considered here will always contain inconsistencies, irrespective of the RD classification approach. The objectives here are therefore simply to illustrate the principles and to check whether the combination of several independently RD classified maps may provide a reasonable final RD map of the Forsmark area.

In order to obtain a basis for the RD classification, the groundwater discharge areas identified using the topographical RD model (Section 3.1) are in Tables 3-2 and 3-3 compared to the ground layer in the vegetation/land use map (Table 3-2) and the QD map (Table 3-3). Using the “Union” function in ArcGIS, all areas classified as MLD (Most likely discharge areas) according to the topographical RD model were combined with these two background maps. The result is a number of polygons for each map combination. The areas of these polygons quantify the distributions of ground layer vegetation types and QD types in areas classified as MLD, according to the topographical RD model. Simple RD classifications were also made of the remaining background maps (the soil map, and the field layer of the vegetation/land use map), see Tables 3-4 to 3-6.

**Table 3-2. Comparison between ground layer vegetation types in MLD areas and in the whole map area, classified using the topographical RD model. R = recharge, D = discharge, U = undefined.**

Ground layer type	MLD areas (%)	Whole map area (%)	Interpreted RD class
Not peatland – other (wetland)	10.9	4.2	D
Not peatland – moss type (wetland)	1.2	0.9	D
Moss land – forest	35.2	71.5	R
Moss land (pasture and meadow)	1.5	1.2	D
Arable land (other)	< 1	< 1	U
Peatland – other (wetland)	0.6	0.3	D
Peatland – white moss type (wetland)	17.0	7.0	D
Water	30.3	8.2	D
Buildings, sand or stone pits etc. (other)	2.1	5.8	U

**Table 3-3. Comparison between QD types in MLD areas and in the whole map area, classified using the topographical RD model. R = recharge, D = discharge, U = undefined.**

QD type	MLD areas (%)	Whole map area (%)	RD class
Organic soil	14.3	5.1	D
Clay	20.8	7.3	D
Sand	2.2	1.6	R
Gravel	< 1	< 1	R
Till	40.3	68.7	U
Rock-till	0	< 1	R
Rock	0.5	3.2	R
Artificial fill	1.6	2.4	U
Water	20.8	11.1	D

**Table 3-4. Simplified RD classification of the soil map. R = recharge, D = discharge, U = undefined.**

Soil type	RD class
HI (Histosol)	D
GL (Gleysol)	D
GL/CM (Gleysol/Cambisol)	D
RG/GL (Regosol/Gleysol)	R
RG/GLA-a (Regosol/Gleysol, arable land)	D
AR/GL (Arenosol/Gleysol)	D
RG (Regosol)	R
LP (Leptosol)	R
Water	D
No class	U

**Table 3-5. Simplified RD classification of the field layer of the vegetation map. R = recharge, D = discharge, U = undefined.**

Field layer type	RD class
No field layer – forest	U
No field layer – other land	U
Sedge-heath type	D
Sedge-reed type	D
Sedge-herb type	D
Dry heath type	R
Outside mapped area	U
Water	D
Wet herb type	D
Arable land	U
Herb-heath type	U
Herb type	D



**Table 3-6. Rules for RD classifications of map overlays. R = recharge, D = discharge, U = undefined. For the map overlays, an “extra” class (Unclassified) is assigned in areas where none of the other classes (R, D, or U) can be assigned according to the rules.**

RD combination for individual maps	RD classification for map overlays
RRR	R
DDD	D
RRD	Unclassified
DDR	Unclassified
RRU	R
DDU	D
RDU	Unclassified
RUU	R
DUU	D
UUU	Undefined

According to Table 3-2, the ground layer vegetation types Not peatland – other (wetland), Not peatland – moss type (wetland), Moss land (pasture and meadow), Peatland – other (wetland) and Water are overrepresented in the MLD areas, compared to the whole common area for the topographical RD map and the vegetation map. These vegetation types are therefore interpreted as discharge areas, whereas the others (except Moss land – forest, classified as recharge, R) are classified as undefined (U).

In Table 3-3, the QD types Organic soil, Clay and Water are overrepresented in the whole common map area. These QD types are therefore interpreted as discharge areas. Moreover, areas classified as rock-till and rock are underrepresented, why these areas are interpreted as recharge areas. The other classes on the QD map are classified as undefined.

Figures 3-3 and 3-4 show the map overlays, produced by overlay of the four considered background maps in two combinations: Figure 3-3 shows the overlay of the RD classified QD map, soil map, and ground layer of the vegetation/land use map, whereas Figure 3-4 shows the overlay of the RD classified QD map, soil map, and field layer of the vegetation/land use map. The adopted “rules” for the RD classifications for the map overlays are summarized in Table 3-6. These rules mean that a rather weak correlation is accepted between the RD classifications of the individual background maps for the map overlay classification. As an example, combination of an area classified as U (Undefined) in two background maps, and D in the third background map, yields D as the “combined” RD classification of that particular area.

There are obviously many limitations of a simple RD classification scheme, as the one used here. One drawback with the classification rules in Table 3-6 is that they may overestimate the extents of R and D areas in map overlays, compared to areas classified as U (Undefined). Moreover, a more advanced classification scheme would include the use of different weights to the background maps, e.g. that the vegetation/land use map could be given a larger weight compared to the QD map.

Most areas in Figures 3-3 and 3-4 obtain similar RD classifications, even though different background maps (vegetation layers) are used. The main difference between the classifications is that there are more Unclassified areas in Figure 3-3 than in Figure 3-4. Using the field layer as background map (Figure 3-4), large areas are classified as discharge; these areas are Unclassified using the ground layer background map (Figure 3-3). In particular, there are large

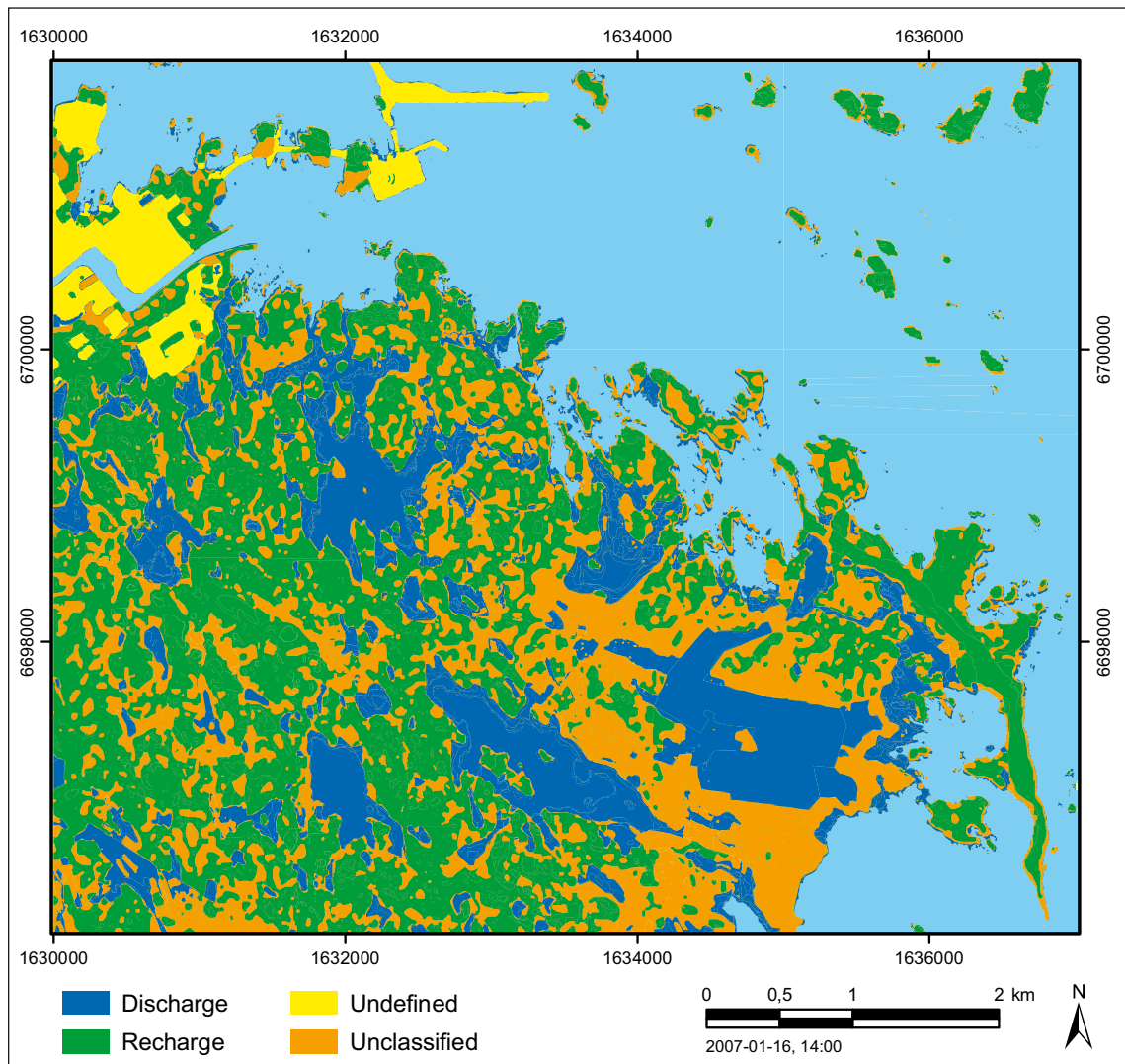


**Figure 3-3.** RD classification, produced by overlay of the QD map, the soil map, and the ground layer of the vegetation/land use map.

discharge areas in the south-eastern part of the map area in Figure 3-4, which are Unclassified in Figure 3-3. In the field layer of the vegetation/land use map, these areas mainly consist of herb types, which according to the classification scheme correspond to discharge (Table 3-5). In the ground layer, large areas (including the south-eastern parts of the map area in Figure 3-3) consist of Moss land – forest, which corresponds to recharge (Table 3-2). This explains the main differences between the two RD maps. These examples illustrate the difficulties in making consistent RD classifications, based on these types of background maps. It should be noted that the use of “weights” and calibration are possible also here (cf. Section 3.1), but no such attempts have been made within the present study.

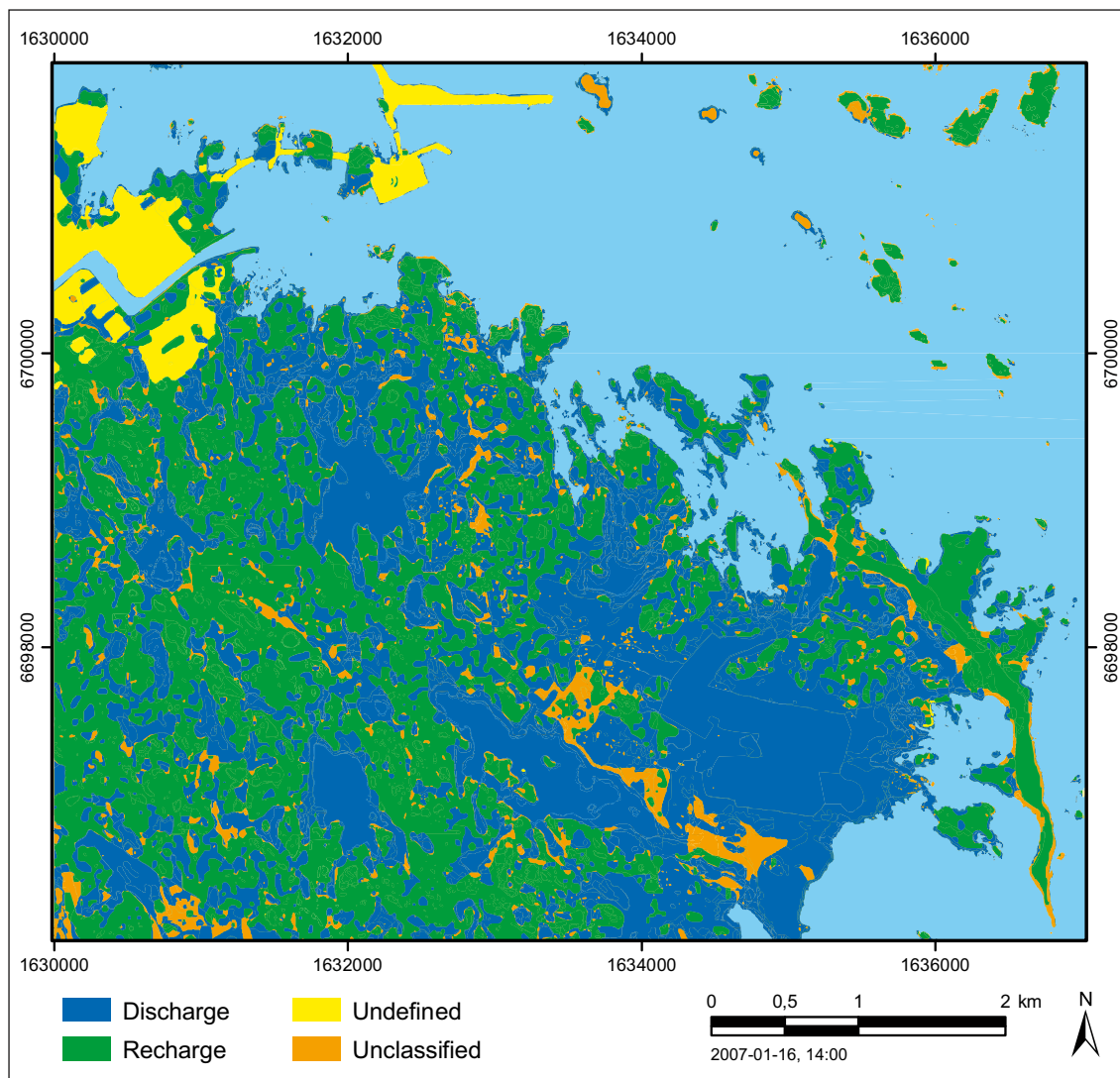


*Figure 3-4. RD classification, produced by overlay of the QD map, the soil map, and the field layer of the vegetation/land use map.*

### 3.3 Hydrological-hydrogeological modelling using MIKE SHE

The water flow model used in this study is established using the numerical modelling tools MIKE SHE and MIKE 11 (referred to as MIKE SHE, for brevity). This model was set up and used for descriptive modelling of near-surface and surface water flow at the Forsmark site /Johansson et al. 2005/, and also for quantification of the hydrological-hydrogeological effects of the construction and operation of a geological repository in Forsmark /Bosson and Berglund 2006/.

MIKE SHE is a physically based and distributed water flow model. It can be used for stationary or transient simulations of all the main processes of the hydrological cycle, including the saturated and unsaturated zones, evapotranspiration/interception, and overland flow /DHI Software 2004/. MIKE SHE is fully integrated with the channel-flow code MIKE 11, which can simulate stationary or transient surface water flow in watercourses and lakes. MIKE SHE and MIKE 11 may be run in parallel, with a continuous exchange of water.

The inputs to MIKE SHE include data describing topography (a DEM), meteorology, vegetation/land use, geology, and hydrogeology. In addition, MIKE 11 requires information on the so called river network (including bottom elevations, widths and depths of watercourses and lakes) within the model area. The inputs to the MIKE SHE model used here consist of data available as of July 31, 2004, which was the Forsmark 1.2 “data freeze”. A more detailed description of

the model set up and the input data can be found elsewhere /Johansson et al. 2005, Bosson and Berglund 2006/.

The MIKE SHE model area (size 37.6 km<sup>2</sup>) comprises most of the on-shore parts of what is referred to as the Forsmark regional model area. Note that the upstream (inland) MIKE SHE boundary follows the water divide towards the watercourse Forsmarksån, see Figure 3-5.

The established MIKE SHE model was used to generate a map of recharge and discharge areas, using model-calculated annual average hydraulic heads in the two uppermost calculation layers (layers 1 and 2; layers are numbered from the top and downwards). Note that the thicknesses of these layers vary across the model area, since the calculation layers in principle follow the geological (QD) layers /Johansson et al. 2005/. In MIKE SHE, calculation layers must be continuous throughout the modelled area, whereas geological layers can have zero thickness in parts of the model area. In the model set up, calculation layers are assigned a minimum thickness of 1 m, since there are some areas with very thin QD above rock.

Following the definitions of groundwater recharge and discharge (Section 2.1), discharge areas are in MIKE SHE identified as areas with a higher hydraulic head in layer 2 (i.e. the lower of the considered layers) than in layer 1. The opposite relation defines recharge areas. The thereby generated RD map is shown in Figure 3-6. Note that this RD map contains two classes (recharge and discharge), whereas five classes were identified using the topographical RD model in Section 3.1.

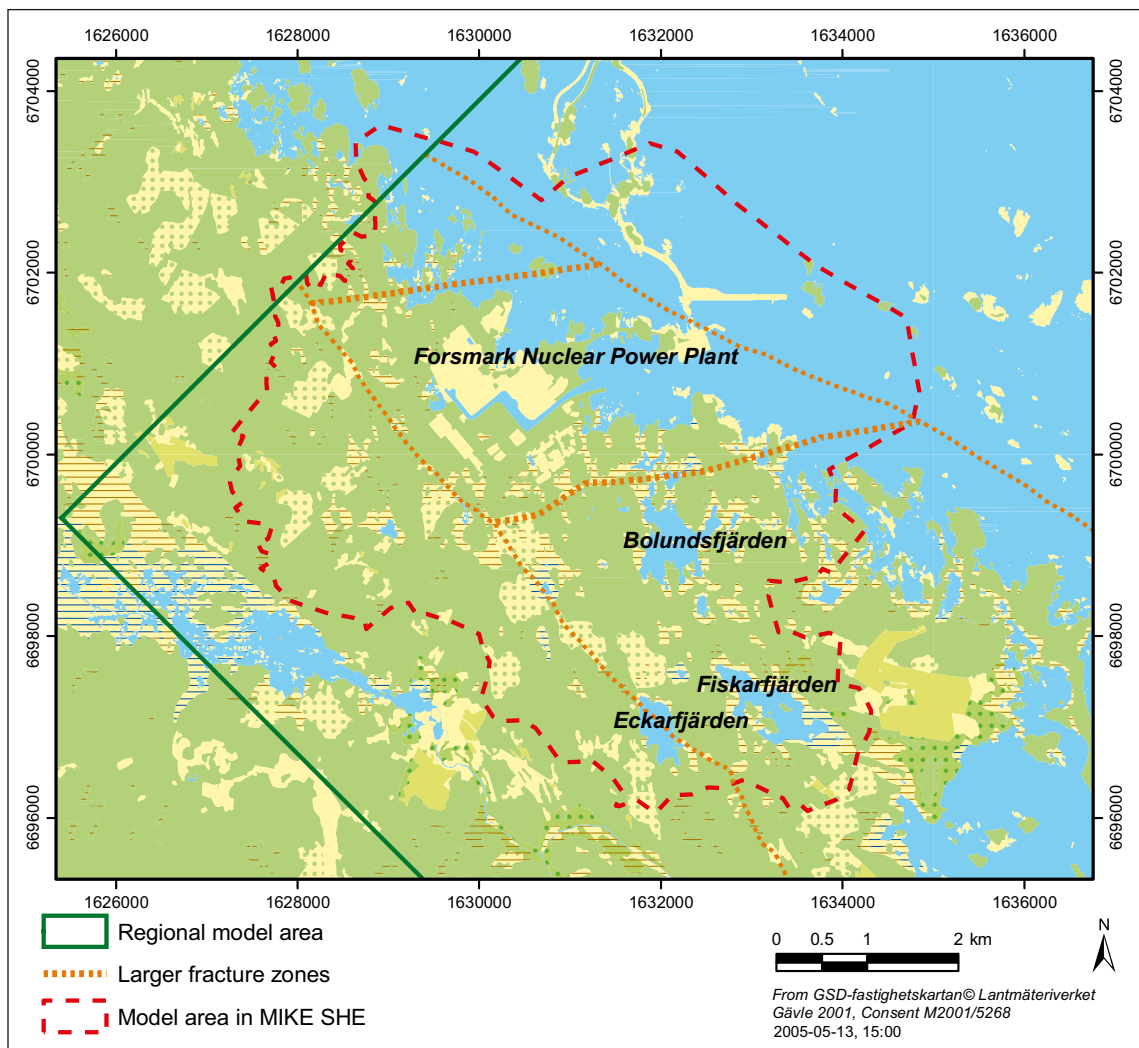


*Figure 3-5. Overview map of the MIKE SHE model area.*

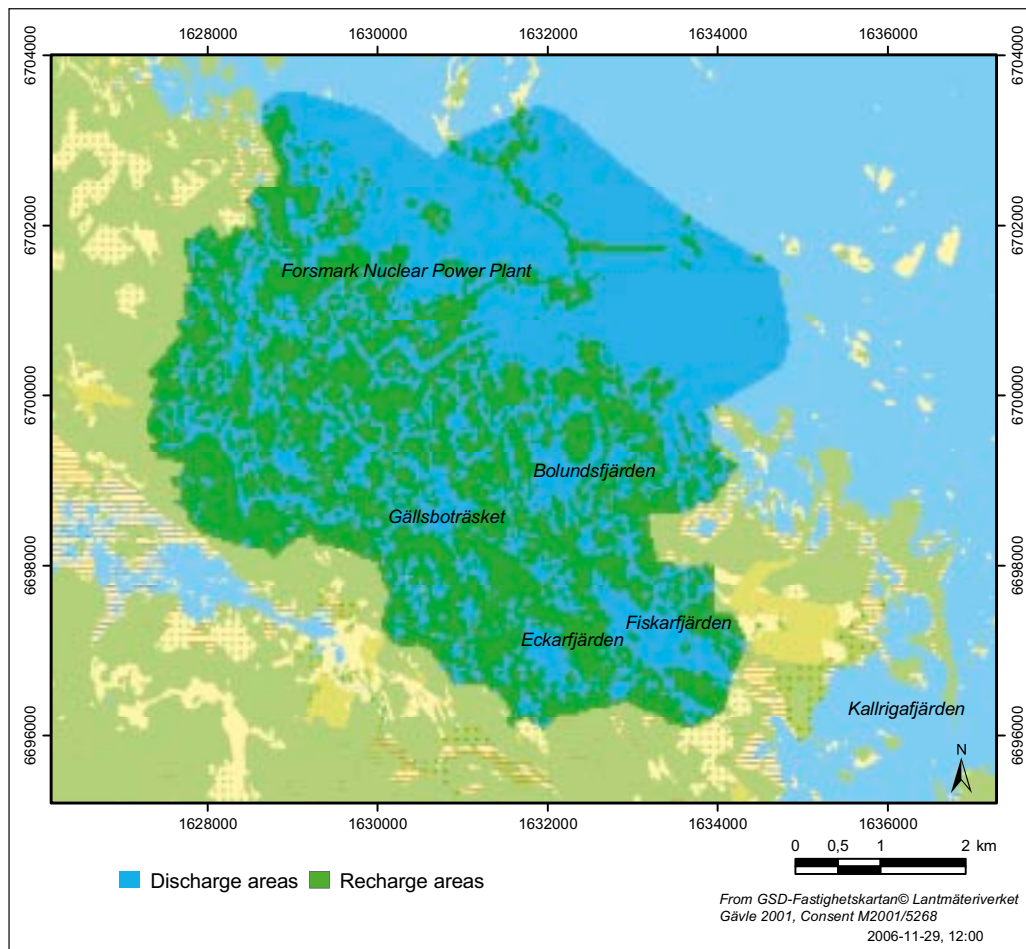


Figure 3-6. RD map of Forsmark, generated by the MIKE SHE model.

Previous MIKE SHE modelling of the Forsmark area /Johansson et al. 2005/ has shown that permanent recharge and discharge areas are located in (major) topographic highs and in watercourses and lakes, respectively. However, previous modelling has also shown areas that switch in time between recharge and discharge, due to temporally variable meteorological conditions (cf. Sections 2.1 and 2.2). Even though such transient conditions are simulated in MIKE SHE, it should be noted that Figure 3-6 represents “average” RD conditions.

According to Figure 3-6, the inland parts of the MIKE SHE model area are dominated by recharge areas (green). Areas classified as discharge (blue) include surface waters, i.e. the major lakes (Bolundsfjärden, Gällsboträsket, Fiskarfjärden and Eckarfjärden) and the sea. It should again be noted that the sea is set as a prescribed head boundary, whereas water flows and water levels in inland surface waters (lakes and watercourses), and their interactions with groundwater, are simulated explicitly through the MIKE SHE-MIKE 11 integration. The MIKE SHE recharge-discharge classification is further discussed in Section 4.2, comparing the MIKE SHE and topographical RD classifications.

### 3.4 Field classification of groundwater monitoring well locations

Recharge-discharge classification have been performed in the field, including 56 groundwater monitoring wells and 3 BAT filter tips in Quaternary deposits. The objectives of the classification are to support the conceptual modelling of near-surface groundwater flow, and to support interpretations of groundwater level time series and hydrochemical data from monitoring wells.

### 3.4.1 Methodology

Seven parameters were considered in the RD classification of the well locations. The classes of the parameters were, if applicable, adapted to the topographical classification in Section 3.1, and to the mappings of vegetation/land use and soil in Section 3.2. For some parameters, the classes were also given numerical values, allowing quantitative correlations studies. The following parameters were used:

- Local topography (areas 20 m by 20 m, and 100 m by 100 m)
  - Peak (1)
  - Ridge (2)
  - Pass (3)
  - Slope (upper (4), mid (5), flat (6), lower (7))
  - Channel (8)
  - Pit (9)
- Influence from surface water (distance)
  - Lake
  - Wetland
  - Brook
- Vegetation, ground layer, % coverage (areas 20 m by 20 m, and 100 m by 100 m)
  - Lichen
  - Lichen/moss
  - Moss
  - Sphagnum
  - Wet moss
  - Other
- Vegetation, field layer, % coverage (areas 20 m by 20 m, and 100 m by 100 m)
  - Heather
  - Lingonberry
  - Bilberry
  - Herb
  - Grass
  - Sedge
  - Reed
  - Other
- Vegetation, bush layer, % coverage (areas 20 m by 20 m, and 100 m by 100 m)
  - Pine
  - Spruce
  - Juniper
  - Birch
  - Aspen
  - Alder
  - Other
- Vegetation, tree layer, % coverage (areas 20 m by 20 m, and 100 m by 100 m)
  - Pine
  - Spruce
  - Birch
  - Aspen
  - Alder
  - Other
- Site hydrology
  - Dry (1)
  - Fresh (2)
  - Fresh/moist (3)
  - Moist (4)
  - Wet (5)
  - Open water

A specific form was used for classification in the field of each of the above parameters. Finally, the RD classification was completed by an overall judgement of recharge-discharge in five classes (cf. Section 3.1):

- Recharge (R) (1)
- Probable recharge (PR) (2)
- Varying (V) (3)
- Probable discharge (PD) (4)
- Discharge (D) (5)

### 3.4.2 Results

The results of the recharge-discharge well classification are shown in Table 3-7 and Figure 3-7.

**Table 3-7. Field classification of groundwater monitoring wells and BAT filter tips according to recharge/discharge location. R = recharge, PR = probable recharge, V = varying, PD = probable discharge, D = discharge.**

Well ID	RD classification	Well ID	RD classification
SFM0001*	D	SFM0031	D
SFM0002*	R	SFM0032	D
SFM0003*	V	SFM0033*	D
SFM0004*	R	SFM0034*	D
SFM0005*	R	SFM0035	D
SFM0006*	R	SFM0036*	D
SFM0007	R	SFM0037	D
SFM0008*	R	SFM0049*	D
SFM0009*	D	SFM0051	D
SFM0010*	V	SFM0053	D
SFM0011*	D	SFM0056	R
SFM0012	D	SFM0057*	R
SFM0013*	D	SFM0058*	R
SFM0014*	D	SFM0059*	R
SFM0015	D	SFM0060	R
SFM0016*	D	SFM0061*	R
SFM0017*	D	SFM0062	D
SFM0018*	D	SFM0063	D
SFM0019*	R	SFM0065	D
SFM0020*	V	SFM0067	D
SFM0021*	PD	SFM0068	PD
SFM0022	D	SFM0069	D
SFM0023	D	SFM0070	R
SFM0024	D	SFM0071	R
SFM0025	D	SFM0072	R
SFM0026*	D	SFM0073	D
SFM0027	D	SFM0074	D
SFM0028*	D	SFM0075	R
SFM0029	D	SFM0076	R
SFM0030*	D		

\* Well included in the correlation analysis presented below.

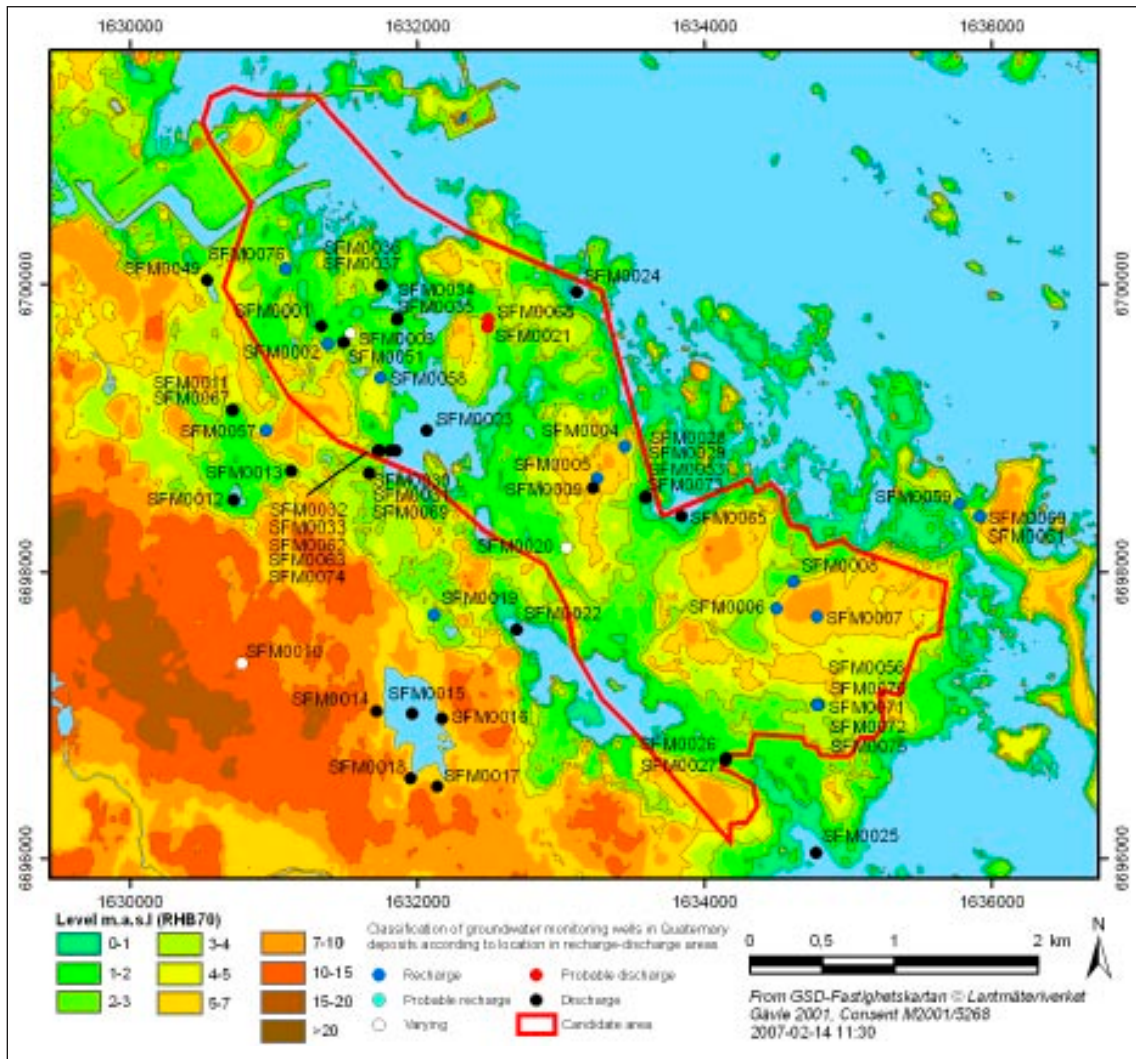


**Figure 3-7.** Field classification of groundwater monitoring wells and BAT filter tips according to recharge-discharge conditions.

Summarizing Table 3-7, 18 wells were classified as located in recharge areas, 3 wells in areas with varying recharge-discharge conditions, 2 wells in probable discharge areas, and 36 wells in discharge areas. A subset of 29 of the classified wells (excluding BAT filter tips, wells below open water, and wells with less than 150 days of observations), is used in the correlation analysis presented below. The considered wells are indicated (\*) in Table 3-7. The topographical index used in the analysis refers to a 100 m by 100 m area, centred on the well.

Figures 3-8 and 3-9 show the correlations between the RD classification and the topographical index, and between the RD classification and the site hydrology index. Note that some of the 29 wells included in the analysis are overlapping in Figures 3-8 and 3-9; points representing more than one well are shown in the figures. As expected, the general trend in Figure 3-8 is that wells in convex topographical positions are classified as located in recharge areas, whereas wells in concave positions are classified as located in discharge areas. Wells located in “flat” topographical positions cover the whole range of RD classes. As also expected, Figure 3-9 shows a trend with “dry” recharge locations to “wet” discharge locations. The site hydrology index fresh/moist (3) covers the whole range of RD classes.



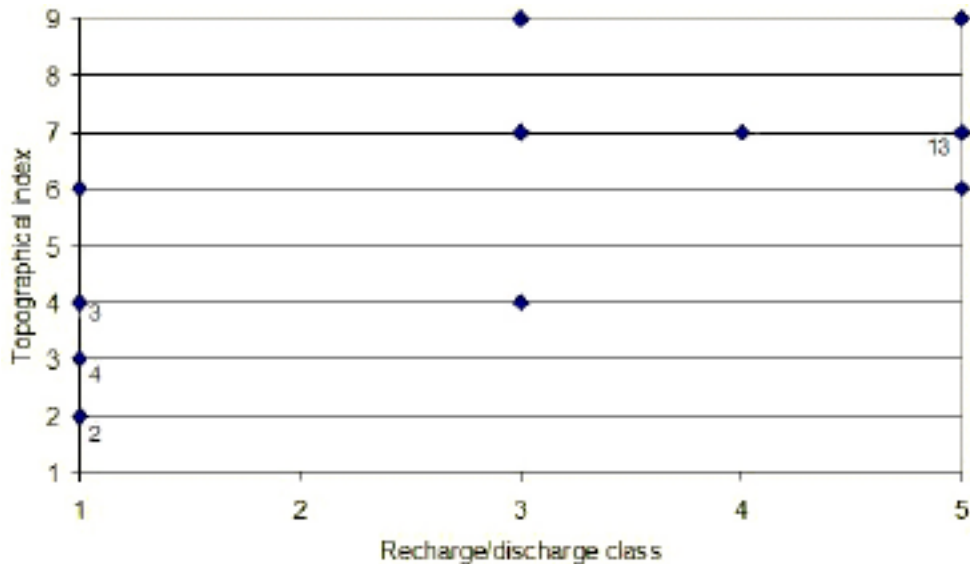


**Figure 3-8.** Cross-plot of recharge-discharge field classification and topographical index. Recharge-discharge classes: 1 = recharge, 2 = probable recharge, 3 = varying, 4 = probable discharge, 5 = discharge. Topographical indices: 1 = peak, 2 = ridge, 3 = pass, 4 = slope, upper; 5 = slope, mid, 6 = flat, 7 = slope lower; 8 = channel, 9 = pit.

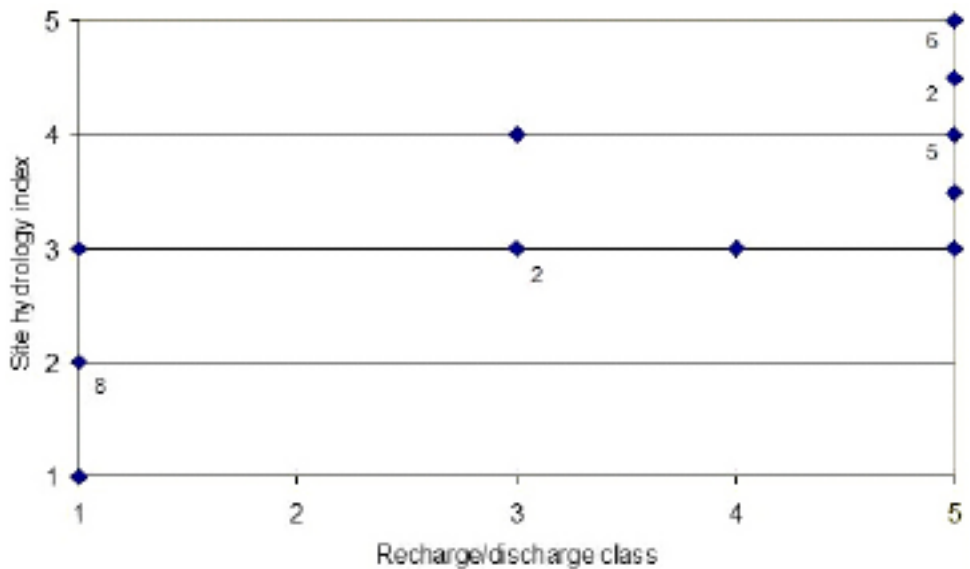


**Figure 3-9.** Cross-plot of recharge-discharge classes and site hydrology indices. Recharge-discharge classes: 1 = recharge, 2 = probable recharge, 3 = varying, 4 = probable discharge, 5 = discharge, Site hydrology indices: 1 = dry, 2 = fresh, 3 = fresh/moist, 4 = moist, 5 = wet.

Measured groundwater levels were not used in the RD classification. Figures 3-10 to 3-12 show cross-plots of the mean, minimum and maximum groundwater levels relative to ground surface, and recharge/discharge class. The mean groundwater levels are generally deeper in wells classified as located in recharge areas. However, there is a large range in the mean groundwater depths. The two deepest wells are located in the esker Börstilåsen. However, also in the “recharge wells” installed in till, the mean groundwater depths vary between 0.5 and 4.5 m. The range of mean groundwater depths for the “discharge wells” is much smaller, varying from c. 0 to 0.7 m below ground.

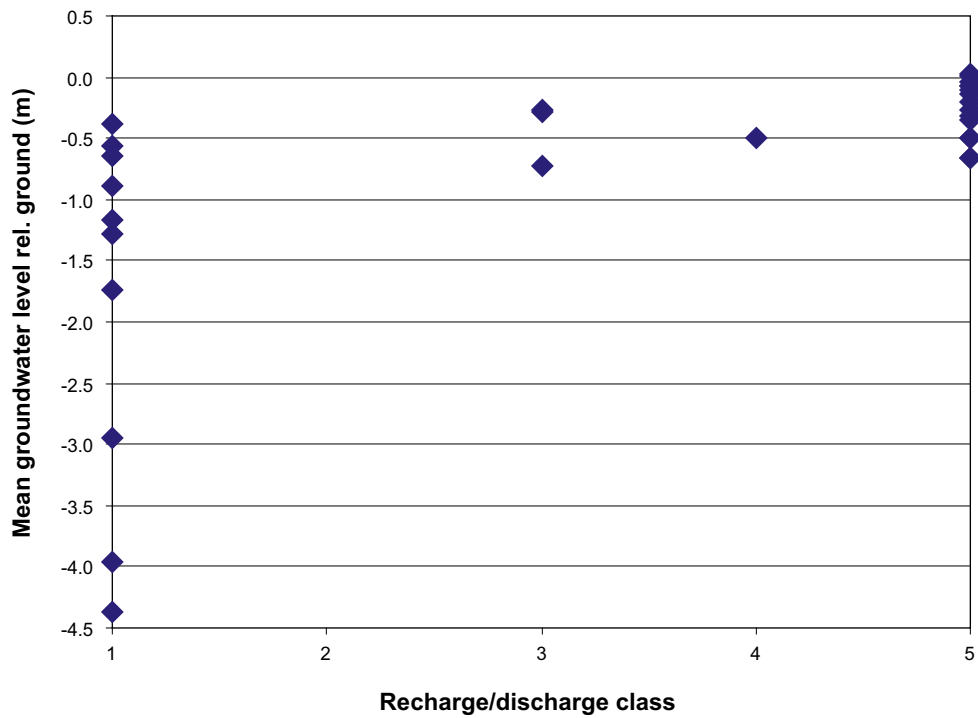


**Figure 3-10.** Cross-plot of recharge-discharge classes and mean groundwater levels below ground. Recharge-discharge classes: 1 = recharge, 2 = probable recharge, 3 = varying, 4 = probable discharge, 5 = discharge.

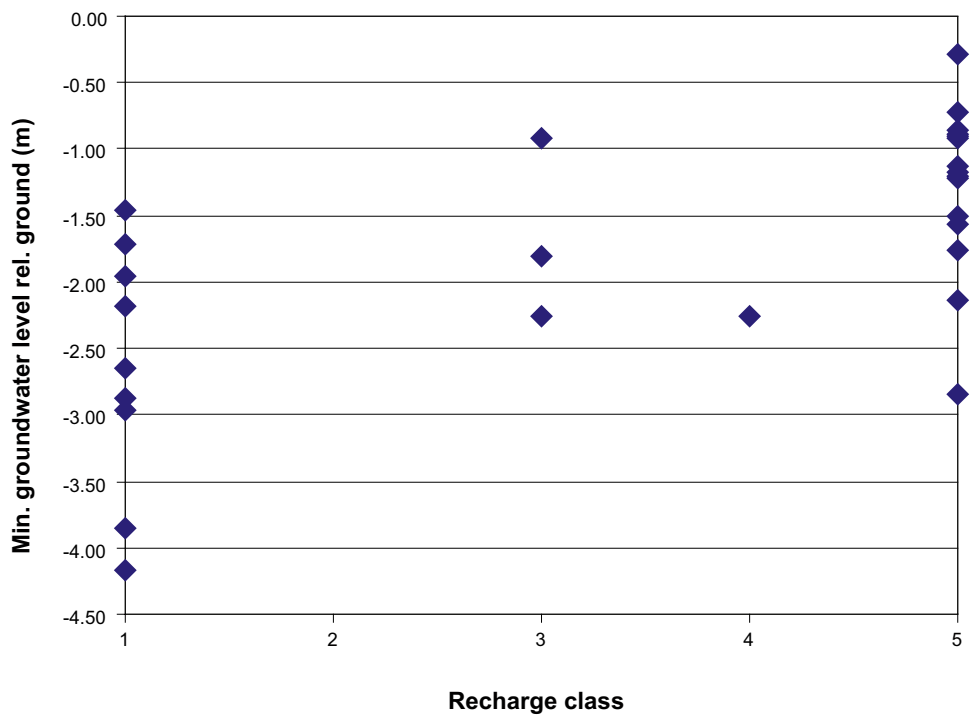


**Figure 3-11.** Cross-plot of recharge-discharge classes and minimum groundwater levels below ground. Recharge-discharge classes: 1 = recharge, 2 = probable recharge, 3 = varying, 4 = probable discharge, 5 = discharge.

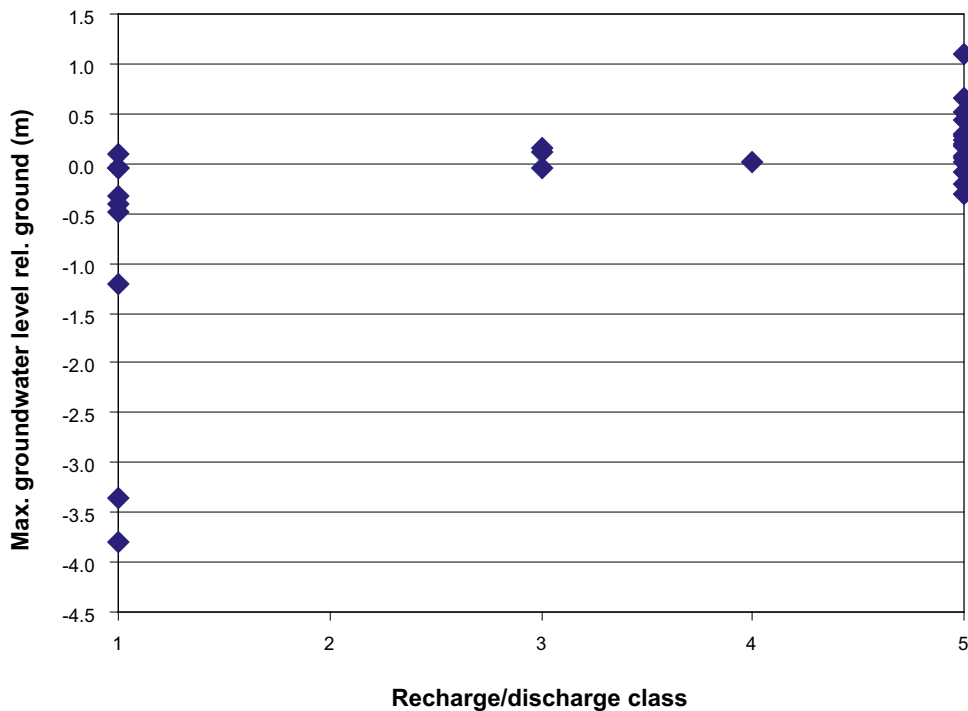
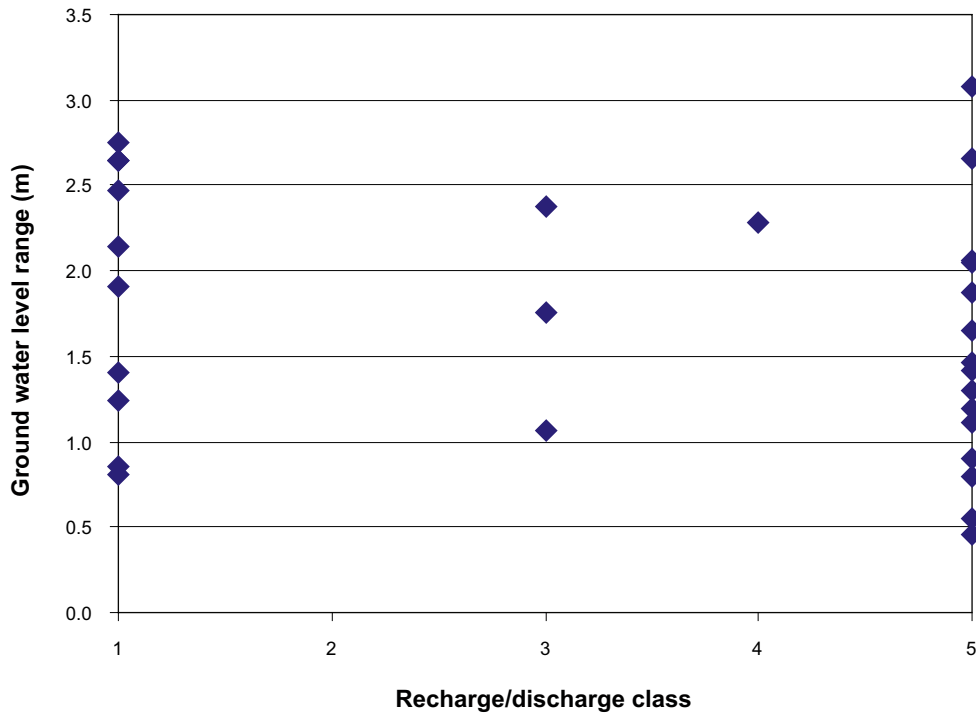


**Figure 3-12.** Cross-plot of recharge-discharge classes and maximum groundwater levels below ground. Recharge-discharge classes: 1 = recharge, 2 = probable recharge, 3 = varying, 4 = probable discharge, 5 = discharge.

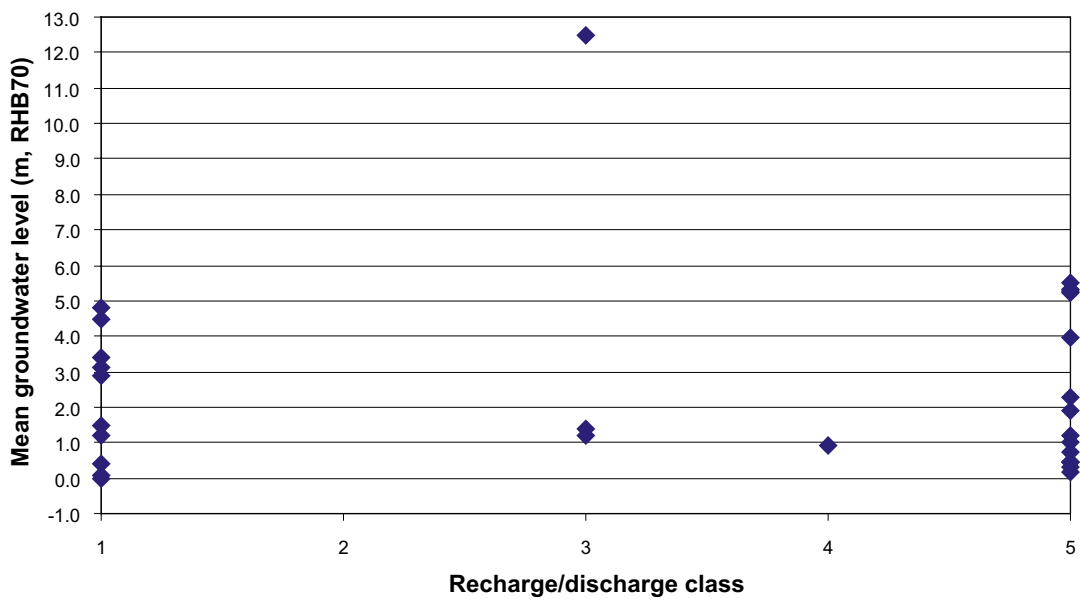
Compared to mean groundwater depths, minimum groundwater depths at the “discharge wells” have a much larger range (Figure 3-11). A possible explanation is a spatially variable influence of indirect and direct root-water uptake depending on the vegetation. Maximum groundwater depths (Figure 3-12) demonstrate a relatively small range, both for the “recharge” and “discharge wells” (c. 1 m for most wells); this phenomenon is probably an effect of high hydraulic conductivity close to the ground surface. For many of the “discharge wells”, the maximum groundwater levels are above ground. This is also the case for one of the “recharge wells” (SFM0057). This indicates that the area surrounding well SFM0057 changes to a discharge area, at least for short periods. Three more wells (SFM0002, SFM0004 and SFM0019), classified as located in recharge areas, have maximum groundwater levels less than 0.1 m below ground, indicating that also these three wells may be located in areas with varying recharge-discharge conditions, although not identified as such in the RD classification.

Figure 3-13 shows the ranges in groundwater level of each well. Theoretically, the range should be smaller for the wells located in discharge areas. However, the ranges are approximately the same for wells located in recharge and discharge areas. A possible explanation is that the groundwater levels in discharge areas are strongly influenced by water uptake from vegetation, resulting in groundwater level changes not directly coupled to groundwater flow, cf. Section 2.2.3 and Figure 2-16.

Figures 3-14 and 3-15 show cross-plots of the recharge-discharge classification and mean groundwater levels in m (elevation system RHB70), and the recharge-discharge classification and ground surface elevations. In contrast to the cross-plot of the recharge-discharge classes and the groundwater depths below ground surface above, no correlations can be seen in these plots. This indicates that local topography dominates over regional slope as a controlling factor for near-surface RD patterns in Forsmark. As mentioned previously, local recharge and discharge areas may at some locations coincide with intermediate or even regional recharge and discharge areas.



**Figure 3-13.** Cross-plot of recharge-discharge classes and maximum groundwater level range. Recharge-discharge classes: 1 = recharge, 2 = probable recharge, 3 = varying, 4 = probable discharge, 5 = discharge.



**Figure 3-14.** Cross-plot of recharge-discharge classes and mean groundwater level, m (elevation system RHB70). Recharge-discharge classes: 1 = recharge, 2 = probable recharge, 3 = varying, 4 = probable discharge, 5 = discharge.

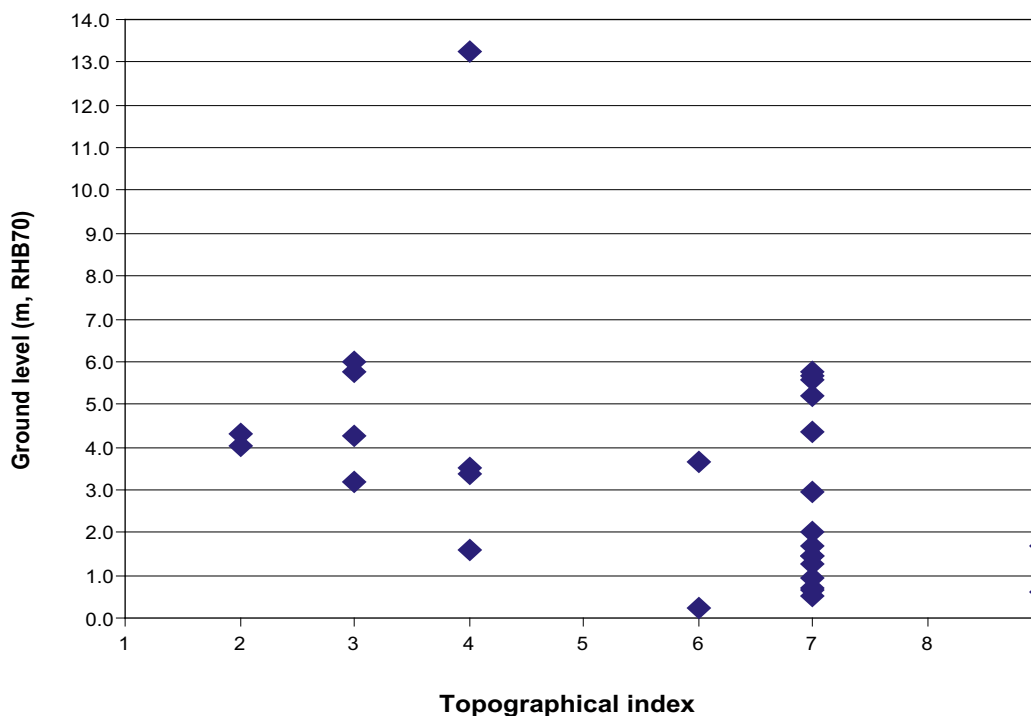


**Figure 3-15.** Cross-plot of topographical indices and mean groundwater levels, m (elevation system RHB70). Topographical indices: 1 = peak, 2 = ridge, 3 = pass, 4 = slope, upper, 5 = slope, mid, 6 = flat, 7 = slope lower, 8 = channel, 9 = pit.

### 3.5 Hydrochemical classification of groundwater monitoring well locations

#### 3.5.1 Some observations concerning RD-hydrochemistry relations in the Forsmark area

The spatial and temporal distributions of hydrochemical parameters may potentially be used to distinguish “water types” and to evaluate the overall groundwater flow pattern, including spatial distributions of recharge and discharge areas and residence times of water in different parts of the flow system. Examples of hydrochemical data include main elements and specific chemical components (such as isotopes) in groundwater, sampled in groundwater monitoring wells in QD and boreholes in the rock.

/Tröjbom and Söderbäck 2007/ present a general overview of the patterns of “recharge and discharge wells”, identified in the physical-hydrological RD classification (Section 3.4), using various types of hydrochemical plots. For instance, a so called Langelier-Ludwig plot was used to visualize the relative fractions of the cations Na, K, Mg and Ca on the x-axis, and the anions HCO<sub>3</sub>, Cl and SO<sub>4</sub> on the y-axis. Such a plot for groundwater wells in Forsmark shows that most wells field-classified as “recharge wells” are dominated by Ca-HCO<sub>3</sub> type of groundwater. The field-classified “discharge wells” are scattered across the Langelier-Ludwig plot, and hence do not demonstrate any clear pattern.

A plot of total sulphate versus an estimated fraction of non-marine sulphate shows that field-classified “recharge wells” mainly are located in the upper part of the plot, i.e. demonstrating groundwater with a high fraction of non-marine sulphate. The field-classified “discharge wells” are scattered across the plot, and hence do not demonstrate any clear pattern.

A plot of Ca versus  $\text{HCO}_3$  indicates that calcite dissolution is a major calcium source in near-surface groundwaters in the Forsmark area. The field-classified “recharge wells” are located along the saturation line for calcite dissolution, whereas the field-classified “discharge wells” do not demonstrate any clear pattern in the plot.

Generally, there seems to be more apparent patterns in the RD-hydrochemistry relations for field-classified “recharge wells” in the cited plots, compared to “discharge wells”. These conclusions indicate that surface/near-surface hydrochemical data can not be used as the single input for identification of near-surface discharge areas. Rather, hydrochemical data are thought to support RD classifications made by other methods.

Detailed data analyses using PCA (Principal Component Analysis) have been performed to investigate the statistical correlations (or lack of correlations) between the field-based RD classification of groundwater monitoring wells (Section 3.4) and the hydrochemical characteristics of groundwater sampled from these wells /Tröjbom and Söderbäck 2007/. The analyses are based on a range of data collected within the hydrogeochemical programme at Forsmark. The programme includes both chemical parameters and some basic physical parameters, such as groundwater temperature.

The results of the PCA show a positive correlation between the RD classification and the average and the temporal variability of “redox parameters” (such as the concentration of dissolved oxygen and Eh), the chloride concentration, and the groundwater temperature. In addition, a positive correlation was found between the RD class and the temporal variability of tritium (for a further discussion on tritium, see Section 3.5.3) and the electrical conductivity. On the contrary, weak or no correlations were found between the RD classification and the temporal variability of deuterium (see Section 3.5.3), the oxygen isotope  $^{18}\text{O}$ , and the average concentration of DOC (dissolved organic carbon).

The PCA shows that wells classified as “recharge wells” according to the field-based RD classification are characterized by low chloride concentrations, but with large temporal variability, high Eh, and a small temporal variability of tritium. In addition, these wells demonstrate low average groundwater temperatures, with small temporal variability. In general, the opposite was found for the field-classified “discharge wells”. The PCA also shows that the averages of hydrochemical parameters that “typically” are used to identify groundwater recharge and discharge (such as chloride, DOC, Eh, and tritium) demonstrate much larger variability between field-classified “discharge wells” compared to “recharge wells”. The following sections exemplify the use of three hydrochemical data sets for RD classification, namely major chemical elements, redox and tritium.

### 3.5.2 Major chemical elements

A so called Piper-plot was used to classify 42 of the groundwater monitoring wells in Forsmark, according to relative compositions of major chemical elements in groundwater samples /Tröjbom and Söderbäck 2007/. In this RD classification scheme, groundwater of  $\text{Ca-HCO}_3$  type is assumed to indicate groundwater recharge, and groundwater of  $\text{Na-HCO}_3$  to  $\text{Na-Cl}$  types is assumed to indicate groundwater discharge. The result of the classification is shown in Figure 3-16.

Of the 42 Piper plot-classified wells, 24 are classified as “recharge wells”, and 18 as “discharge wells”. Most of the field-classified recharge wells (red triangles in Figure 3-16) are found in the left part of the Piper plot, hence corresponding to recharge wells also in the hydrochemical classification. On the other hand, field-classified “discharge wells” are far more scattered in the Piper plot. The Piper-plot based hydrochemical RD classification is further discussed in Section 4.3.2, where it is compared to the results of the field-based RD classification.

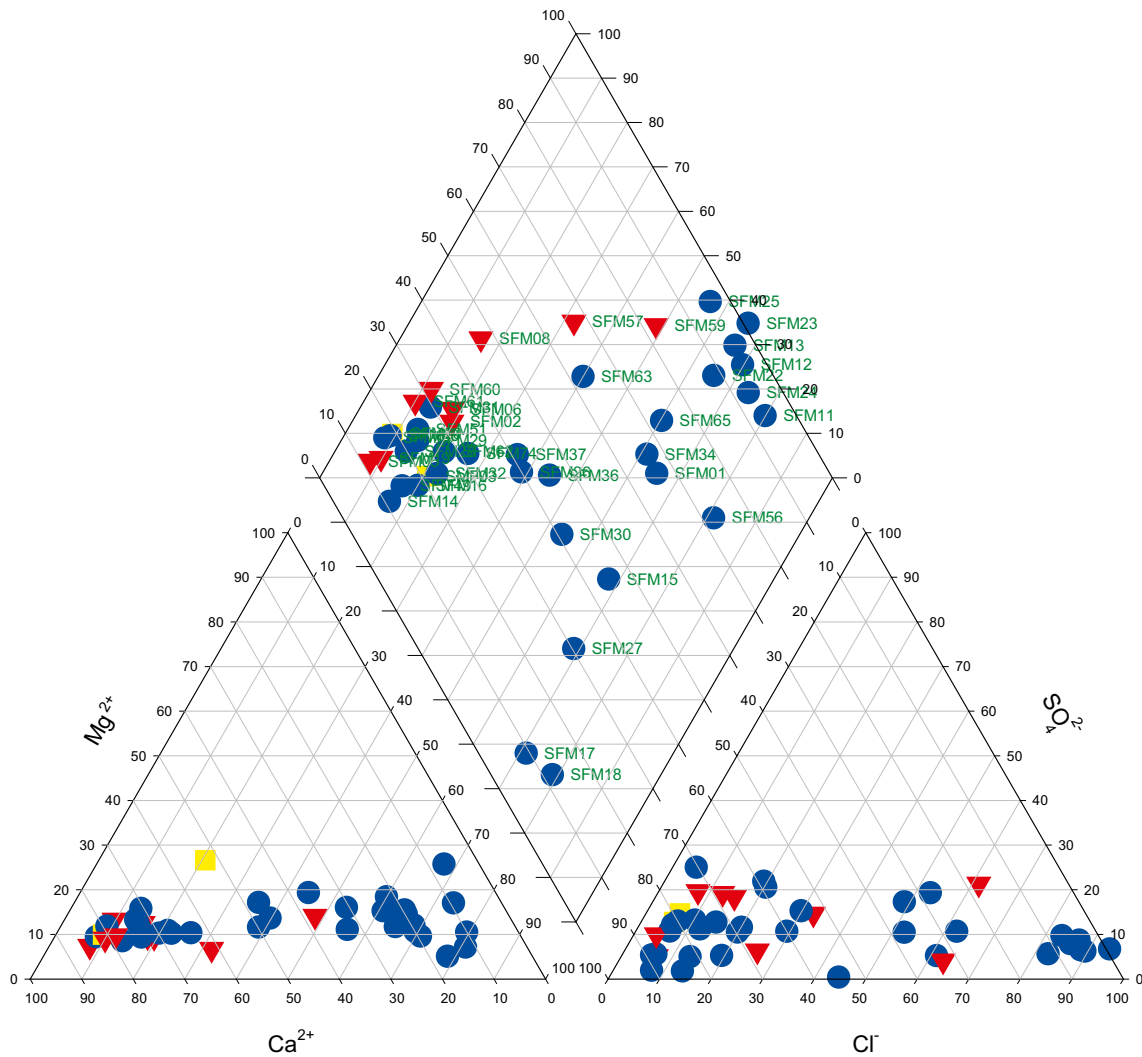


**Figure 3-16.** Piper plot of groundwater monitoring wells in Forsmark /Tröjbom and Söderbäck 2007/. The plot is based on average concentrations of major chemical elements in groundwater sampled in each well. The encircled wells are chemically classified as recharge wells. According to the hydrological field classification (Section 3.4), red triangles in the plot were classified as recharge wells, yellow dots as wells with varying RD characteristics, and blue dots as discharge wells.

### 3.5.3 Redox and groundwater age

#### Redox-based classification

Based on averages of the total contents of iron, manganese and sulphate, /Tröjbom and Söderbäck 2006/ classified groundwater monitoring wells in Forsmark into four classes, following the national Swedish environmental quality criteria for groundwater /Naturvårdsverket 1999/. According to this classification scheme, class 1 corresponds to high redox potential (aerobic groundwater, which can be assumed to characterize a recharge area), and class 4 very low redox potential (anaerobic groundwater, which can be assumed to characterize a discharge area). This redox-based classification is summarized in the comparison between RD classifications of groundwater well locations in Section 4.3.2.

### **Classification of estimated groundwater age using isotopes**

Groundwater age dating, based on isotopes, can potentially be used to interpret groundwater flow patterns and groundwater residence times (see, e.g. /Cook and Herczeg 2000, Appelo and Postma 2005/. Examples of isotopes available for age dating groundwaters within certain age intervals include the following:

- Young (modern) groundwaters (< 50 years): Isotopes include tritium ( $^3\text{H}$ ) and krypton-85 ( $^{85}\text{Kr}$ ). Tritium is analyzed within SKB's hydrogeochemical programme for Forsmark. The practical use of  $^{85}\text{Kr}$  for groundwater age dating is limited due to sampling and interpretation difficulties.
- Old groundwaters (< 30,000 years): An example is the carbon isotope carbon-14 ( $^{14}\text{C}$ ), analyzed within SKB's hydrogeochemical programme for Forsmark. The main practical limitation related to the use of  $^{14}\text{C}$  for groundwater age dating is a complicated task, requiring a number of corrections. These corrections are due to "dead" carbon derived from carbonate dissolution, and/or degradation of organic carbon /Appelo and Postma 2005/.
- Very old groundwaters (< 400,000 years): Isotopes include krypton-81 ( $^{81}\text{Kr}$ ) and chloride-36 ( $^{36}\text{Cl}$ ). One specific problem with  $^{36}\text{Cl}$  is that this isotope also may be produced from  $^{35}\text{Cl}$  in U/Th-rich rock. Another example is the (stable) helium isotope  $^4\text{He}$ , which can be used to indicate the presence of very old groundwaters (hundreds of thousands to a few million years).  $^4\text{He}$  is produced in the geosphere by radioactive decay of  $^{238}\text{U}$  to  $^{206}\text{Pb}$ , and by fission of  $^6\text{Li}$  in uraniferous rocks. The practical use of  $^4\text{He}$  as a hydrogeological tracer is limited due to uncertainties related to in situ and external  $^4\text{He}$  sources /Van der Hoven et al. 2005/. Of interest for the present subject is that previous studies have shown that high groundwater concentrations of dissolved helium gas may be expected in areas of groundwater discharge, particularly in granitic areas (e.g. /Gascoyne and Sheppard 1993/). Helium data have not been used in the present study, but may be utilized to support updated RD classifications of the Forsmark area.

The brief summary above shows that there are many practical limitations and uncertainties related to the use of isotopes and isotope ratios for groundwater age dating. This implies that such age dating methods require rather thorough analyses and corrections, which are outside the scope of the present study. A relatively simple example will be demonstrated here, using the radioactive hydrogen isotope tritium ( $^3\text{H}$ ) for groundwater age dating. The reason for choosing this isotope is that it has been used in many previous studies (see e.g. /Appelo and Postma 2005/ and references therein). Further, data are available in the scientific literature for first-tier estimates of groundwater age simply from the tritium concentration /Clark and Fritz 1997/.

Hydrogen has two stable isotopes:  $^1\text{H}$  (protium; light hydrogen), and  $^2\text{H}$  (deuterium (D); heavy hydrogen). The tritium isotope ( $^3\text{H}$ ), which has a half life of c. 12.32 years, decays to the stable helium isotope  $^3\text{He}$ . Tritium is produced naturally in the upper atmosphere (by cosmic bombardment of nitrogen with neutrons), as well as in the geosphere (by neutrons produced during the spontaneous fission of uranium and thorium). In principle, the ratio  $^3\text{H}/^3\text{He}$  offers an absolute groundwater age dating method, since the initial  $^3\text{H}$  concentration is given by the sum of  $^3\text{H}$  and  $^3\text{He}$  in a groundwater sample. However, there are practical limitations in the use of this direct age dating method, since the estimated age is affected by dispersion and also by different diffusion rates of  $^3\text{H}$  and  $^3\text{He}$  (see, e.g. /LaBolle et al. 2006/). Moreover, the  $^3\text{He}$  concentration in the sample needs to be subtracted in order to account for the in situ production of  $^3\text{H}$ .



Tritium concentrations are usually presented in tritium units (TU); 1 TU equals one molecule of  $^3\text{H}$  per  $10^{18}$  molecules of  $^1\text{H}$  (corresponding to an activity of c. 3.2 pCi per litre of water from the emitted  $\beta$  particles). The natural production of tritium in the atmosphere is very low: natural (pre-nuclear age) levels of tritium in precipitation are on the order of 1 to 5 TU. Beginning in the 1950's, large amounts of tritium were produced by the above-ground testing of thermo-nuclear bombs. The above-ground testing was banned (USA, USSR, and UK) in 1963, which led to a reduction of the anthropogenic tritium production.

Knowledge of the large tritium input to the hydrological cycle during the 1960's can be used as a basis to estimate groundwater age. High tritium concentrations ( $> 30$  TU) characterize water that was recharged during the late 1950's or early 1960's. Moderate concentrations characterize modern recharge, whereas concentrations close to the detection limit (c. 1 TU) are likely submodern or "paleo" groundwaters, which have been mixed with shallow (and modern) groundwaters /Clark and Fritz 1997/. General guidelines for age dating of groundwater using tritium are summarized in Table 3-8.

It must be observed that the use of tritium for groundwater age dating is limited by a number of factors, including uneven global distributions, partly due to continued nuclear releases at some locations. Based on relatively few samples, it has been estimated that present-day precipitation in the Forsmark area has a tritium concentration of c. 8–12 TU /SKB 2005/. The large variability of the "tritium input function" to the groundwater system obviously makes it difficult to use tritium as an indicator of near-surface groundwater recharge and discharge. For instance, a near-surface groundwater sample with a tritium concentration of, say, 15 TU may be 100% recent. On the other hand, this sample may also contain a mixture of more or less tritium-free (i.e. very old) groundwater, and groundwater recharge during the 1960's (i.e. with a high tritium concentration).

Table 3-9 shows age-dating estimates, based on the general guidelines in Table 3-8. It can be seen that a vast majority of the wells have a tritium concentration in the range 5–15 TU, corresponding to "modern" groundwater (age  $< 5$  to 10 y). Most of the other wells are estimated to contain either submodern groundwater (recharge prior to the 1950's), or a mix of submodern and modern groundwater. The estimated groundwater ages in Table 3-9 are further discussed in Section 4.3.2, comparing RD classifications of groundwater monitoring well locations.

**Table 3-8. General guidelines for groundwater age dating using tritium /Clark and Fritz 1997/**

Range (TU)	Age dating
$< 0.8$	Submodern (prior to the 1950's)
0.8–4	Mix of submodern and modern
5–15	Modern ( $< 5$ –10 years)
15–30	Some anthropogenic (bomb) tritium
$> 30$	Recharge in the 1960's to 1970's
$> 50$	Recharge in the 1960's

**Table 3-9. Estimates of groundwater age using tritium (data from /Tröjbom and Söderbäck 2007/).**

Well ID	Tritium (TU) Average	Minimum	Groundwater age (based on the TU average)
SFM0001	11.4	< 6	Modern (< 5 to 10 y)
SFM0002	11.7	9.6	Modern (< 5 to 10 y)
SFM0003	14.5	< 6	Modern (< 5 to 10 y)
SFM0005	11.2	10.5	Modern (< 5 to 10 y)
SFM0006	10.2	7.8	Modern (< 5 to 10 y)
SFM0008	10.5	8.1	Modern (< 5 to 10 y)
SFM0009	11.8	10.6	Modern (< 5–10 years)
SFM0010	< 0.8	< 0.8	Submodern (prior to the 1950's)
SFM0011	2.0	2.0	Mix of submodern and modern
SFM0012	2.6	< 0.8	Mix of submodern and modern
SFM0013	7.0	7.0	Modern (< 5 to 10 y)
SFM0014	13.5	13.5	Modern (< 5 to 10 y)
SFM0015	4.2	< 0.8	Mix of submodern and modern (< 4 TU); modern (< 5 to 10 years) (> 5 TU)
SFM0016	13.8	13.8	Modern (< 5 to 10 y)
SFM0017	7.8	7.8	Modern (< 5 to 10 y)
SFM0018	7.1	7.1	Modern (< 5 to 10 y)
SFM0019	12.7	12.7	Modern (< 5 to 10 y)
SFM0020	10.1	10.1	Modern (< 5 to 10 y)
SFM0021	12.0	12.0	Modern (< 5 to 10 y)
SFM0022	1.0	< 0.8	Mix of submodern and modern
SFM0023	3.7	2.4	Mix of submodern and modern
SFM0024	10.2	4.8	Modern (< 5 to 10 y)
SFM0025	7.9	5.0	Modern (< 5 to 10 y)
SFM0026	15.7	15.7	Some bomb tritium
SFM0027	10.5	8.8	Modern (< 5 to 10 y)
SFM0028	15.5	15.5	Some anthropogenic (bomb) tritium
SFM0029	11.9	10.7	Modern (< 5 to 10 y)
SFM0030	11.8	11.8	Modern (< 5 to 10 y)
SFM0031	12.3	9.9	Modern (< 5 to 10 y)
SFM0032	11.3	5.6	Modern (< 5 to 10 y)
SFM0034	12.9	12.9	Modern (< 5 to 10 y)
SFM0036	11.5	11.5	Modern (< 5 to 10 y)
SFM0037	12.1	9.2	Modern (< 5 to 10 y)
SFM0049	12.0	9.6	Modern (< 5 to 10 y)
SFM0051	10.5	7.3	Modern (< 5–10 years)
SFM0053	9.4	1.2	Modern (< 5–10 years)
SFM0056	< 0.8	< 0.8	Submodern (prior to the 1950's)
SFM0057	10.4	8.6	Modern (< 5 to 10 y)
SFM0059	9.0	9.0	Modern (< 5 to 10 y)
SFM0060	9.9	8.5	Modern (< 5 to 10 y)
SFM0061	10.8	9.9	Modern (< 5 to 10 y)
SFM0062	9.9	9.8	Modern (< 5 to 10 y)
SFM0063	9.0	9.0	Modern (< 5 to 10 y)
SFM0074	10.3	8.7	Modern (< 5 to 10 y)
SFM0082	10.6	10.6	Modern (< 5 to 10 y)

## 4 Comparison between RD classification methods

### 4.1 Topographical model and map overlays

This section compares the topographical RD classification (Section 3.1) with the RD classification made using map overlays (Section 3.2). Areas classified as MLD (most likely discharge areas) and PD (probable discharge areas) according to the topographical model were selected for the comparison, whereas areas classified as discharge were chosen from the map overlays. Figures 4-1 and 4-2 show the results of the comparison, indicating areas classified as discharge according to one of the two models only (red = map overlay only, lilac = topographical model only). Areas classified as discharge according to both models are displayed in blue.

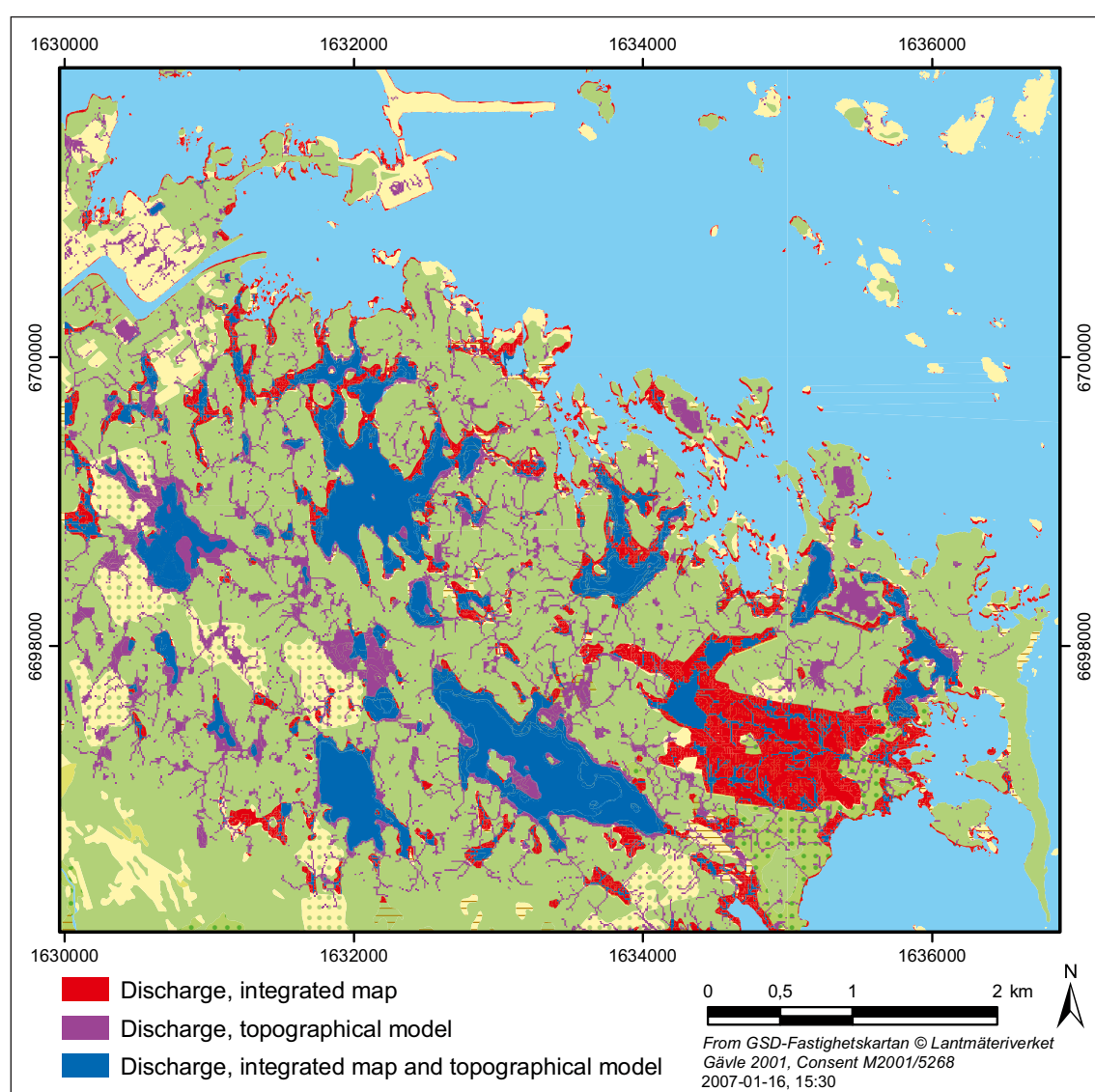


**Figure 4-1.** Comparison between discharge areas according to the topographical RD model, and the RD classification based on overlay of the QD map, the soil map, and the ground layer of the vegetation/land use map (“integrated map”).

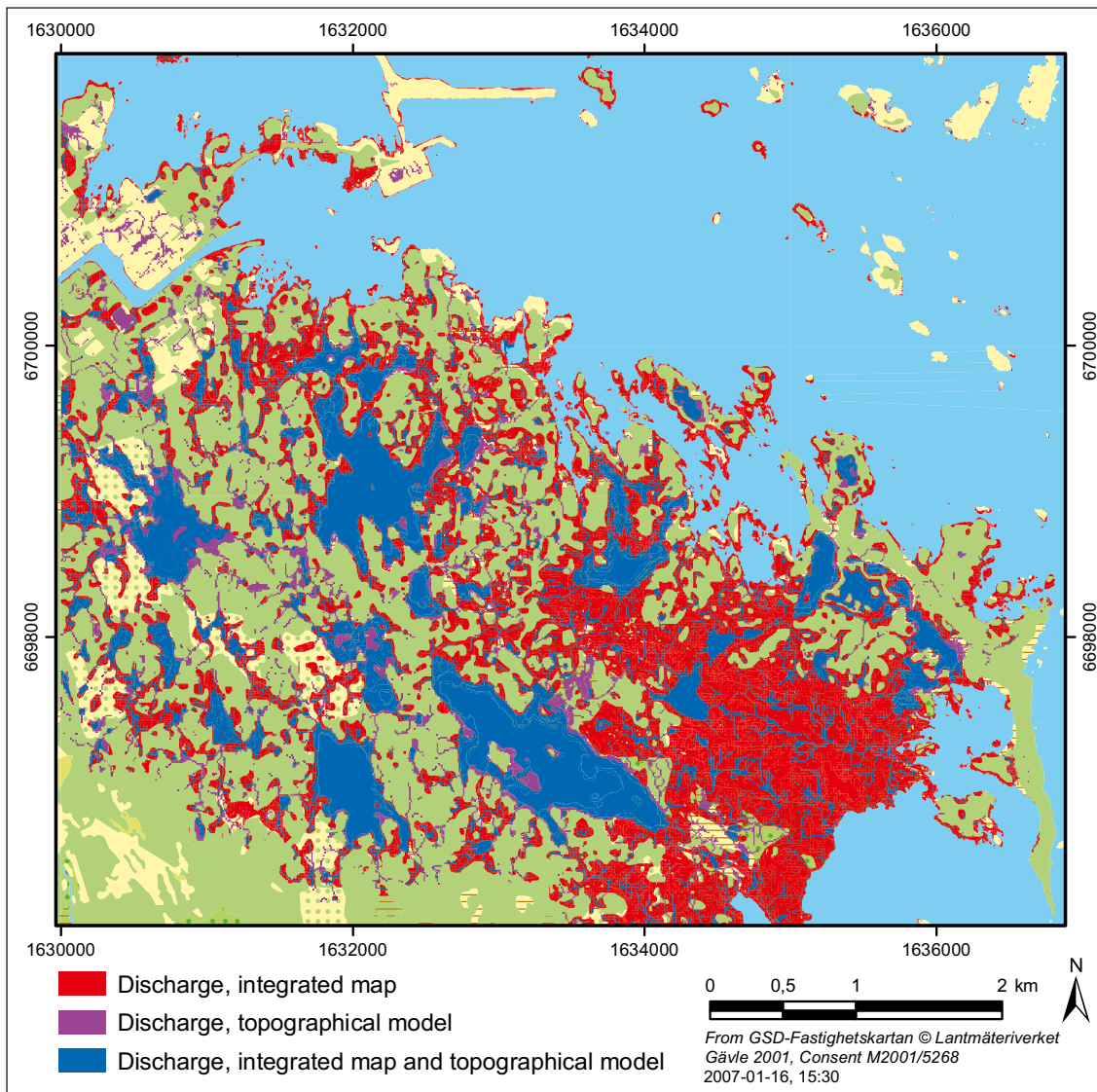


**Figure 4-2.** Comparison between extents of discharge areas according to the topographical RD model, and the RD classification based on overlay of the QD map, the soil map, and the field layer of the vegetation/land use map (“integrated map”).

The figures above indicate that a combination of the QD map, the soil map and the ground layer of the vegetation/land use map yields the most realistic identification of discharge areas (this could be suspected already when producing the map overlays in Section 3.2). Obviously, this conclusion is based on one subset of all the potential background map combinations and RD classification rules.

Even the “best” background map combination demonstrates large differences to the topographical model, in particular in the form of large discharge areas in the south-eastern part of the map area (Figure 4-1), which are not identified as discharge areas in the topographical RD model. Further, the topographical RD model (which has been developed directly from the 10-metre DEM) shows a much more detailed resolution compared to the map overlays. The map overlays are based on maps that by necessity involve a higher degree of generalization than a high resolution DEM. The illustrative examples presented here show that RD classifications based on map overlays require background maps with relatively high spatial resolution (possibly complemented with field checks to obtain higher accuracy), and also detailed RD classifications to provide realistic results.

## 4.2 Topographical model and MIKE SHE

This section compares the RD classifications performed using the topographical model (Section 3.1) and the MIKE SHE model (Section 3.3). As described in these sections, the topographically determined RD map contains five classes, whereas two classes were used in the MIKE SHE modelling. Figures 4-3 and 4-4 compare the two RD classifications, in terms of recharge and discharge areas, respectively. Note that the classes MLD (most likely discharge areas) and PD (probable discharge areas) are used from the topographical model. Also note that the “empty” areas in Figure 4-3 are recharge areas in neither of the two RD models.

In order to quantify the match between these two RD classification methods, all grid cells classified as “recharge cells” using the MIKE SHE model were assigned the flag value +1 in ArcGIS, whereas all “discharge cells” were assigned the flag value -1. The ArcGIS tool “Zonal statistics” (available in Spatial analyst, an ArcGIS extension) was subsequently used to calculate the average MIKE SHE flag value for the grid cells located within each of the five topographically determined RD classes. Note that the area for which the model comparison is made consists of the onshore parts of the Forsmark area where the two model areas coincide (cf. Figures 3-2 and 3-4).

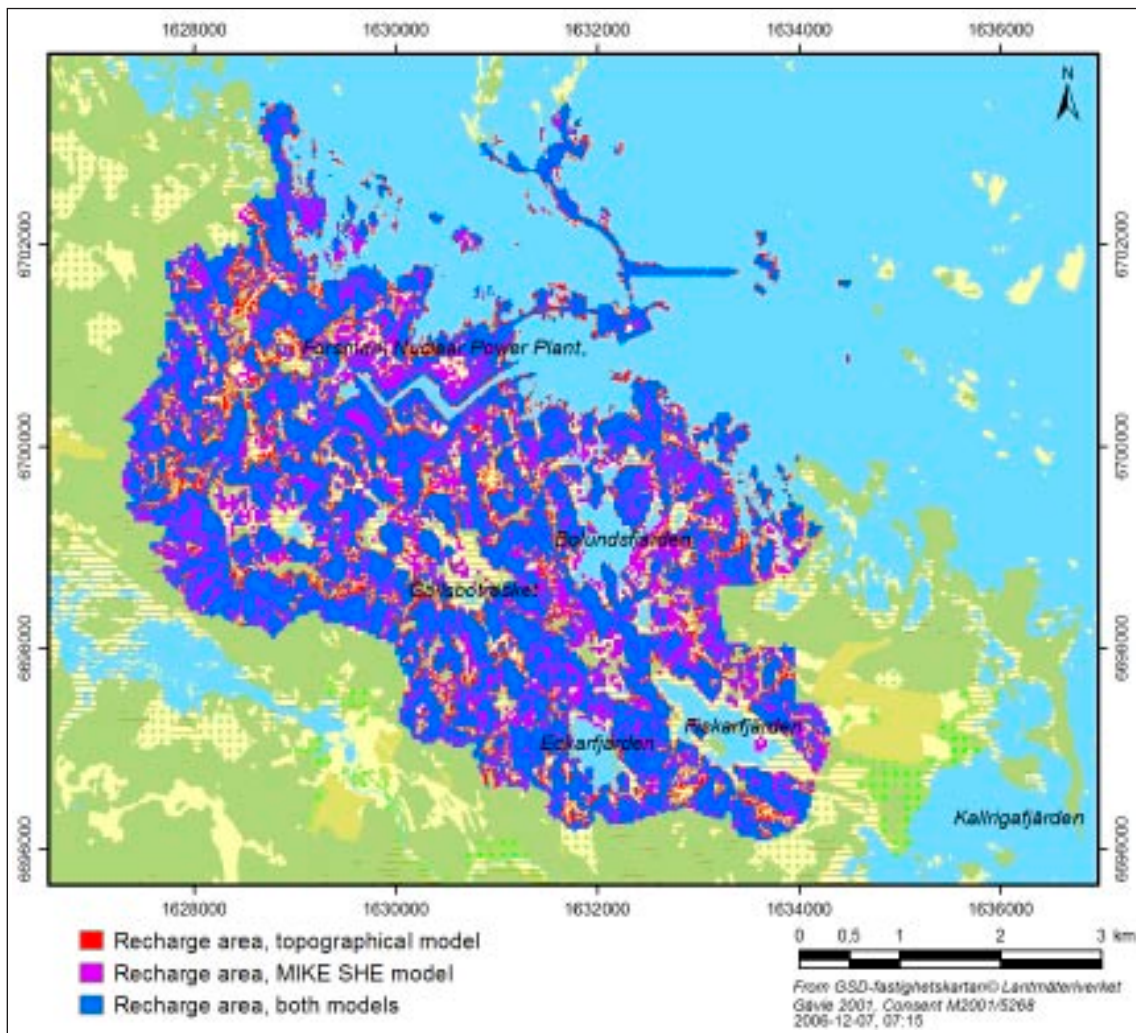


**Figure 4-3.** Comparison between recharge areas identified using the topographical RD model and the MIKE SHE model. Blue areas are classified as recharge areas according to both models, whereas red and lilac areas are recharge areas according to one of the models only.

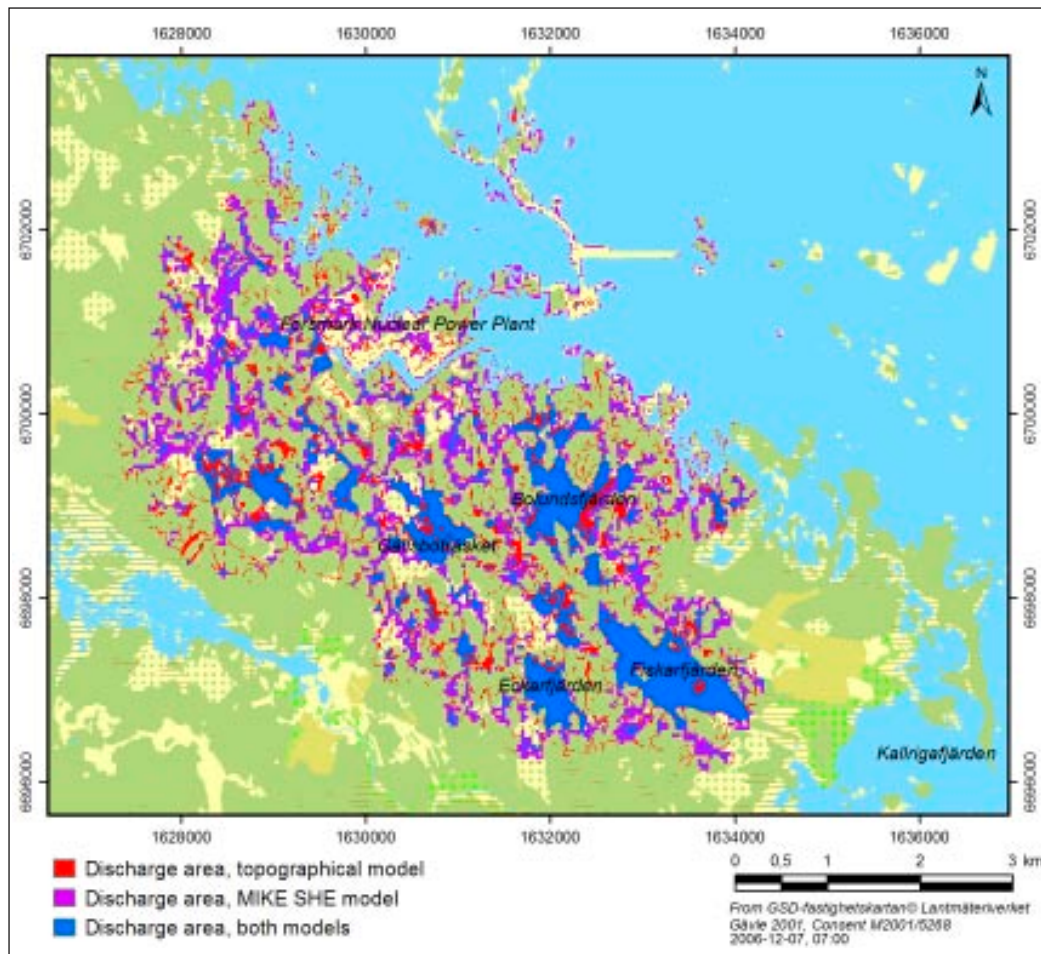


**Figure 4-4.** Comparison between discharge areas identified using the topographical RD model and the MIKE SHE model. Blue areas are classified as discharge areas according to both models, whereas red and lilac areas are discharge areas according to one of the models only.

The results (Figure 4-5) indicate a good agreement between the topographical RD model and the MIKE SHE recharge-discharge classification. The average MIKE SHE flag value within the topographical MLR class is 0.92; a perfect match between the models would give an average flag value of 1.00. The corresponding flag value within the topographical MLD class is  $-0.47$  (perfect match:  $-1.00$ ). One possible reason for the discharge area mismatch is associated with the observation that the Basin fill function, used in the topographical modelling (cf. Section 3.1) produces somewhat larger and deeper lakes in Forsmark than the real lakes. Another reason is likely due to the different spatial resolutions of the two models: MIKE SHE has a grid cell size of 40 m by 40 m, whereas the grid cell size of the DEM used in the topographical modelling is 10 by 10 m.

The excellent (recharge areas) and the less good (discharge areas) agreement between the two models are further illustrated in Table 4-1. The table compares the total areas of the two “topographical extremes” (MLR and MLD) to the total areas of MIKE SHE grid cells with flag values +1 (MIKE SHE “recharge”) and  $-1$  (MIKE SHE “discharge”). Also this comparison illustrates that the best agreement between the models is obtained for the recharge areas: The total area of the DEM grid cells classified as MLR is 3.44 km<sup>2</sup>, whereas the total area of the MIKE SHE grid cells with flag value +1 (recharge) is 3.3 km<sup>2</sup>. The total area of the MIKE SHE discharge grid cells within the MLR areas is 0.12 km<sup>2</sup>, corresponding to c. 3.5% of the MLR areas. Note that the difference between the total areas computed by the two models is due to different spatial resolutions. The total area of the MIKE SHE recharge grid cells within the MLD areas is 0.93 km<sup>2</sup>, corresponding to c. 23% of the MLD areas (total area = 4.04 km<sup>2</sup>).

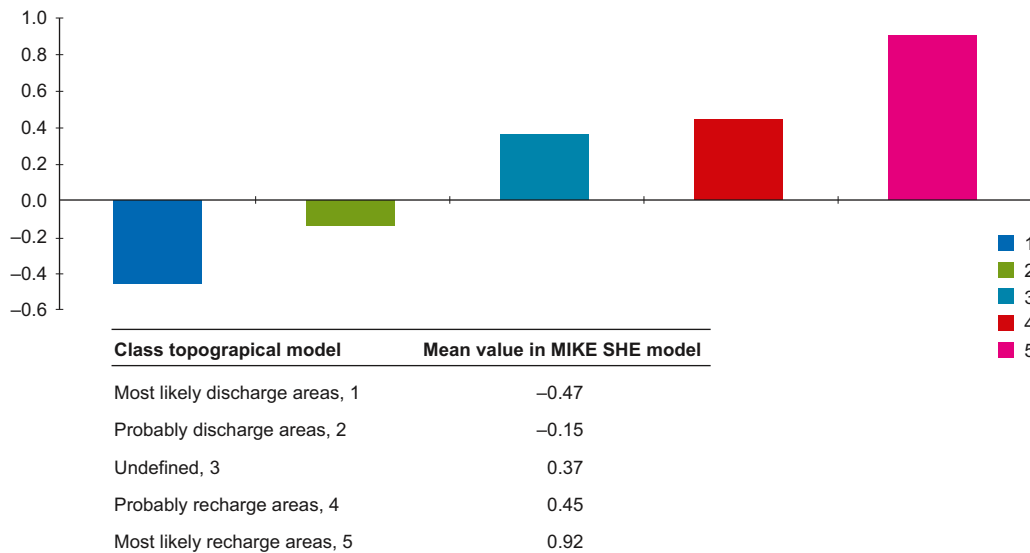


**Figure 4-5.** Comparison between the RD classifications produced by the topographical model and the MIKE SHE model. The figure compares the average MIKE SHE flag values (vertical axis) within each of the five RD classes (from the left to the right: 1/blue = most likely discharge areas, 5/lilac = most likely recharge areas) according to the topographical model.

**Table 4-1. Comparison between the RD classifications according to the topographical model and the MIKE SHE model.**

	Area (km <sup>2</sup> )
Topographical model, "Most likely recharge areas" (MLR)	3.44
MIKE SHE model, "Recharge" (flag value +1), located within MLR	3.30
MIKE SHE model, "Discharge" (flag value -1), located within MLR	0.12
Topographical model, "Most likely discharge areas" (MLD)	4.04
MIKE SHE model, "Discharge" (flag value -1), located within MLD	3.08
MIKE SHE model, "Recharge" (flag value +1), located within MLD	0.93

### 4.3 Methods for classification of groundwater monitoring well locations

This section compares the previously outlined methods used for topographical and RD classifications of groundwater monitoring well locations in the Forsmark area:

- The topographical model (Section 3.1; both topographical and RD classifications are evaluated).
- The field-based classification (Section 3.4; both topographical and RD classifications are evaluated).
- The hydrochemical RD classification (Section 3.5; only the RD classifications are evaluated).

Section 4.3.1 compares two methods used for topographical classifications of well locations (the classification based on the DEM, and a field classification), whereas Section 4.3.2 compares RD classification methods.

### 4.3.1 Topographical classifications

According to the general principles of groundwater recharge and discharge (Section 2.1.1), topography has large influence on recharge-discharge patterns. This motivates a separate comparison of the methods that explicitly classify the topography. Table 4-2 compares the topographical classification made in the field (Section 3.4) and a topographical (geomorphological) classification that was made from the 10-m DEM /Johansson et al. 2005/. According to the methodology described in Section 3.1, the geomorphological classification was made using the Landserf software /Wood 1996/. For each DEM grid cell, the result is one of the geomorphological features peak, ridge, pass, plane, channel, and pit. Note that in the DEM-based geomorphological classification, only wells with ID numbers SFM0001 to -0060 were analyzed. Moreover, in cases of immediately nearby wells, only one well was classified. Neither wells installed below open water nor wells with very short time series (at the time of classification) are classified /Johansson et al. 2005/.

The geomorphological classification was performed with different windows sizes and slope tolerance values (cf. Section 3.2). Most groundwater wells obtained the same geomorphological classification, irrespective of window size and slope tolerance. For a few wells, the geomorphological classification differs between the parameter sets, see Table 4-2. For instance, well SFM0001 is classified as located either at a ridge or a plane, which should be interpreted as the presence of a low and indistinct ridge at this well location.

Most striking from Table 4-2 is that the field classification of the topography is more detailed for slopes. Out of the 31 wells locations classified using the DEM, 25 are classified as plane on 30 m by 30 m-scale, even with a low slope tolerance. In comparison, in the field classification only 14 of 56 well locations are classified as flat on the 20 m by 20 m-scale. Obviously, different resolutions of the topographical classifications influence also the RD classifications, since the local topography has a large impact on near-surface recharge-discharge patterns; cf. Sections 2.1 and 2.2. This finding is further demonstrated in Section 4.3.2.

### 4.3.2 RD classifications

Table 4-3 compares the field-based RD classification of well locations (Section 3.4), the topography-based RD classification (using the DEM, Section 3.2), and the hydrochemical RD classification, based on major elements (Piper plot, Section 3.5.1). The table also includes tritium-based estimates of groundwater age (Section 3.5.2). The abbreviations used in the table are explained in the table heading. Note that the DEM-based RD classification refers to the DEM cell (cell size 10 by 10 m) associated with the geographical coordinate of each well.

Table 4-4 summarizes the comparisons in Table 4-3; note that Table 4-4 considers the 42 wells that have been classified using all three methods in Table 4-3. Grey-toned cells in Table 4-4 quantify “between-method-agreements” for the same (lumped) RD classes, e.g. the discharge class according to one method versus the discharge class according to another method. The percentages (ratios) shown in the table are calculated as the classes along the horizontal divided by the classes along the vertical. For instance, the upper left grey-toned table cell indicates that of the totally 9 wells classified as R or PR in the field-based RD classification (FIELD), 3 wells (33%) are classified as MLR or PR according to the topography-based RD model (TOPO).



**Table 4-2. Comparison between a topographical classification made in the field, and a topographical classification based on the 10-m DEM.**

Well ID	Field classification (Section 3.4)		Geomorphological classification based on 10-m DEM /Johansson et al. 2005/			
	20 m by 20 m	100 m by 100 m	Slope tolerance > 1 degrees, curvature > 0.1		Slope tolerance > 0.5 degrees, curvature > 0.05	
			30 m by 30 m	110 m by 110 m	30 m by 30 m	110 m by 110 m
SFM0001	Ridge	Slope-lower	Ridge	Plane	Ridge	Ridge
SFM0002	Slope-mid	Slope-mid	Plane	Plane	Plane	Plane
SFM0003	Slope-lower	Slope-lower	Plane	Channel	Plane	Plane
SFM0004	Slope-mid	Slope-mid	Plane	Channel	Plane	Pass
SFM0005	Slope-mid	Slope-upper	Plane	Plane	Ridge	Plane
SFM0006	Slope-upper	Slope-upper	Plane	Plane	Plane	Plane
SFM0007	Slope-upper	Slope-upper	Plane	Plane	Plane	Plane
SFM0008	Slope-mid	Slope-mid	Plane	Plane	Plane	Plane
SFM0009	Slope-lower	Slope-lower	Plane	Plane	Plane	Plane
SFM0010	Slope-lower	Slope-mid	Plane	Plane	Channel	Plane
SFM0011	Flat	Slope-lower	Plane	Plane	Plane	Plane
SFM0012	Open water	Open water				
SFM0013	Flat	Slope-lower	Plane	Plane	Plane	Channel
SFM0014	Slope-lower	Slope-lower	Plane	Plane	Plane	Plane
SFM0015	Open water	Open water				
SFM0016	Slope-lower	Slope-lower	Plane	Plane	Plane	Plane
SFM0017	Flat	Flat	Plane	Channel	Plane	Channel
SFM0018	Flat	Slope-lower	Plane	Channel	Plane	Channel
SFM0019	Flat	Flat	Plane	Plane	Plane	Plane
SFM0020	Pit	Pit	Plane	Channel	Plane	Plane
SFM0021	Slope-lower	Slope-lower	Plane	Plane	Plane	Plane
SFM0022	Open water	Open water				
SFM0023	Open water	Open water				
SFM0024	Open water	Open water				
SFM0025	Open water	Open water				
SFM0026	Flat	Slope-lower	Plane	Plane	Channel	Channel
SFM0027	Slope-lower	Slope-lower	Plane	Plane	Plane	Plane
SFM0028	Flat	Flat	Plane	Plane	Plane	Plane
SFM0029	Flat	Flat				
SFM0030	Slope-lower	Slope-lower	Pass	Plane	Channel	Plane
SFM0031	Slope-lower	Slope-lower				
SFM0032	Flat	Slope-lower				
SFM0033	Flat	Slope-lower	Plane	Channel	Plane	Plane
SFM0034	Slope-lower	Slope-lower, Channel	Channel	Channel	Plane	Plane
SFM0035	Slope-lower	Slope-lower				
SFM0036	Pit	Pit	Plane	Plane	Channel	Plane
SFM0037	Pit	Pit				
SFM0049	Slope-lower	Slope-lower	Plane	Plane	Plane	Channel
SFM0057	Slope-lower	Slope-upper	Plane	Plane	Plane	Plane
SFM0058	Slope-upper	Slope-upper	Ridge	Plane	Plane	Ridge
SFM0059	Ridge	Ridge	Plane	Plane	Plane	Plane
SFM0060	Peak	Ridge	Plane	Plane	Plane	Plane
SFM0061	Peak	Ridge				
SFM0062	Open water	Open water				
SFM0063	Open water	Open water				
SFM0065	Open water	Open water				
SFM0067	Flat	Slope-lower				
SFM0068	Slope-lower	Slope-lower				
SFM0069	Slope-lower	Slope-lower				
SFM0070	Slope-mid	Slope-mid				
SFM0071	Slope-mid	Slope-mid				
SFM0072	Slope-mid	Slope-mid				
SFM0073	Flat	Flat				
SFM0074	Flat	Slope-lower				
SFM0075	Slope-mid	Slope-mid				
SFM0076	Flat	Peak				

**Table 4-3. Comparison of methods for RD classification of groundwater monitoring wells in the Forsmark area. D = discharge, R = recharge, P = probably, V = varying, U = undefined.**

Well ID	Field classification (Section 3.4)	Topographical model (Section 3.1)	Major chemical elements (Piper plot, Section 3.5.2)	Redox potential class (Section 3.5.3) <sup>1</sup>	Groundwater age (tritium; Section 3.5.3)
SFM0001	D	PR	D	3	Modern (< 5 to 10 y)
SFM0002	R	U	R	3	Modern (< 5 to 10 y)
SFM0003	V	PR	R	3	Modern (< 5 to 10 y)
SFM0004	R	PD	No data		
SFM0005	R	D	R	2	Modern (< 5 to 10 y)
SFM0006	R	U	R	2	Modern (< 5 to 10 y)
SFM0007	R	U	No data		
SFM0008	R	PR	R	3	Modern (< 5 to 10 y)
SFM0009	D	U	R	1	Modern (< 5 to 10 y)
SFM0010	V	PR	R		Submodern (prior to the 1950's)
SFM0011	D	D	D		Mix of submodern and modern
SFM0012	D	D	D	3	Mix of submodern and modern
SFM0013	D	D	D		Modern (< 5 to 10 y)
SFM0014	D	U	R		Modern (< 5 to 10 y)
SFM0015	D	D	D	4	Mix of submodern and modern / modern
SFM0016	D	D	R		Modern (< 5 to 10 y)
SFM0017	D	PD	D		Modern (< 5 to 10 y)
SFM0018	D	PR	D		Modern (< 5 to 10 y)
SFM0019	R	D	R		Modern (< 5 to 10 y)
SFM0020	V	D	R		Modern (< 5 to 10 y)
SFM0021	PD	U	R		Modern (< 5 to 10 y)
SFM0022	D	D	D	2	Mix of submodern and modern
SFM0023	D	D	D	3	Mix of submodern and modern
SFM0024	D	D	D		Modern (< 5 to 10 y)
SFM0025	D	D	D	3	Modern (< 5 to 10 y)
SFM0026	D	D	R		Some anthropogenic (bomb) tritium
SFM0027	D	PR	D	2	Modern (< 5 to 10 y)
SFM0028	D	PD	R		Some anthropogenic (bomb) tritium
SFM0029	D	PD	R	3	Modern (< 5 to 10 y)
SFM0030	D	U	D		Modern (< 5 to 10 y)
SFM0031	D	U	R	3	Modern (< 5 to 10 y)
SFM0032	D	PR	R	3	Modern (< 5 to 10 y)
SFM0033	D	PR	No data		
SFM0034	D	D	D		Modern (< 5 to 10 y)
SFM0035	D	D	No data		
SFM0036	D	PR	R		Modern (< 5 to 10 y)
SFM0037	D	PR	R	3	Modern (< 5 to 10 y)
SFM0049	D	D	R	4	Modern (< 5 to 10 y)
SFM0051	D	D	No data		Modern (< 5 to 10 y)
SFM0053	D	PD	No data		Modern (< 5 to 10 y)
SFM0056	R	U	No data		Submodern (prior to the 1950's)
SFM0057	R	PR	D	3	Modern (< 5 to 10 y)
SFM0058	R	R	No data		
SFM0059	R	R	D		Modern (< 5 to 10 y)
SFM0060	R	PD	R	1	Modern (< 5 to 10 y)
SFM0061	R	PD	R		Modern (< 5 to 10 y)
SFM0062	D	D	R	3	Modern (< 5 to 10 y)
SFM0063	D	D	D	2	Modern (< 5 to 10 y)
SFM0065	D	D	D	2	No data
SFM0067	D	D	No data		
SFM0068	PD	U	No data		
SFM0069	D	U	No data		
SFM0070	R	PR	No data		
SFM0071	R	U	No data		
SFM0072	R	U	No data		
SFM0073	D	PD	No data		
SFM0074	D	D	R	3	Modern (< 5 to 10 y)
SFM0075	R	U	No data		
SFM0076	R	R	No data		

<sup>1</sup>Class 1 = high redox potential (recharge characteristics), class 4 = very low redox potential (discharge characteristics).

**Table 4-4. Agreements between the physical-hydrological field classification (FIELD), the DEM-based topographical classification (TOPO) and the chemical classification (PIPER) of groundwater monitoring well locations in Forsmark. R = recharge, D = discharge, ML = most likely, P = probably, V = varying, U = undefined.**

	TOPO (MLR, PR)	TOPO (U)	TOPO (MLD, PD)	PIPER (R)	PIPER (D)
FIELD (R, PR)	33% (3/9)	22% (2/9)	44% (4/9)	78% (7/9)	22% (2/9)
FIELD (V)	66% (2/3)	0%	33% (1/3)	100% (3/3)	0%
FIELD (D, PD)	20% (6/30)	17% (5/30)	63% (19/30)	47% (14/30)	53% (16/30)
TOPO (MLR, PR)				55% (6/11)	45% (5/11)
TOPO (U)				86% (6/7)	14% (1/7)
TOPO (MLD, PD)				50% (12/24)	50% (12/24)

The following observations can be made from Tables 4-3 and 4-4:

- For wells classified as recharge wells according to the field-based classification, there is relative good agreement (c. 80%) to the Piper-plot classification. The agreement is less good (c. 50%) for field-classified discharge wells.
- The best agreement between the field-based classification and the topographical classification (c. 60%) is for field-classified discharge wells. For the field-classified recharge wells, the agreement is less good (c. 30%).
- The agreement between the topographical classification and the Piper-plot classification is generally less good (c. 50%).
- The average tritium concentrations (TU) show no clear pattern compared to the recharge-discharge classifications, at least not among wells field-classified as discharge. However, groundwater sampled in most wells field-classified as recharge can be age dated as “modern” (< 5 to 10 y).

As mentioned in Section 3.5.1, hydrochemical parameters that typically are used to identify groundwater recharge and discharge areas (such as chloride, DOC, Eh, and tritium) demonstrate much larger variability between wells that are field-classified as discharge wells, compared to those field-classified as recharge wells. This is exemplified in Figures 4-6 and 4-7, showing the field-based RD classification (horizontal axes) versus the average Cl concentration (vertical axis in Figure 4-6) and the average tritium concentration (vertical axis in Figure 4-7).

Piper-plot based RD classifications, using Ca-HCO<sub>3</sub>, Na-HCO<sub>3</sub> and Na-Cl as main RD indicators, become difficult in areas with calcite-rich soils. Further, this type of classification assumes that discharging groundwater is characterized by high content of Na and Cl. In calcite-rich soils, recharging groundwater may be saturated with respect to calcite at relatively shallow depths. This implies that groundwater sampled in recharge areas hydrochemically may be interpreted as groundwater discharge. Further, shallow groundwater flow paths (cf. Section 2.1) implies that discharging groundwater may have low content of Na and Cl, which hydrochemically is interpreted as groundwater recharge.

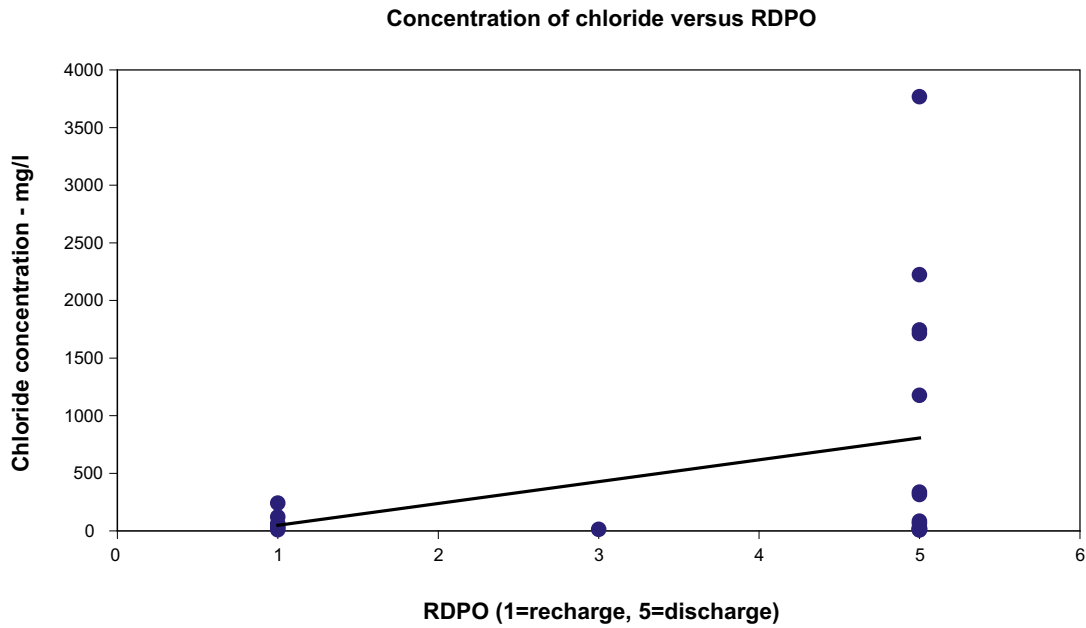


**Figure 4-6.** Plot showing the field-based RD classification on the horizontal axis (1 = recharge, 5 = discharge) and the average Cl concentration (mg/l) in groundwater monitoring wells on the vertical axis. The plot includes 21 groundwater monitoring wells, with 3 or more sampling occasions.

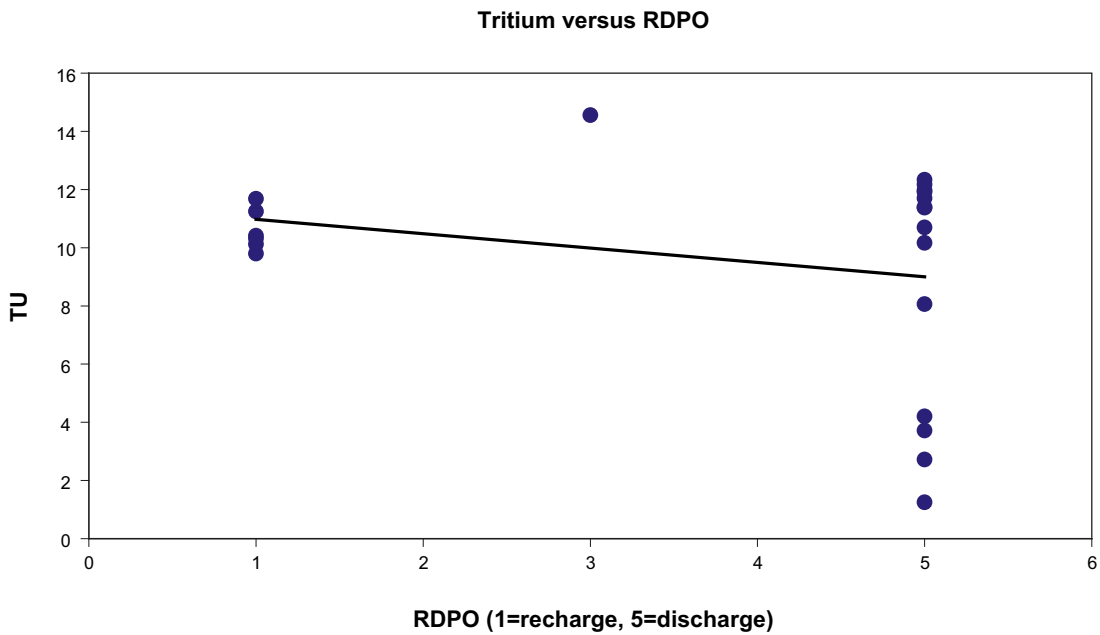


**Figure 4-7.** Plot showing the field-based RD classification on the horizontal axis (1 = recharge, 5 = discharge) and the average tritium concentration (TU) in groundwater monitoring wells on the vertical axis. The plot includes 21 groundwater monitoring wells, with 3 or more sampling occasions.

Figure 4-8 (cf. Table 4-4) shows an overview map of the Forsmark area, comparing the field-based RD classification and the hydrochemical RD classification of groundwater monitoring wells /Tröjbom and Söderbäck 2007/. In this map, one can identify three principal types of disagreements between these two classification methods (denoting field-based classification = field, Piper plot-based classification = hydrochemical, recharge = R, discharge = D, and V = variable):

- Field = R and hydrochemical = D (H1-C5 in Figure 4-8): This group contains two wells, located close to water divides (hence indicating recharge) but at the same time located close to surface waters (hence indicating discharge). One possible explanation for the classification mismatch is thus that the hydrochemistry indicates discharge, since the wells are in areas with discharge to eskers (SFM0059) and close to surface waters/a local discharge area (SFM0057). As an alternative explanation, these wells may be influenced by modern or old sea water, and therefore “erroneously” classified according to the hydrochemistry.
- Field = V and hydrochemical = R (H3-C1 in Figure 4-8): This group contains three wells, located relatively far from both water divides and surface waters. One possible explanation is that the field classification is unclear due to the generally small topographical gradients, whereas the hydrochemical classification (not having an “intermediate” class) also should be “Intermediate”, since it is influenced by local recharge.
- Field = D or PD, and hydrochemical = R (H5-C1 in Figure 4-8): This group contains 14 wells, of which 12 are located in the vicinity of lakes. One possible interpretation is that there are local recharge-discharge patterns in wetlands, clumps of reeds and shores around the lakes. It is possible that the hydrochemical-based classification of these wells in reality is based on rain- or surface water, which has accumulated on the ground surface. Further, water sampled in discharge areas associated to near-surface flow systems is characterized by short residence time in the subsurface, and small content of Na and Cl. This implies that this water hydrochemically is interpreted as groundwater recharge. Deviating wells in this group are SFM0009 and -21, both located on or close to water divides. For these wells, it is possible that there is some error in the field classification.

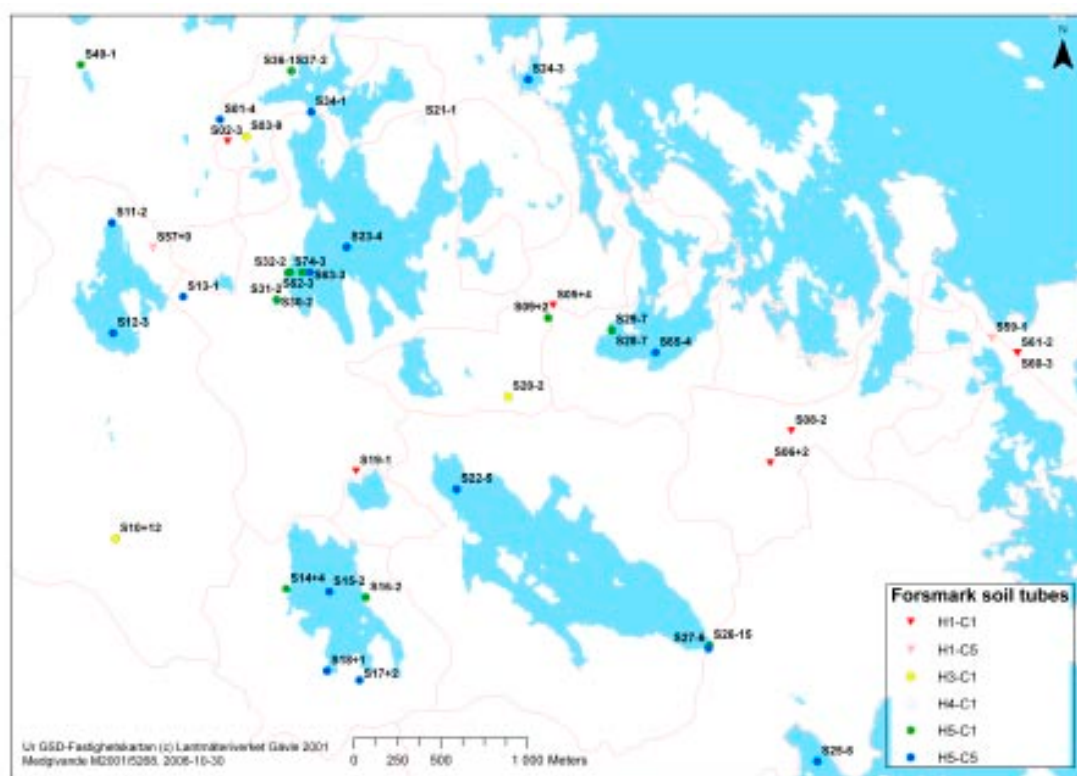


**Figure 4-8.** Overview map of the Forsmark area, comparing the field-based (H) and the hydrochemical (Piper plot; C) RD classifications of groundwater monitoring wells /Tröjbom and Söderbäck 2007/. 1 = R, 2 = PR, 3 = I, 4 = PD, 5 = D.

## 5 Summary and conclusions

Data and models were presented and compared for identification of near-surface groundwater recharge and discharge (RD) areas in Forsmark. One objective was to demonstrate how different types of data and models independently can be utilized to identify RD areas. Another objective was to investigate the results of different RD classification methods, and to identify and discuss possible reasons for observed differences.

In order to provide a problem description, some general principles of groundwater recharge and discharge were demonstrated, focusing on the influences of topography and geological variability on groundwater RD patterns on different scales. The presented concepts were applied to interpret hydrological and hydrogeological observations made in the Forsmark area, providing an up-to-date summary of the preliminary conceptual model of water flow at the site.

The study includes both “continuous” and “discrete” RD classification methods. Continuous methods include topographical modelling, map overlays, and hydrological-hydrogeological flow modelling. Discrete (point) methods include field-based and hydrochemistry-based RD classifications of groundwater monitoring well locations.

The topographical RD modelling, which uses the digital elevation model as the only input, was performed by means of geomorphological classification (Landserf) and hydrological functions in ArcGIS. The resulting RD map contains five classes, ranging from most likely recharge to most likely discharge (and including 22% unclassified areas). Model validation (using a separate validation area in Forsmark) showed that the topographical RD model only produces a deviating classification of c. 1% of recharge and discharge areas, respectively. In the validation, the RD classification was checked for some hundreds random DEM cells, coinciding with rock outcrops (assumed to be typical recharge areas), and lakes, watercourses and wetlands (assumed to be typical discharge areas). It should be noted that the topographical RD model assumes that discharge occurs at lakes, watercourses and wetlands, but nowhere else.

The RD classifications using map overlays were based on background maps of Quaternary deposits, soils, and ground- and field layers of the vegetation/land use map. RD classifications were made of each individual background map, and simple RD classification rules were used to produce “integrated” RD maps (map overlays) in four classes: Recharge, discharge, undefined, and unclassified. In some parts of the classified map area, the resulting RD classifications were quite similar, even though different background maps were combined. However, some major differences were noticed, in particular for the south-eastern part of the map area. This may be explained by contradictory RD classifications of the field layer and the ground layer of the vegetation/land use map. The map overlay exercise illustrated the difficulties in making detailed, consistent (and realistic) RD classifications, based on these types of background maps. It should be noted that the use of “weights” and also calibration are possible for map-based RD classifications, even though no such attempts were made here.

Hydrological-hydrogeological modelling was performed using the MIKE SHE-MIKE 11 software packages. The established spatially and temporally distributed water flow model takes into account all the main processes of the hydrological cycle. Apart from the topography, this numerical water flow model needs many types of input data, including meteorology, vegetation/land use, geology, hydrogeology, and bottom elevations, widths and depths of watercourses and lakes. The resulting RD map had two classes (recharge and discharge), identified using near-surface head gradients (based on the difference in the model-calculated annual average hydraulic heads in the two uppermost calculation layers). The results show that the onshore parts of the considered model area are dominated by recharge areas. Areas classified as discharge mainly include surface waters, such as the major lakes and the sea.

The comparison between the topographical RD map and the map overlays shows that a combination of the QD map, the soil map and the ground layer of the vegetation/land use map yields the most realistic identification of discharge areas, based on the used subset of potential background map combinations and simple RD classification rules. However, this “best” map combination shows large differences compared to the topography-based model. Further, the topographical RD model, which is based on the 10-m DEM, has a much more detailed resolution compared to the map overlays; the map overlays by necessity involve a higher degree of generalization. The simple map comparisons made in the study show that RD classifications based on map overlays require background maps with high spatial resolution, detailed type divisions, and/or a larger number of background maps, in order to produce realistic results.

The comparison between the topographical RD map and the MIKE SHE RD map shows an excellent agreement, at least in areas topographically classified as recharge. The match is less good in areas topographically classified as discharge. Possible reasons for this mismatch are that the ArcGIS “Basin fill” function, used in the topographical modelling, overestimates the sizes and depths of the lakes in Forsmark, and that the models have different spatial resolutions (topographical model: 10 m by 10 m; MIKE SHE: 40 m by 40 m); the model comparison would benefit from using models with similar spatial resolutions.

The field-based RD classification was performed of 59 of the groundwater monitoring wells (including 3 BAT filter tips) in Forsmark. The classification scheme is based on many location-specific factors, including local topography, distance from surface water, vegetation (ground layer, field layer, bush layer, and tree layer), and site hydrology. Well locations were classified in five classes: Recharge, probable recharge, varying, probable discharge, and discharge. Most wells (38) were classified as discharge or probable discharge, and 18 as recharge. 3 well locations were classified as varying.

A hydrochemical RD classification of 42 of the groundwater monitoring wells was presented, using Piper plots of the relative composition of major chemical elements. The Piper plot identifies groundwater of Ca-HCO<sub>3</sub> type (assumed to indicate recharge) and Na-HCO<sub>3</sub> to Na-Cl types (assumed to indicate discharge). This hydrochemical classification resulted in 24 wells classified as recharge, and 18 wells as discharge.

Table 5-1 summarizes the findings from the study, in terms of the agreements between the considered RD models. Overall, the best agreements are found between the topography-based model and the MIKE SHE model. The agreement between the topographical model and the map overlays is less good. The agreement between the map overlays on the one hand, and the MIKE SHE and field-based RD classifications on the other, is thought to be less good, as inferred from the comparison made with the topography-based model. However, much improvement of the map overlays can likely be obtained, e.g. by using “weights” and calibration (such exercises were outside the scope of the present study).

The comparison between the field-based and the hydrochemistry-based methods for well classification showed that there is a good agreement (80%) for wells that are field-classified as “recharge wells”. The agreement is less good (< 50%) for field-classified “discharge wells”. The undulating terrain in Forsmark implies that discharge areas may contain a mix of groundwaters, associated to local, intermediate, and/or regional groundwater flow systems. This limits the applicability of Piper plots, in which major chemical elements in near-surface groundwater samples are used for RD classification. In support of this conclusion, the concentration of the hydrogen isotope tritium, which is commonly used for age-dating of groundwaters, shows low variability among field-classified recharge wells, but a large spread among field-classified discharge wells.

**Table 5-1. Cross-plot summary of the RD model comparisons<sup>1</sup>.**

	Topography-based (top.):		Map overlays (m.o.):		MIKE SHE (M. SHE):		Field classification:		Hydrochem. (Piper plot; Pip.):	
	R	D	R	D	R	D	R	D	R	D
<b>Topography-based:</b>										
R			(+)		+		-		-	
D				(+)		(+)		-		-
<b>Map overlays:</b>										
R					(+) (*m.o. /top.)		(+) (*m.o. /top.)		N.C.	
D						(+) (*m.o. /top.)		(+) (*m.o. /top.)		N.C.
<b>MIKE SHE:</b>										
R							+		-	
D								(+) (*M. SHE /top.)		- (*Pip. /top.)
<b>Field classification:</b>										
R									+	
D										-

<sup>1</sup> + indicates good agreement, – indicates less good agreement. (+) implies that there is potential for better agreement by further model refinement. \* indicates that the RD model agreement was not investigated in the study, but can be inferred from the performed model comparisons. N.C. means that no comparison was made, and no conclusions should be inferred from the performed model comparisons.

The study demonstrates the importance of using several types of data and models for supporting interpretations of groundwater flow systems in Forsmark. The results of the method comparisons show that relatively simple RD models may be used, depending on the purpose and spatial/temporal scale of the analysis. For instance, “time-averaged” recharge-discharge patterns are probably identified with sufficient accuracy using a topographical RD model. On the other hand, quantification of the influences of e.g. subsurface features (geological variability) and flow transients on recharge-discharge patterns require (numerical) water flow models, taking into account both spatial variability and temporally variable meteorological conditions.

It can be concluded that topography-based modelling and numerical water flow modelling constitute important tools for identification of near-surface groundwater recharge-discharge areas. Field-based RD classifications are obviously time consuming, and thereby restricted to limited numbers of objects in the field; the study demonstrated an RD classification of groundwater monitoring wells. For instance, such objects may be locations where flow modelling indicates that radionuclides, originating at repository depth (400–700 m), may enter the surface system. Further, groundwaters in some near-surface discharge areas in Forsmark seem to contain a mix of groundwaters, possibly associated to multi-scale groundwater flow systems. This implies that hydrochemical data potentially may be used to support topography- and flow modelling-based interpretations of groundwater flow patterns in Forsmark, e.g. for identification of potential areas with discharge of “deep” groundwater.



Updated RD classifications of the Forsmark area should be made when further data and updated models are available. Based on the findings in this study, it is recommended that the MIKE SHE model primarily is used for this purpose. MIKE SHE (in combination with groundwater flow models of the deep bedrock) has the largest potential to identify the most important subset of the groundwater discharge areas, i.e. discharge areas receiving groundwater that passes the intended repository volume along its flow path. Further motivations for choosing MIKE SHE are that this model provides a spatially “continuous” RD classification, and incorporates many processes and data (including transients) that are not considered in the other models. For instance, the topography-based RD model uses only the DEM, which will not be updated further. MIKE SHE takes into account many other types of data (such as meteorology and geology) that will be updated and also incorporated in the MIKE SHE model. The other methods presented in the study should primarily be used as support for the MIKE SHE modelling. This supporting data set should include a field-based RD classification of the entire set of monitoring wells in Forsmark (and possibly also other objects of interest), as well as an updated hydrochemistry-based RD classification. However, the present results indicate that Piper plots and single “age parameters” (such as tritium, used as example here) provide too inconsistent information to be of practical use for RD classification. In order to evaluate the applicability of hydrochemistry-based methods to assess water flow patterns in Forsmark, hydrochemical data need to be analyzed further and compared to updated MIKE SHE modelling results.

## References

- Appelo C A J, Postma D, 2005.** Geochemistry, groundwater and pollution. A. A. Balkema Publishers, Rotterdam, Netherlands.
- Beven K J, Kirkby M J, 1979.** A physically based variable contributing area model of basin hydrology. *Hydrol Sci Bull* 24(1), 43–69.
- Boresjö Bronge L, Wester K, 2002.** Vegetation mapping with satellite data of the Forsmark and Tierp regions. SKB R-02-06, Svensk Kärnbränslehantering AB.
- Boresjö Bronge L, Wester K, 2003.** Vegetation mapping with satellite data of the Forsmark, Tierp and Oskarshamn regions. SKB P-03-83, Svensk Kärnbränslehantering AB.
- Bosson E, Berglund S, 2006.** Near-surface hydrogeological model of Forsmark. Open repository and solute transport applications. SKB R-06-52, Svensk Kärnbränslehantering AB.
- Brydsten L, 2006.** Modelling groundwater discharge areas using only digital elevation models as input data. SKB TR-06-39, Svensk Kärnbränslehantering AB.
- Clark I D, Fritz P, 1997.** Environmental isotopes in hydrogeology. Lewis Publishers, New York.
- Cook P G, Herczeg A L (eds), 2000.** Environmental tracers in subsurface hydrology. Kluwer Academic Press, Boston.
- DHI Software, 2004.** MIKE SHE User's Guide. DHI Water and Environment, Hørsholm, Denmark.
- Ericsson L O, Holmén J, Rhén I, Blomquist N, 2006.** Storregional grundvattenmodellering – fördjupad analys av flödesförhållanden i Östra Småland. Jämförelse av olika konceptuella beskrivningar. SKB R-06-64, Svensk Kärnbränslehantering AB.
- Eriksson B, 1981.** Den potentiella evapotranspirationen i Sverige. SMHI RMK Nr 28. Sveriges Meteorologiska och Hydrologiska Institut (SMHI). (In Swedish.)
- Fitts C, 2004.** TWODAN. Two-dimensional analytical groundwater flow model. Fitts Geosolutions, Scarborough, ME, USA.
- Follin S, Stigsson M, Svensson U, 2005.** Regional hydrogeological simulations for Forsmark – Numerical modelling using DarcyTools. Preliminary site description Forsmark area – version 1.2. SKB R-05-60, Svensk Kärnbränslehantering AB.
- Freeze R A, Cherry J A, 1979.** Groundwater. Prentice Hall, Inc., Englewood Cliffs, N.J., USA.
- Freeze R A, Witherspoon P A, 1967.** Theoretical analysis of regional groundwater flow: 2. Effect of water-table configuration and subsurface permeability variation. *Water Resour Res* 3, 623–634.
- Gascoyne M, Sheppard M I, 1993.** Evidence of terrestrial discharge of deep groundwater on the Canadian Shield from helium in soil gases. *Env Sci Tech* 27, 2420–2426.
- Gentzschein B, Levén J, Follin S, 2006.** A comparison between well yield data from the site investigation in Forsmark and domestic wells in northern Uppland. SKB P-06-53, Svensk Kärnbränslehantering AB.
- Gokall-Norman K, Ludvigson J-E, 2006.** Hydraulic interference test in borehole HFM14. SKB P-06-196, Svensk Kärnbränslehantering AB.

- Gokall-Norman K, Ludvigson J-E, Jönsson S, 2005.** Hydraulic interference test in borehole HFM01. SKB P-05-236, Svensk Kärnbränslehantering AB.
- Grip H, Rodhe A, 1985.** Vattnets väg från regn till bäck. Hallgren & Fallgren Studieförlag AB (in Swedish).
- Gustafsson Y, 1968.** The influence of topography on groundwater formation. In: Ground water problems (eds. Eriksson E, Gustafsson Y, Nilsson K), 3–21. Pergamon Press, Oxford, UK.
- Hedenström A, 2003.** Investigation of marine and lacustrine sediments in lakes. SKB P-03-24, Svensk Kärnbränslehantering AB.
- Hedenström A, 2004.** Investigation of marine and lacustrine sediments in lakes. Stratigraphical and analytical data. SKB P-04-86, Svensk Kärnbränslehantering AB.
- Holmén J, Forsman J, 2005.** Flow of groundwater from great depths into the near surface deposits – modelling of a local domain in northeast Uppland. SKB R-04-31, Svensk Kärnbränslehantering AB.
- Johansson P-O, Werner K, Bosson E, Berglund S, Juston J, 2005.** Description of climate, surface hydrology and near-surface hydrogeology. Preliminary site description Forsmark area – version 1.2. SKB R-05-06, Svensk Kärnbränslehantering AB.
- Juston J, Johansson P-O, Levén J, Tröjbom M, Follin S, 2007.** Analysis of meteorological, hydrological and hydrogeological monitoring data. SKB R-06-49, Svensk Kärnbränslehantering AB.
- LaBolle E M, Fogg G E, Eweis J B, 2006.** Diffusive fractionation of  $^3\text{H}$  and  $^3\text{He}$  in groundwater and its impact on groundwater age estimates. Water Resour Res 42, W07202.
- Lind B, Lundin L, 1990.** Saturated hydraulic conductivity of Scandinavian tills. Nordic Hydrol 21, 107–118.
- Lundin L, Lode E, Stendahl J, Melkerud P-A, Björkvald L, Thorstensson A, 2004.** Soils and site types in the Forsmark area. SKB R-04-08, Svensk Kärnbränslehantering AB.
- Naturvårdsverket, 1999.** Bedömningsgrunder för miljö kvalitet. Grundvatten. Naturvårdsverket Rapport 4915 (in Swedish).
- Nyman H, Strömgren M, Hedenström A, 2007.** SKB-report (yet untitled) to be published, Svensk Kärnbränslehantering AB.
- SKB, 2005.** Preliminary site description. Forsmark area – version 1.2. SKB R-05-18, Svensk Kärnbränslehantering AB.
- SKB, 2006.** Site descriptive modelling Forsmark stage 2.1. Feedback for completion of the site investigation including input from safety assessment and repository engineering. SKB R-06-8, Svensk Kärnbränslehantering AB.
- SMHI, 2005.** Månadsnederbörd Forsmark och Oskarshamn. PM for Svensk Kärnbränslehantering AB (in Swedish).
- Sohlenius G, Hedenström A, Rudmark L, 2004.** Mapping of unconsolidated Quaternary deposits 2002–2003. Map description. SKB R-04-39, Svensk Kärnbränslehantering AB.
- Tóth J, 1962.** A theory of groundwater motion in small drainage basins in Central Alberta, Canada. J Geophys Res 67(11), 4375–4387.
- Tóth J, 1963.** A theoretical analysis of groundwater flow in small drainage basins. J Geophys Res 68(16), 4795–4811.

**Tröjbom M, Söderbäck B, 2006.** Chemical characteristics of surface systems in the Forsmark area. SKB R-06-19, Svensk Kärnbränslehantering AB.

**Tröjbom M, Söderbäck B, 2007.** SKB-report (yet untitled) to be published. Svensk Kärnbränslehantering AB.

**Van der Hoven S J, Wright R E, Carstens D A, 2005.** Radiogenic  $^4\text{He}$  as a conservative tracer in buried-valley aquifers. Water Resour Res 41, W11414.

**Vikström M, 2005.** Modelling of soil depth and lake sediments. An example from the Forsmark site. SKB R-05-07, Svensk Kärnbränslehantering AB.

**Werner K, Lundholm L, 2004.** Pumping test in well SFM0074. SKB P-04-142, Svensk Kärnbränslehantering AB.

**Wood J D, 1996.** The geomorphological characterisation of digital elevation models. Ph.D. Thesis, University of Leicester, UK.